DOKUZ EYLÜL UNIVERSITY

GRADUATE SCHOOL OF NATURAL AND APPLIED SCIENCES

AN INVESTIGATION OF VOLUME DEFORMATION, HYDRAULIC CONDUCTIVITY AND WATER RETENTION BEHAVIOR OF GLASS FIBER ADDED BENTONITE UNDER HIGH TEMPERATURES

by

Yusuf BATUGE

February, 2024

İZMİR

AN INVESTIGATION OF VOLUME DEFORMATION, HYDRAULIC CONDUCTIVITY AND WATER RETENTION BEHAVIOR OF GLASS FIBER ADDED BENTONITE UNDER HIGH TEMPERATURES

A Thesis Submitted to the
Graduate School of Natural and Applied Sciences of Dokuz Eylül University
In Partial Fulfillment of the Requirements for Master of Science in
Department of Civil Engineering, Geotechnics Program

by

Yusuf BATUGE

February, 2024

İZMİR

M.Sc THESIS EXAMINATION RESULT FORM

We have read the thesis entitled **"AN INVESTIGATION OF VOLUME DEFORMATION, HYDRAULIC CONDUCTIVITY AND WATER RETENTION BEHAVIOR OF GLASS FIBER ADDED BENTONITE UNDER HIGH TEMPERATURES"** completed by **YUSUF BATUGE** under supervision of **PROF.DR. YELİZ YÜKSELEN AKSOY** and we certify that in our opinion it is fully adequate, in scope and in quality, as a thesis for the degree of Master of Science.

Prof.Dr. Yeliz YÜKSELEN AKSOY

Supervisor

Jury Member

Jury Member

Prof. Dr. Okan FISTIKOĞLU

Director

Graduate School of Natural and Applied Sciences

ACKNOWLEDGMENT

First of all, I would like to thank my thesis advisor Prof. Dr. Yeliz YÜKSELEN AKSOY for always supporting me with her valuable knowledge during my thesis process.

I consider my dear friend Şükran Gizem ALPAYDIN as my second teacher for being with me in all experimental studies and supporting me in every subject.

I would like to thank my valuable lab mates Cihat AŞÇI, Emir OKUCU and Emir Can KARABULUT for being with me during this thesis process. I would also like to thank Res. Assist. Tuğçe ÖZDAMAR KUL for her valuable contributions to my laboratory process.

Finally, I would like to express my gratitude to my life partner Duygu AYDOĞAN, who gave me the strength to endure and always believed in me, and to my parents who never withheld any support from me.

I would like to thank TUBITAK for the financial support for the scholarship and test equipment for conducting the studies within the scope of the project titled "Improvement of Short and Long Term Engineering Performance and Thermal Conductivity Properties of Bentonite as a Buffer Material for Energy Geostructures" and grant No. 120M470.

Yusuf BATUGE

AN INVESTIGATION OF VOLUME DEFORMATION, HYDRAULIC CONDUCTIVITY AND WATER RETENTION BEHAVIOR OF GLASS FIBER ADDED BENTONITE UNDER HIGH TEMPERATURES

ABSTRACT

In line with the world's need for energy; heat piles, buried high voltage cables and high level nuclear waste (HLW) storage areas, which have emerged in the last century to meet energy needs, are examples of energy geo-structures. These energy geo-structures emit high temperatures and increase the temperature of the soil with which they interact, investigating and improving the behavior of soils under high temperatures has become a major issue. Bentonite is a clay with high montmorillonite content, which is preferred as a buffer material in energy geo-structures due to its high swelling capacity and low hydraulic conductivity.

In this study, a series of experiments were carried out in the laboratory to investigate the volumetric deformation, hydraulic conductivity and water retention behavior of bentonite under high temperature (80 °C). Experiments were carried out on samples kept at 80 °C to observe the effect of high temperature on the volume deformation of bentonite in short (6 months) and long (1 year) term. The effect of high temperature curing for 3 months was also investigated for hydraulic conductivity properties of bentonite. Glass fiber has been used as a bentonite additive because of its good engineering properties at high temperatures. In accordance with the literature, high temperature increased the compressibility and hydraulic conductivity of bentonite mixtures, while decreasing the swelling behavior and causing a negative effect. The compressibility of the mixtures under curing effect decreased. In the water retention behavior, a decrease in the total suction value was observed, while a negligible change was observed in the water retention curve (WRC). Glass fiber additive significantly increased the swelling behavior of bentonite at room temperature. This effect decreased at high temperature. It also has a negative effect on hydraulic conductivity, while its effect on water retention behavior and compressibility is negligible.

Keywords: Bentonite, glass fiber, high temperature, volume deformation, water retention capacity, hydraulic conductivity, curing effect

CAM ELYAF KATKILI BENTONİTİN YÜKSEK SICAKLIK ALTINDA HACİMSEL DEFORMASYON, GEÇİRİMLİLİK VE SU TUTMA DAVRANIŞININ İNCELENMESİ

ÖZ

Dünyanın enerji ihtiyacı doğrultusunda son yüzyılda ortaya çıkan ısı kazıkları, gömülü yüksek gerilim kabloları ve yüksek seviyeli nükleer atık (HLW) depolama alanları yenilenebilir ve temiz enerjinin çeşitli türleri enerji geo-yapılarına örnektir. Bu enerji geo-yapılarının yüksek sıcaklık yaydıkları ve etkileşimde bulundukları zeminin sıcaklığını artırdıkları düşünüldüğünde, artan sıcaklık altında zemin davranışlarının araştırılması ve iyileştirilmesi önemli bir konu haline gelmiştir. Bentonit, yüksek şişme kapasitesi ve düşük hidrolik iletkenliği nedeniyle enerji geo-yapılarında tampon malzeme olarak tercih edilen yüksek montmorillonit içeriğine sahip bir kildir.

Bu çalışmada, bentonitin yüksek sıcaklık (80 °C) altında hacimsel deformasyonunu, hidrolik iletkenliğini ve su tutma davranışını araştırmak için laboratuvarda bir dizi deney gerçekleştirilmiştir. Deneyler, yüksek sıcaklığın bentonitin hacimsel deformasyonu üzerindeki etkisini kısa (6 ay) ve uzun (1 yıl) vadede gözlemlemek için 80 °C'de tutulan numuneler üzerinde gerçekleştirilmiştir. Bentonitin hidrolik iletkenlik özellikleri için 3 ay boyunca yüksek sıcaklıkta kürlemenin etkisi de araştırılmıştır. Cam elyaf, yüksek sıcaklıklardaki iyi mühendislik özellikleri nedeniyle bentonit katkısı olarak kullanılmıştır. Literatüre uygun olarak, yüksek sıcaklık bentonit karışımlarının sıkıştırılabilirliğini ve hidrolik iletkenliğini artırırken, şişme davranışını azaltarak olumsuz bir etkiye neden olmuştur. Kür etkisi altındaki karışımların sıkıştırılabilirliği azalmıştır. Su tutma davranışında ise toplam emme basıncı değerinde azalma gözlenirken, su tutma eğrisinde (WRC) ihmal edilebilir bir değişim gözlenmiştir. Cam elyaf katkısı oda sıcaklığında bentonitin şişme davranışını önemli ölçüde artırmıştır. Bu etki yüksek sıcaklıkta azalmıştır. Ayrıca hidrolik iletkenlik üzerinde olumsuz bir etkiye sahipken, su tutma davranışı ve sıkıştırılabilirlik üzerindeki etkisi ihmal edilebilir düzeydedir.

Anahtar kelimeler: Bentonit, cam elyaf, yüksek sıcaklık, hacimsel deformasyon, su tutma kapasitesi, hidrolik iletkenlik, kürleme etkisi

CONTENTS

Page

LIST OF FIGURES

Page

LIST OF TABLES

Page

LIST OF SYMBOLS

C_c : Compression index

C_s : Swelling index

c_v : Coefficient of consolidation

σ'_p : Pre-consolidation pressure

ε_v : Vertical Deformation

ρ_d : Dry density

ψ : Suction

G_s : Specific gravity

k : Hydraulic conductivity

m_v : Coefficient of volume compressibility

e : Void ratio

σ_{vc} : Effective stress

ABBREVIATIONS

HLW : High level waste

THM : Thermo-hydro-mechanical

WRC : Water retention curve

FSI : Free swell index

VET : Vapor equilibrium technique

BBM : Bentonite based material

NC : Normally consolidated

OC : Over consolidated

OCR : Over consolidation ratio

SWCC : Soil water characteristic curve

RH : Relative humidity

CEC : Cation exchange capacity

Ca : Calcium

Na : Sodium

Mg : Magnesium

DDL : Diffuse double layer

XRD : X-ray diffraction

MBI : Methylene blue index

LL : Liquid limit

PL : Plastic limit

GF : Glass fiber

SSA : Specific surface area

NH_4OAc : Ammonium acetate

K_2CO_3 : Potassium carbonate

$CaNO_3$: Calcium nitrate

$NaNO_2$: Sodium nitrite

NaCl : Sodium chloride

KCl : Potassium chloride

$ZnSO_4$: Zinc sulfate

K_2SO_4 : Potassium sulfate

0.5% GF : 0.5% Glass fiber added bentonite mixture

1% GF : 1% Glass fiber added bentonite mixture

RT : Room Temperature

CHAPTER ONE
INTRODUCTION

1.1 Statement of the Problem

In parallel to increasing world population, the need for energy is also increasing significantly. Considering the limited availability of fossil fuels and their harmful effects on the environment, it is inevitable that the trend towards environmentally friendly and sustainable energy sources increases in the last century.

In this respect, other than wind and solar energies, which are thought to be a solution to the energy problem, energy geo-structures that come to mind are also taking their place. These structures are high-power buried cables used to distribute electricity, heat piles that meet the heating and cooling needs of buildings through heat transfer, and high level nuclear waste repositories for storing radioactive wastes generated in nuclear energy production in deep geological waste areas.

These energy geo-structures are structures that interact with the soil surrounding them and transmit high temperatures and thermal cycles to the soils for long periods of time. Hence, there is an increased emphasis on studies examining the thermo-hydro-mechanical behavior of soils has been observed over the past two decades. Studies have shown that the engineering behavior of soils can undergo alterations in the presence of high temperatures. Examining and improving the engineering behavior of soils that will be exposed to thermal changes for many years under high temperatures is of great importance for the integrity of energy geo-structures, and thus to prevent harm to the environment and human beings.

While investigating the engineering properties of soils under high temperatures is important in the literature, special emphasis should be placed on understanding the engineering properties of bentonite clay. This clay is often used as buffer material in energy geo-structures. It is very important to understand how it responds to prolonged exposure to high temperatures because of its performance as a buffer material.

1.2 Objective and Scope

Within the scope of this study, it was aimed to observe the changes in the volumetric deformation, hydraulic conductivity and water retention behavior of bentonite clay under high temperatures for short-term and long-term periods. In addition, glass fiber additive, which is frequently used for soil improvement and shows good thermal properties, was used as an additive material to bentonite, considering that it would improve the engineering properties of bentonite.

For this purpose, glass fiber additives were used in the experiments at the contents of 0.5% and 1% of the dry weight of bentonite. To observe the change in engineering parameters in the presence of high temperature, experiments were conducted both at room temperature and 80 °C. To examine the compressibility and swelling properties of bentonite exposed to high temperatures for long-term periods, the samples were kept in hot water pools at 80 °C for 6 months and 1 year, and then consolidation experiments were performed on these samples. Additionally, to examine the long-term change of the hydraulic conductivity, the samples were kept in permeameters at 80 °C for 3 months. To better understand the swelling property under high temperature, free swell index (FSI) tests were performed both at room temperature and 80 °C. To examine the water retention behavior of highly compacted bentonite, its suction value was examined using the vapor equilibrium technique (VET).

1.3 Outline of the Thesis

The thesis was organized as five chapters. These chapters are listed below:

In Chapter 1, the statement of the problem and the purpose and scope of the thesis are explained, respectively.

In Chapter 2, after discussing the high level nuclear waste repositories that can produce high temperatures in detail, the effects of high temperatures on the volumetric deformation, suction and hydraulic conductivity behaviors of the soils were given.

In Chapter 3, the characterization of the materials used in the thesis and the experimental methods are introduced.

In Chapter 4, the results and discussions obtained from the experiments within the scope of the thesis are presented.

In Chapter 5, conclusions and recommendations for future studies are presented.

CHAPTER TWO
BACKGROUND

Examining the effect of high temperatures on soils engineering behavior at dates back to the past century. The first documented experimental study exploring the effects of temperature on soil consolidation behavior was belongs to Gray (1936). The initial conference dedicated to examining the impact of temperature and heat on the engineering properties of soils was convened in Washington in 1969 (Abuel-Naga et al., 2006). In the early stages, research endeavors primarily concentrated on grasping how temperature changes affected the volumetric and strength parameters of soil specimens during their collection and transportation to the laboratory (Virdi & Keedwell, 1988). Previous studies therefore examined the engineering behavior of soils at temperatures up to 50 °C (Abuel-Naga et al., 2006).

With advancing technological developments, interest in examining the changes of soils under high temperatures has also increased. One of the main reasons for this interest stems from the increase in energy geo-structures in the past decades. It requires examining the engineering behavior of soils under temperature due to the temperatures emitted by energy geo-structures such as heat piles, buried power cables and especially nuclear waste storage areas.

2.1 High Level Nuclear Waste Repositories

Nuclear energy stands out as the most efficient energy field today. It plays an active role in the fight against climate change, especially by providing less carbon emissions compared to other energy sources. As with all other energy sources, waste materials are generated during the production of nuclear energy. Nuclear wastes are classified as low, medium and high level waste according to their radioactivity. Although most of these wastes are low radioactivity wastes, there are also high radioactivity wastes called spent fuel. According to Wang (2008), China produces approximately 10.3 metric tons of high level radioactive waste (HLW) annually, originating from nuclear power plants and other nuclear facilities.

Because of its high radioactive nature and high temperatures it releases, the high level nuclear wastes necessitate storage for centuries to prevent environmental harm. Nuclear waste will continue to decay after being stored in the disposal repository and will release a large amount of decay heat, which will cause changes in the temperature field in the repository (Zhou et al., 2021). Many countries have adopted the concept of deep geological disposal to separate high level radioactive waste (HLW) from the biological environment (Zhang et al., 2013; Xu et al., 2016; Shao et al., 2022). Several countries are intending to construct geological repositories for high-level radioactive waste (HLW) at significant depths, typically ranging from 500 to approximately 1000 meters below the ground level, within intact host rock formations (Tripathy & Schanz, 2007; Ye et al., 2012).

A high-level radioactive waste (HLW) disposal facility is typically connected to a multiple barrier system designed to separate the waste from the biosphere. This system usually includes a natural geological barrier formed by the bedrock of the repository and its surroundings, as well as an engineered barrier system. The engineered barrier system includes man-made materials strategically positioned within the repository, including the waste form, waste canisters, buffer material, backfill and seals (Zhang et al., 2012). General concept of the HLW repositories is shown in Figure 2.1.

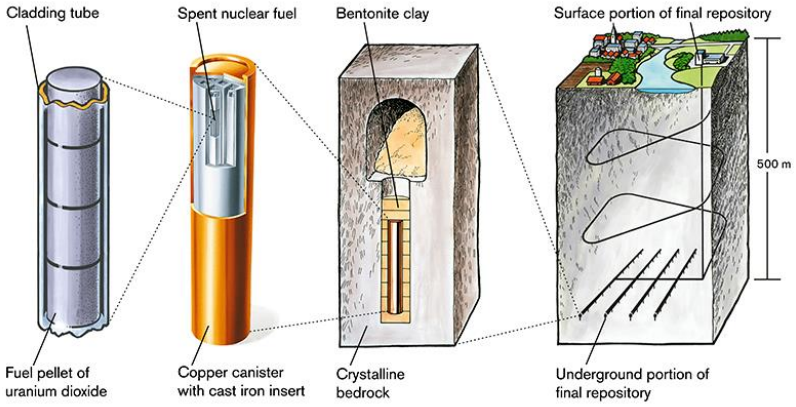

Figure 2.1 General concept of HLW repositories (Hedin, 2006)

Several countries have opted for bentonite-based materials (BBM) as buffer materials in the multi-barrier system due to their suitable swelling capacity, which seals structural cracks upon hydration, and their low permeability and high absorption

capacity, which effectively hinder potential leakage of radioactive substances (Pusch, 1983; Komine & Ogata, 1996; Villar, 2006; Ye et al., 2020). The main reasons for the high swelling and low hydraulic conductivity of bentonite clay are its high content of montmorillonite, high plasticity index, high specific surface area.

Until now, various types of bentonites have been selected as buffer material for HLW repositories. MX-80 bentonite extracted in Wyoming, USA has been selected as buffer and sealing material in many countries such as Germany (Herbert & Moog, 1999), Finland (Dixon, 2000), and Sweden (Nakashima, 2006). FEBEX bentonite mined in Almeria, Spain has been approved by ENRESA (The Spanish Agency for Radioactive Waste Management) for buffer material (Villar, 1999). GaoMiao-Zi (GMZ) bentonite was selected as a suitable buffer material for HLW storage in China (Liu et al., 2001). Kunigel V1 bentonite was presented as a suitable bentonite for Japan (Imbert & Villar, 2006), while FoCa bentonite was selected in France (Tang et al., 2008).

A bentonite-based buffer material (BBM) can be produced by static or dynamic compaction such as bentonite itself and bentonite–sand mixture (Ito and Komine, 2008). Mostly pure bentonite blocks or bentonite pellets are used and the dry densities of compacted bentonite range from 1.2 to 2 Mg/m^3 with void ratios between 0.4-1.3 (Tripathy & Schanz, 2007). The performance indicators required for the material to be used as a buffer are given in Table 2.1.

Shen et al. (2000) reported that the maximum temperature at the edge of the repository occurs after 10 years after the repository is closed and the maximum temperature is about 90 °C. At HLW repositories around the world, the maximum design temperature is 100 °C or below, such as, POSIVA in Finland (Posiva, 2003), ANDRA in France (ANDRA, 2005), SKB in Sweden (Hedin, 2006), NWMO in Canada (Maak, 2006), SCK in Belgium (Delage et al., 2010) and KORAD in South Korea (Cho et al., 2012). In this study, in order to examine the behavior of bentonite under high temperature, 80 °C was used as the maximum temperature preferred by many researchers (Cho et al., 1999; Villar & Lloret, 2004; Ye et al., 2012).

Table 2.1 Performance indicators of the buffer materials (Kim et al., 2011)

Performance indicator	**Criterion**	**Background**
Hydraulic conductivity	$k^{buffer}<10^{-12}$m/s	Limit mass transport to a diffusion-dominated process
Swelling pressure	$P_{swell}>1$ MPa	Ensure sealing, self-healing capacity
Maximum temperature	T^{buffer} <100 °C	Ensure that the buffer retains its properties for long periods of time
Minimum temperature	T^{buffer} >-5 °C	Prevent freezing
Swelling pressure against the canister	$P_{swell}>0.2$ MPa	Prevent the canister from sinking
Swelling pressure around the canister	$P_{swell}>2$ MPa	Prevent microbial activity
Density around the canister	$\rho_{bulk}>1.650$ kg/m^3	Prevent transport of particles through the buffer
Density around the canister	$\rho_{bulk}<2.10$ kg/m^3	Limit shear stresses on the canister due to rock movements

In the following sections, the changes in consolidation, water retention and hydraulic conductivity of soils and bentonite under high temperatures were given. Finally, the general properties of glass fiber used as bentonite additive in the study were introduced.

2.2 Temperature Effects on Consolidation Behavior of Clayey Soils

In this section, the consolidation behavior of clayey soils under high temperature conditions will be given with former studies in the literature. Until now, many researchers have investigated the consolidation behavior of clayey soils under the influence of temperature. The main focus of these investigations has ranged widely in terms of the types of soils used, the experimental methods used, the soil properties investigated, etc. Among the most important factors affecting the compressibility

parameter of soils under the influence of temperature are temperature range, stress range, mineralogical structure of the soil, and stress history.

In one of the earliest studies, drained isotropic consolidation experiments of remolded and water-saturated illite samples were performed at three temperature conditions (24.7, 37.8, 51.4 °C) and as a result, it was stated that the effect of temperature on the C_c parameter was negligible (Figure 2.2) (Campenella & Mitchell, 1968).

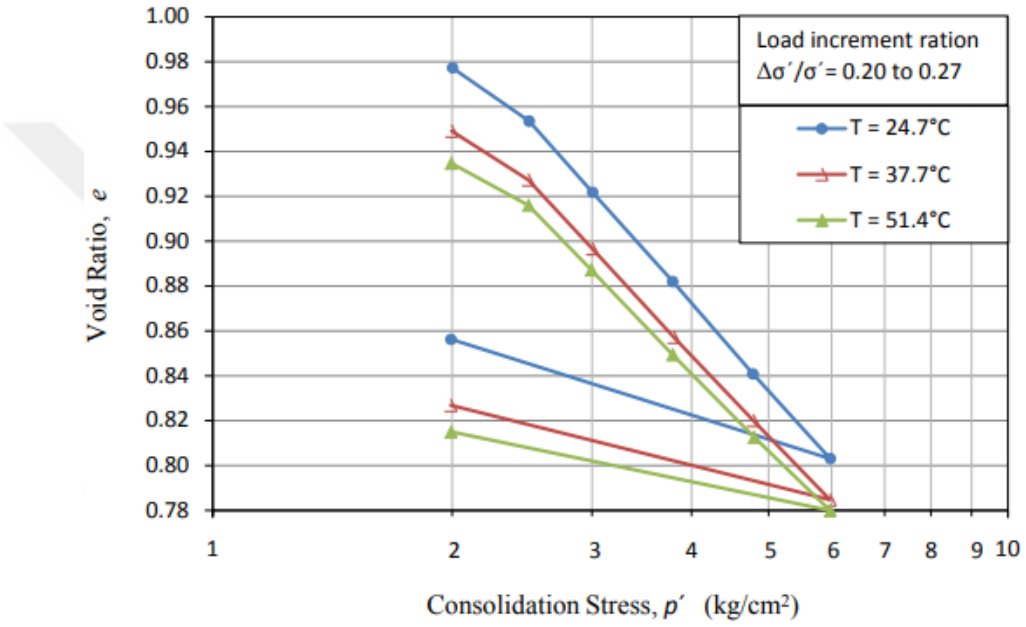

Figure 2.2 Void ratio Vs. consolidation stress at different temperatures (Campanella & Mitchell, 1968; El Tawati, 2010)

Towhata et al. (1993) used normally consolidated (NC) and over consolidated (OC) MC kaolin clay and bentonite with a liquid limit value of 450%. A conventional oedometer test apparatus was used and a temperature range was of 25-90 °C. As a result, it was stated that temperature causes volumetric contraction and volumetric contraction is independent of stress level and OCR. The higher contraction of bentonite than MC clay is related to the plasticity of clays. Delage et al. (2000) investigated the thermal volume change and thermal consolidation of Belgian Boom clay. Tests were carried out with isotropic compression cell up to 100 °C. The following equations are derived to estimate thermal expansion (Campanella & Mitchell, 1968).

$$\Delta V_w = a_w V_w \Delta T \quad (2.1)$$

$$\Delta V_S = a_s V_s \Delta T \quad (2.2)$$

Where ΔV_w is equal to the thermal expansion of the pore water and ΔV_s is equal to the thermal expansion of the soil skeleton, α_w and α_s is the thermal expansion coefficient, while V_w and V_s are the volume of the pore water and soil skeleton, respectively.

The corresponding volumetric strain (ε_v) during the drained heating test is obtained by subtracting the volume due to thermal expansion of water and solids from the total volume of drained pore water (ΔV_{dr}).

$$\varepsilon_v = \frac{[\Delta V_{dr} - (a_w V_W + a_s V_s)\Delta T]}{V} \quad (2.3)$$

In plastic clays with low porosity, Baldi et al. (1988) took into consideration the impact of adsorbed water by applying the double-layer theory. It was posited that the molecules of adsorbed water experience a pressure that decreases exponentially with the distance between the water molecule and the clay platelet. Additionally, it was considered the influence of temperature and pressure on the volume change of the adsorbed water. Given the absence of free water in dense plastic clays, Baldi et al. (1988) derived the following expression for the thermal volumetric strain:

$$\varepsilon_v = \frac{[\Delta V_{dr} - (V \Delta v_a S_S \rho_d + a_s V_s)\Delta T]}{V} \quad (2.4)$$

where Δv_a is the volume of expanded adsorbed water per unit surface area of clay mineral and per °C, S_s is the specific surface of the clay, and ρ_d is the dry unit weight of the soil. Thermal volumetric strains at different temperatures for Boom clay with an

over consolidation ratio (OCR) of 2 are presented in Figure 2.3. In addition, Delage et al., (2000) reported that the coefficient of consolidation (c_v) increases with temperature, but the change after 60 °C is insignificant (Figure 2.4).

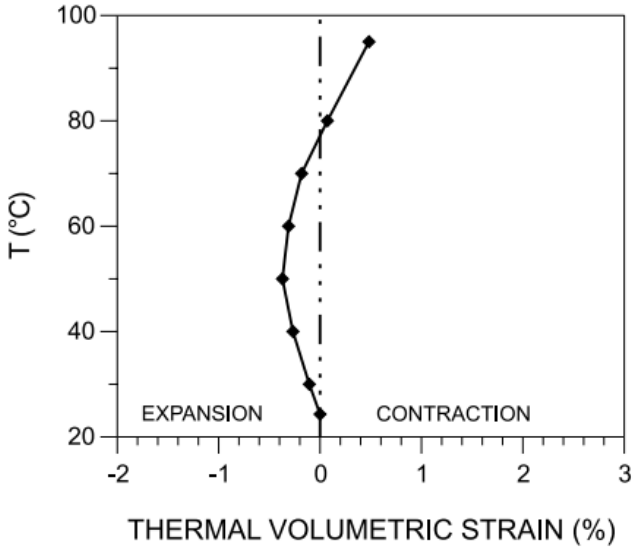

Figure 2.3 Thermal volumetric strains (Delage et al., 2000)

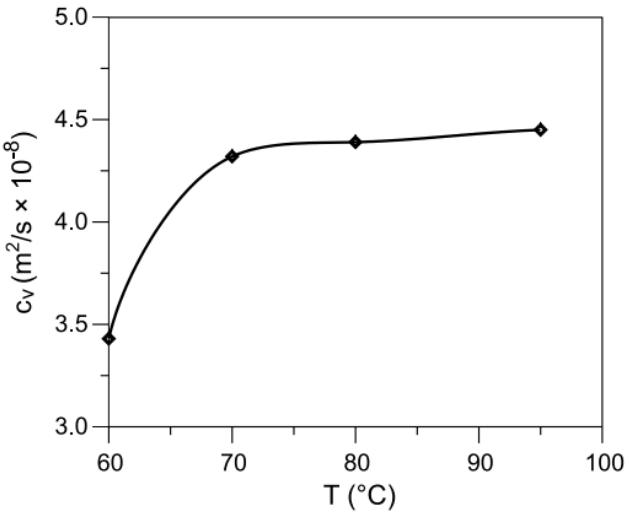

Figure 2.4 Variation of coefficient of consolidation (c_v) with temperature (Delage et al., 2000)

The pre-consolidation pressure serves as the pseudo-elastic threshold that distinguishes between "elastic" behavior before yielding and "plastic" behavior after yielding in isotropic or oedometric conditions (Cekerevac & Laloui, 2004). It plays a

role in determining the magnitude of the yield limit under varying temperatures. Cekerevac & Laloui (2004) observed that the pre-consolidation pressure decreases with increasing temperature in experiments with a modified triaxial cell in a study with kaolin clay (Figure 2.5).

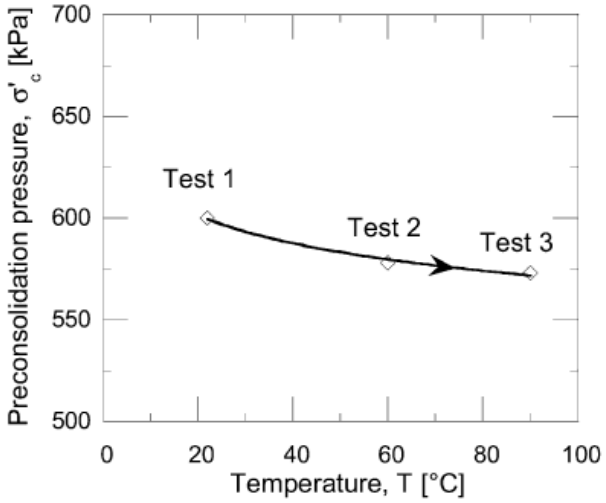

Figure 2.5 Influence of temperature on the pre-consolidation pressure of kaolin (Cekerevac & Laloui, 2004)

Abuel-Naga et al. (2006) studied the thermo-mechanical behavior of natural soft Bangkok clay, with temperature up to 90 °C. When the volumetric strains of the samples with different OCR values were observed with the heating/cooling cycle (22-90-22 °C), it was observed that NC clays experienced an irreversible contraction and increased nonlinearly with increasing temperature, while highly OC clays showed a reversible expansion (Figure 2.6).

Abuel-Naga et al. (2007) compared the plasticity index and volumetric strain of other studies to show the variation of the plasticity of clays to volumetric strain and as a result, it was stated that increasing the plasticity index in clays increases the volumetric strain nonlinearly. Also, they stated that the volumetric strain increased slightly with increasing temperature and the change in compression index (C_c) and swelling index (C_s) was insignificant (Figure 2.7).

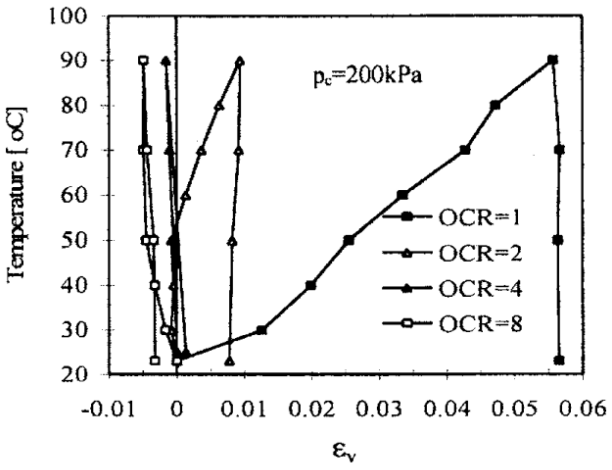

Figure 2.6 Volumetric strain under drained heating/cooling cycle of soft Bangkok clay (Abuel-Naga et al., 2006)

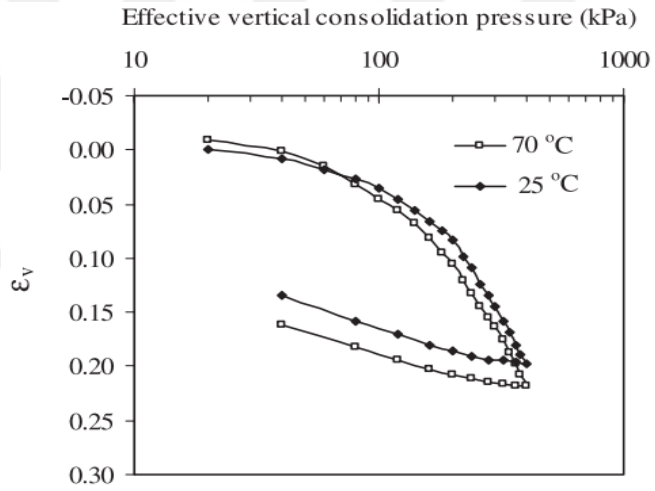

Figure 2.7 Consolidation curve of soft Bangkok clay at different temperatures (Abuel-Naga et al., 2007)

The compacted unsaturated bentonite pellets used in HLW storage areas will take a long time to reach water saturation. Furthermore, the geostatic stress at the top of bentonite pellets at depths of 500-1000 meters is expected to be in the range of about 9-16 MPa (Tripathy and Schanz, 2007). Therefore, it is very important to investigate the thermo-hydro-mechanical properties of compacted unsaturated bentonites. In this respect, some researchers have developed suction and temperature controlled oedometers or isotropic cells (Villar & Lloret, 2004; Tang et al., 2007; Ye et al., 2012).

Ye et al. (2012) conducted experiments with unsaturated compacted GMZ bentonite which has dry density of ρ_d=1.70Mg/m^3 in suction and temperature controlled oedometer. They performed a very wide set of experiments such as suction range from 0-110 MPa, temperature range from 20-80 °C and vertical pressure range from 0.1-80 MPa. As a result, it was observed that temperature causes expansion in bentonite at high suction values and contraction at low suction values. Furthermore, the elastic and plastic compressibility decreased with increasing suction. It was emphasized that the effect of temperature was insignificant in elastic compressibility and a small decrease in plastic compressibility as in the same with saturated soils.

Hoseinimighani & Szendefy (2022) conducted an extensive review study on the studies about volumetric change in fine soils under thermal conditions. They reported that NC clays showed irreversible contractions during drained heating tests (Figure 2.8). For OC clays (OCR>8), an initial expansion followed by a small amount of contraction was observed with increasing temperature, while for lightly over consolidated soils, an initial small expansion followed by contraction was observed as in NC clays (Figure 2.9). They also stated that pre-consolidation pressure decreases with increasing temperature. It was noted that high plasticity decreases pre-consolidation pressure more in temperature change.

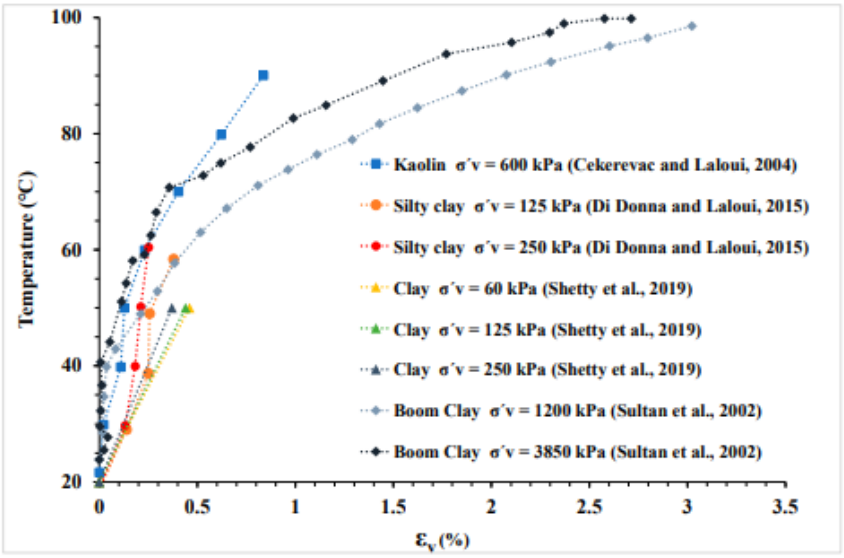

Figure 2.8 Volumetric strain for normally consolidated soils (Hoseinimighani & Szendefy, 2022)

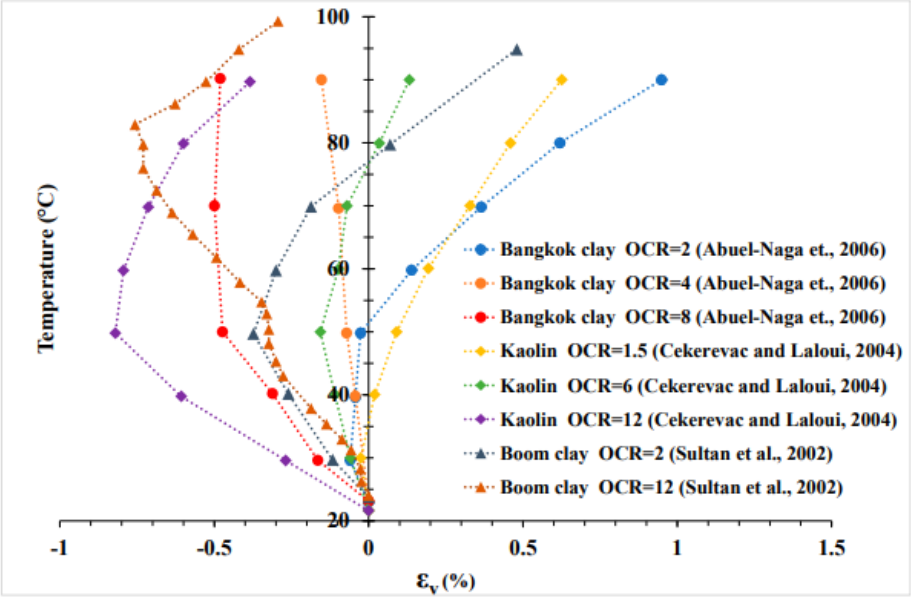

Figure 2.9 Volumetric strain for over consolidated soils (Hoseinimighani & Szendefy, 2022)

The effect of temperature on the compression index (C_c), of clay soils is insignificant, while the swelling index (C_s), decreases slightly. As the temperature increases, the pre-consolidation pressure value decreases. As the temperature increases, the coefficient of consolidation (c_v) increases up to a certain temperature. After a certain temperature level (60 °C), the change in the c_v is insignificant. The behavior of temperature on normally consolidated (NC) and over consolidated (OC) clays is different. NC clays show irreversible contraction, while OC clays show reversible expansion. Studies on clays with different plasticity have shown that clays with higher plasticity undergo higher volumetric strain (ε_v) under the influence of temperature.

2.3 High Temperature Effects on Water Retention Behavior of Soils

One of the crucial parameters for studying the behavior of unsaturated soils is suction. In soils, suction is the ability of the soil to retain water against gravity and is expressed in terms of stress. Richards (1974) divided the suction of soils into three main categories. These are matric suction caused by capillarity, osmotic suction caused by pore fluid chemistry and water adsorption caused by surface clay minerals. Only matric and osmotic suction are used to measure the total suction of soils. Matric suction

is usually the dominant type of suction in non-plastic soils, while osmotic suction is important for high plasticity clays (Blatz et al., 2009).

There are many methods in the literature to measure the suction of soils. Some of these are direct measurements, some are indirect measurements and some measure only matric or osmotic pressure while some measure total suction. These measurement methods are given in Table 2.2. As can be seen from the Table 2.2, the suction ranges of the methods are limited. The maximum range for matric and osmotic suction is 1500 kPa while for total suction it is 30 MPa.

Once placed as a buffer, the compacted bentonite remains unsaturated for some time due to the interaction of decomposition heat from the tailings and groundwater inflow. The movement of groundwater into the buffer during this time is driven by an absorption process. Therefore, suction measurement is essential to investigate groundwater movement in unsaturated compacted bentonite (Lee et al., 2011). Highly compacted unsaturated bentonites in HLW repositories are expected to have total suction values of hundreds of MPa due to their high activity and high swelling capacity (Tang & Cui, 2005). For this reason, the suction measurement and water retention curve (WRC) or also known as soil water characteristic curve (SWCC) of highly compacted bentonite is generally determined by the method with high suction range called vapor equilibrium technique (VET).

This method simply works on the principle of water transfer in the vapor phase between unsaturated soils and the environment due to the relative humidity value in a closed and constant mass system. Desiccators are generally preferred as a closed system with a constant mass. To maintain the relative humidity and therefore the suction inside the desiccator, salt or acid solutions are used, which can be used in different concentrations. Figure 2.10 shows a schematic representation of VET. The advantage of using saturated salt solutions is that there is no change in the concentration of the salt solution while water exchange continues in the vapor phase.

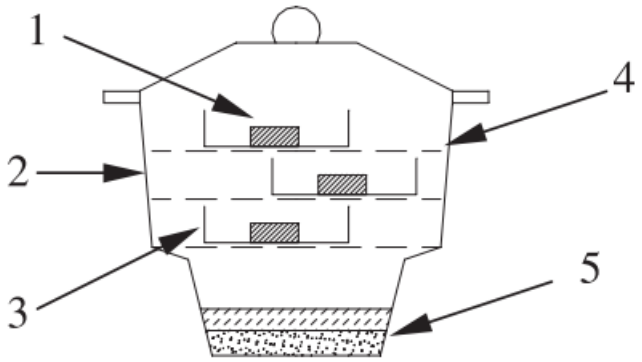

1. Soil sample
2. Desiccator
3. Glass cup
4. Support
5. Oversaturated salt solution

Figure 2.10 Schematic representation of VET (Tang & Cui, 2005)

Table 2.2 Suction measurement methods (Adapted from Pan et al., 2010)

		Technique (Method)	Suction Range (kPa)	Equilibrium Time
Direct suction measurement	Matric suction	axis-transition technique	0-1500	hours
		tensiometer		hours
		suction probe		minutes
Indirect suction measurement	Matric suction	time domain reflectometry	0-1500	hours
		electrical conductivity sensor	50-1500	6-50 hours
		thermal conductivity sensor	0-1500	hours-days
	Osmotic suction	squeezing technique	0-1500	days
	Total suction	psychrometer technique	100-10000	1 h
		relative humidity sensor	100-8000	hours-days
		chilled-mirror hygrometer	150-30000	10 minutes

The net water exchange in the gas phase continues until the relative humidity in the headspace of the system reaches equilibrium. Due to the water retention properties of the soil, the sample hydrates during this water exchange and the water content increases and after a while the water exchange between the soil and the solution is terminated. Equilibrium in a solution is achieved when the sample is periodically weighed and a change of less than a 0.01 g weight change is observed within 7 days (Gao, 2017). The equilibrium is considered to be equal to the concentration in the water content of the soil and the suction value of the soil. The water retention curve (WRC) is obtained by repeating the afore-mentioned events with different salt or acid solutions (or solutions of the same salt prepared at different molar concentrations) that have different suction values.

The main disadvantage of VET is that the equilibrium periods are too long. Tang et al. (1998) stated that the required equilibrium time for a fine-grained soil is between 30-50 days. The soil suction value is defined in Fredlund & Rahardjo, (1993) by the following equation:

$$\psi = \frac{-RT}{Mw\left(\frac{1}{\rho w}\right)} \ln(RH) \tag{2.5}$$

Where R is the universal gas constant (8.31432 J/molK), T is the absolute temperature measured in K, M_w is the molecular weight of water (18.016 kg/kmol), ρ_w is the unit volume weight of water (kg/m^3) as a function of temperature. RH is the measured relative humidity (partial pressure of pore-water vapor divided by the saturation pressure of water vapor over a flat surface of pure water at the same temperature).

Villar & Lloret, (2004) studied the soil-water characteristic curve of compacted FEBEX bentonite under high temperatures. Compacted bentonites at 14% water content were placed in desiccators. Sulfuric acid solutions were used to control relative humidity and vacuum was applied inside the desiccator to accelerate water exchange. Nevertheless, they stated that the equilibrium duration of the experiments was 2 to 3 months. These experiments were conducted on confined and unconfined specimens. For the confined case, the specimens were kept in a non-deformable cell, thus

preventing swelling of the specimen. Confined specimens were prepared at a dry density of 1.65 g/cm^3 and the experiments were carried out at temperatures of 20, 40 and 60 °C. For unconfined specimens, the dry density value ranged between 1.5-1.7 g/cm^3 and experiments were carried out at temperatures of 20, 60 and 80 °C. The wetting followed by drying cycles were performed for both confined and unconfined specimens. Figure 2.11 shows the soil water characteristic curve of the confined sample. A hysteretic behavior is observed in the wetting/drying path at all temperatures. It was also found that the suction value decreased with increasing temperature at the same water content value. The same result is valid for unconfined specimens (Figure 2.12). However, the change for unconfined specimens was not as significant as for confined specimens. Between 60 and 80 °C, there was not much difference in the retention capacity of the unconfined sample. The results showed that the effect of temperature was higher at low suction value, the retention capacity of unconfined samples was higher than confined samples and the suction value increased as the dry density increased.

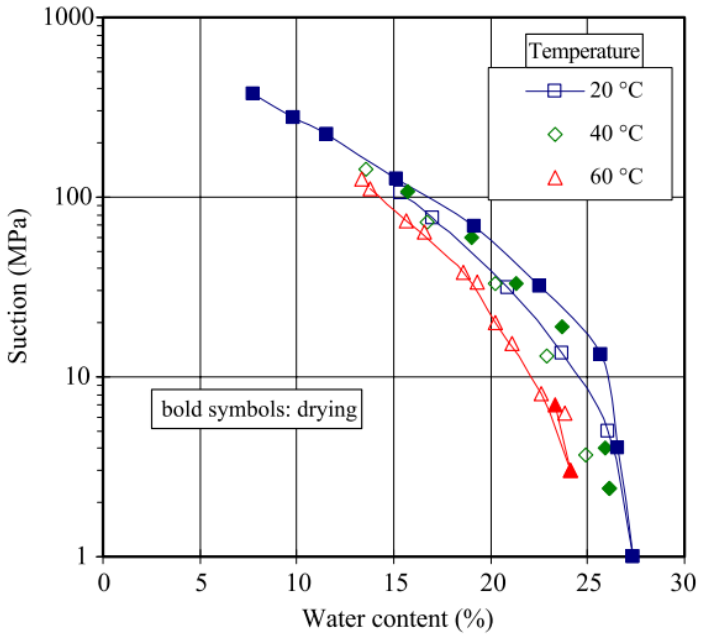

Figure 2.11 Soil water characteristic curve at confined samples and different temperatures for bentonite compacted at dry density 1.65 g/cm^3 (Villar & Lloret, 2004)

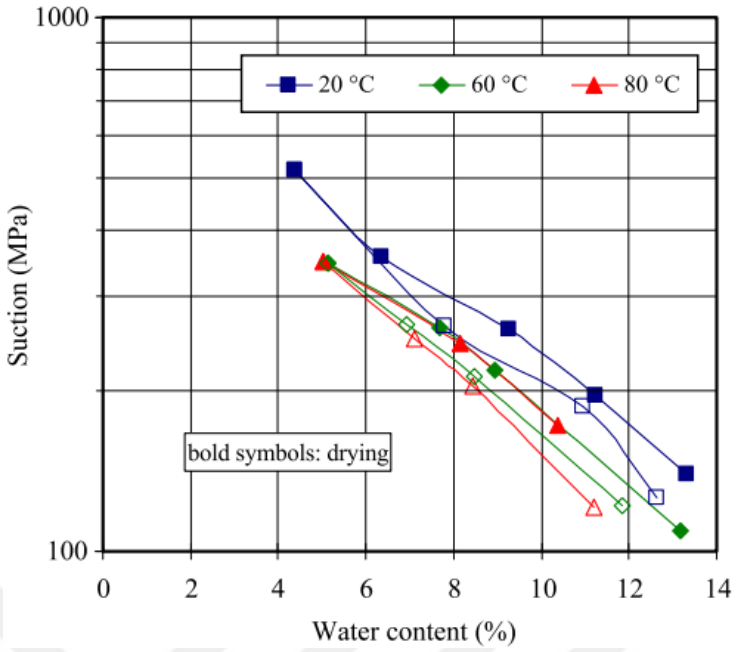

Figure 2.12 Soil water characteristic curve at unconfined samples and different temperatures for bentonite compacted at dry density 1.65 g/cm^3 (Villar & Lloret, 2004)

Tang & Cui (2005) investigated the water retention capacity of MX-80 bentonite at temperatures of 20, 40, 60 and 80 °C. They used saturated salt solutions for relative humidity control and performed temperature dependent relative humidity calibration of salt solutions. The relative humidity values of the solutions decreased as the temperature increased meaning the suction increased. These results were compared with previous studies and showed that the results of Scheineder (1960) can be directly used (Figure 2.13). The specimens were compacted at 8.5% water content at a dry density of 1.65 g/cm^3. At 20 °C, the initial suction value of the specimens was close to 145 MPa, while the initial suction value of the specimens at 80 °C was 67 MPa. The suction-water content plot of the samples at 20, 40, 60 and 80 °C was determined by regression analysis and given in Figure 2.14. It can be seen from the figure that the curve shifts downwards when the temperature increases. In other words, increasing temperature decreased the water retention capacity of the bentonite.

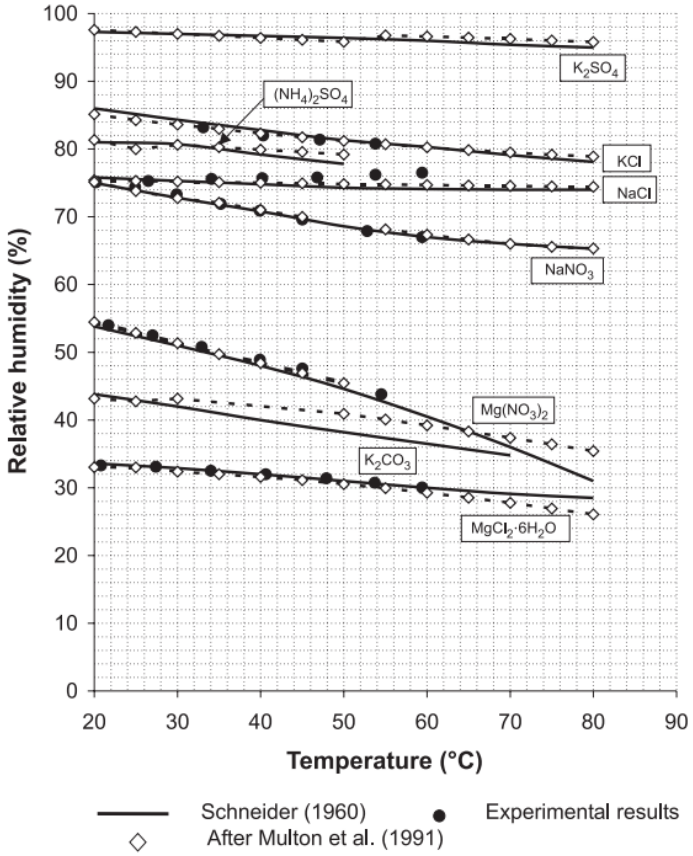

Figure 2.13 Variation of RH with temperature for different saturated salt solutions (Tang & Cui, 2005)

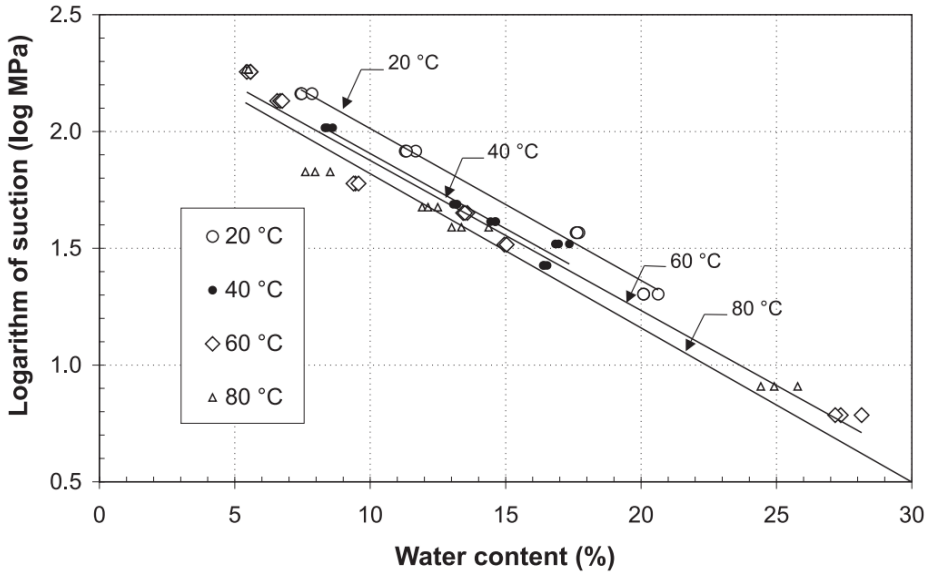

Figure 2.14 Suction-water content plot with regression analysis for different temperatures (Tang & Cui, 2005)

Ye et al. (2009) studied the suction properties of GMZ bentonite by vapor equilibrium technique. The experiments were performed at 20, 40 and 80 °C in confined and unconfined conditions for compacted bentonites with a dry density of 1.7 g/cm^3 and a water content of 10.65%. When applying the vapor equilibrium technique, salt solution was used and an air pump was used to shorten the time (Figure 2.15).

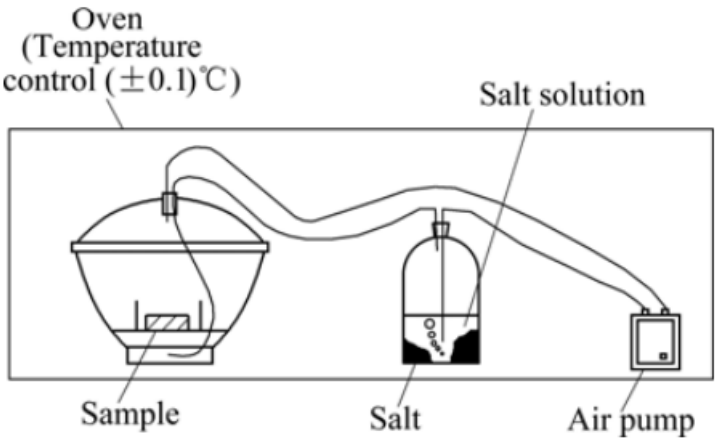

Figure 2.15 Schematic view of Vapor equilibrium technique (Ye et al., 2009)

The soil-water characteristic curve (SWCC) obtained from the results is given in Figure 2.16. According to the results, the water retention capacity decreases with increasing temperature in both confined and unconfined conditions. No effect of confining conditions was observed at high suction values at different temperatures. However, at low suction values, the effect of temperature decreased the water retention capacity in confined condition compared to unconfined condition. Wetting/drying curves and hysteric behavior in unconfined condition at 20 and 40 °C temperatures are as shown in Figure 2.17. As can be seen from the figure, the hysteresis loop shrunk at high temperature. This means that the hysteric behavior decreases with increasing temperature.

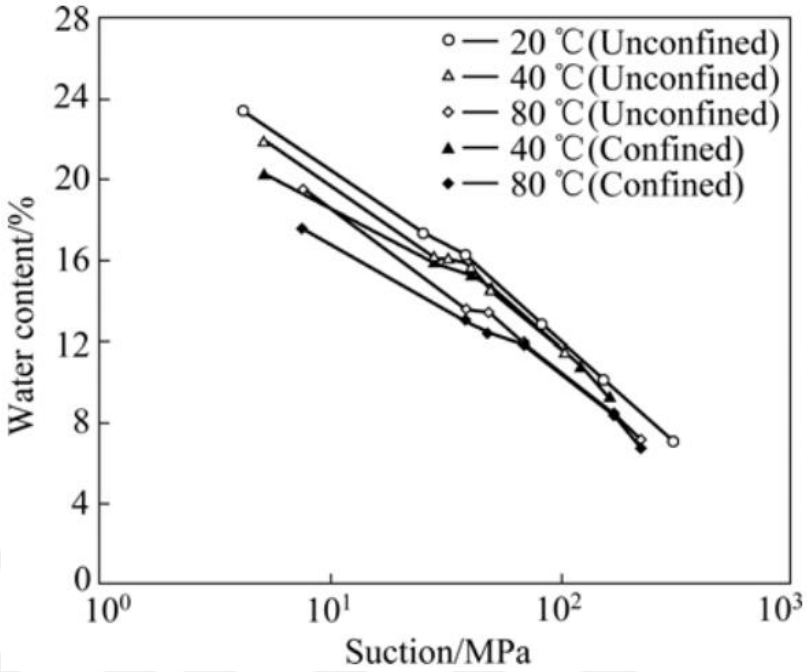

Figure 2.16 Comparision of SWCCs of highly compacted GMZ bentonite with different constraint conditions and temperature (Ye et al., 2009)

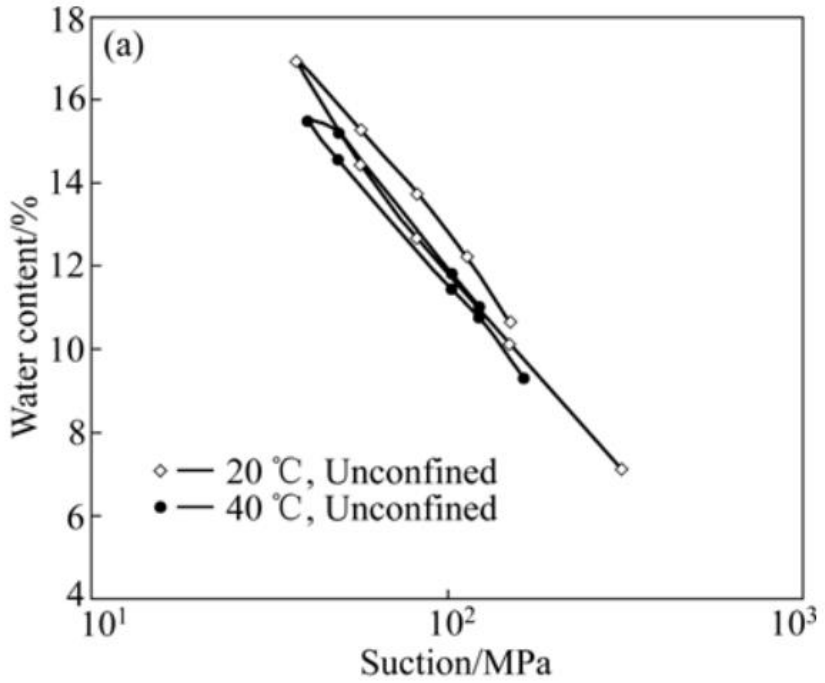

Figure 2.17 Wetting/drying and hysteretic behavior of unconfined GMZ bentonite with two different temperatures (Ye et al., 2009)

Water retention capacity depends on initial water content, dry density and specific surface area of the soil. Suction increases as dry density and specific surface area increase and as initial water content decreases. SWCCs shifts downwards as temperature increases, which means a slight decrease in suction as temperature increases. It can be said that the temperature effect at high suctions is related to the change in clay fabric and intra-aggregate water. At low suctions the temperature effect can be explained by capillary effect and surface tension.

2.4 High Temperature Effects on Hydraulic Conductivity of Soils

Hydraulic conductivity is a property of soil that plays a key role in the movement of water through the soil. It refers to the ability of soil to conduct water and is a key parameter in understanding the hydraulic behavior of soils. Hydraulic conductivity is the most important parameter for bentonite for the safety of HLW repositories. However, temperature increase has a negative effect on the hydraulic conductivity behavior of bentonite, just as it has a negative effect on other engineering behavior. The literature is in agreement that higher temperatures increase the hydraulic conductivity of compacted bentonite (Cho et al., 1999; Delage et al., 2000; Villar & Lloret, 2004). This increase in hydraulic conductivity is mostly related to increase in water viscosity (Cho et al., 1999).

The hydraulic conductivity of compacted bentonite is generally influenced by factors such as mineral composition, density, fluid properties and temperature (Ye et al., 2013). Pusch et al. (1990) stated that the microstructure of soils has a strong effect on the saturated hydraulic conductivity of compacted bentonite due to variations in pore size between clay particles during infiltration. Dixon et al. (1999) found that hydraulic conductivity increased with decreased dry density. Lee & Shackelford, (2005) reported that changing the percentage of sodium montmorillonite in bentonite from 86% to 77% and the cation exchange capacity (CEC) from 93 to 64 meq/100 g increased the permeability by three times. Mishra et al. (2011) found strong empirical correlations between hydraulic conductivity and liquid limit, free swell index and exchangeable sodium percentage in a study with fifteen different bentonites. The temperature effect changes the density and viscosity of the water and thus the hydraulic

conductivity of the soil. The calculation of the hydraulic conductivity found experimentally in the literature with the formulation is as follows:

$$k_s=k_{in}\rho_w g/\eta(T) \quad (2.6)$$

Where k_s is saturated hydraulic conductivity k_{in} intrinsic hydraulic conductivity that found in the tests which is only related to porosity and pore size distribution, ρ_w water density, g acceleration of gravity and $\eta(T)$ water viscosity as a function of temperature. Cho et al. (1999) investigated the saturated hydraulic conductivity of Ca-bentonite at three different dry densities (1.4, 1.6 and 1.8 g/cm^3) and four different temperatures (20, 40, 60 and 80 °C). The hydraulic conductivity value of bentonite decreased as the dry density increased. Also, as the temperature increased, the hydraulic conductivity of bentonite increased (Figure 2.18). It was stated that the hydraulic conductivity measured at 80 °C was three times higher than the hydraulic conductivity measured at 20 °C. They reported that the hydraulic conductivity predicted by the equation given in the above formula and the measured hydraulic conductivity were consistent.

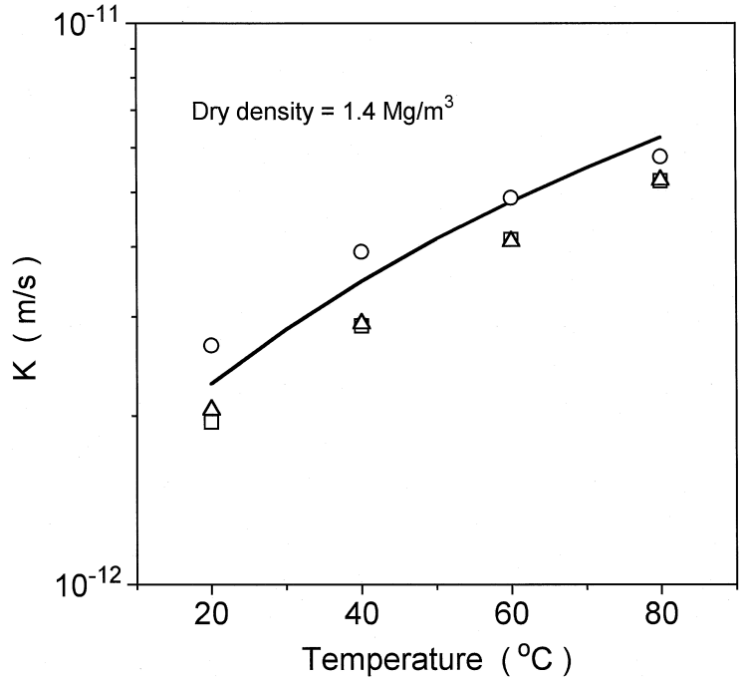

Figure 2.18 Hydraulic conductivities of bentonites at 1.4 g/cm^3 dry density and at different temperatures (Cho et al., 1999)

Villar & Lloret, (2004) determined the hydraulic conductivity of FEBEX bentonite from room temperature to 80 °C in an oedometer cell. Using different hydraulic gradients in the experiments, they concluded that hydraulic gradient has no effect on hydraulic conductivity. They stated that the hydraulic conductivity increased logarithmically as the temperature increased, and they attributed this to the decrease in the kinematic viscosity of water. The hydraulic conductivities determined from the experiment according to Darcy's law and the predicted values found by taking into account the kinematic viscosity of water was compared and the results were found to be consistent (Figure 2.19).

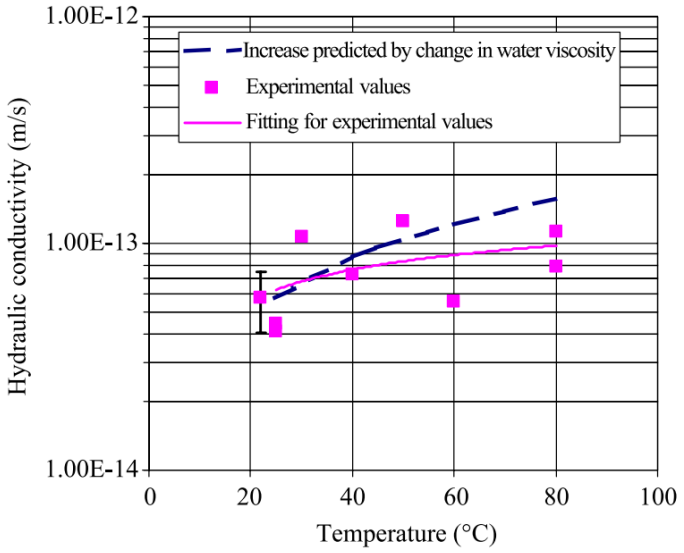

Figure 2.19 Comparison of the experimentally determined and estimated hydraulic conductivity values for FEBEX bentonite at different temperatures (Villar & Lloret, 2004)

Abuel-Naga et al. (2006) obtained the change in hydraulic conductivity of clay at elevated temperatures (25-90 °C) in a triaxial test apparatus in a study with soft Bangkok clay. A strong agreement was observed between the calculated and measured values. Hydraulic conductivity tended to increase with increasing temperature. The hydraulic conductivity at 90 °C was found to be approximately 3 times higher than the hydraulic conductivity at 25 °C (Figure 2.20).

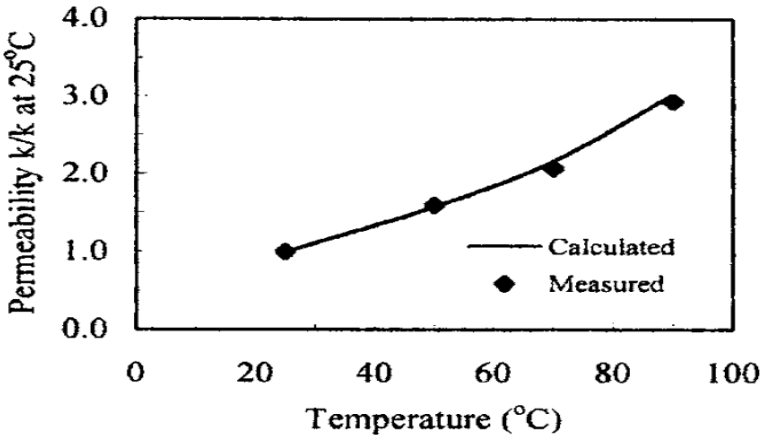

Figure 2.20 Comparison between measured and calculated hydraulic conductivity due to temperature increase (Abuel-Naga et al., 2006)

Ye et al. (2013) performed swelling pressure and saturated hydraulic conductivity tests of GMZ bentonite at 1.7 g/cm^3 dry density and elevated temperatures in a specially designed test apparatus. When the temperature increased from 20 °C to 40 °C, the swelling pressure value increased from 3.02 MPa to 3.41 MPa. They attributed this result to the increase in the repulsion of the double layers of the clays as the temperature increases in the Diffuse Double Layer (DDL) theory. They also observed an increase in the hydraulic conductivity value as the temperature increased in the hydraulic conductivity determination performed up to 60 °C. The measured and calculated hydraulic conductivity values show consistency in the study (Figure 2.21).

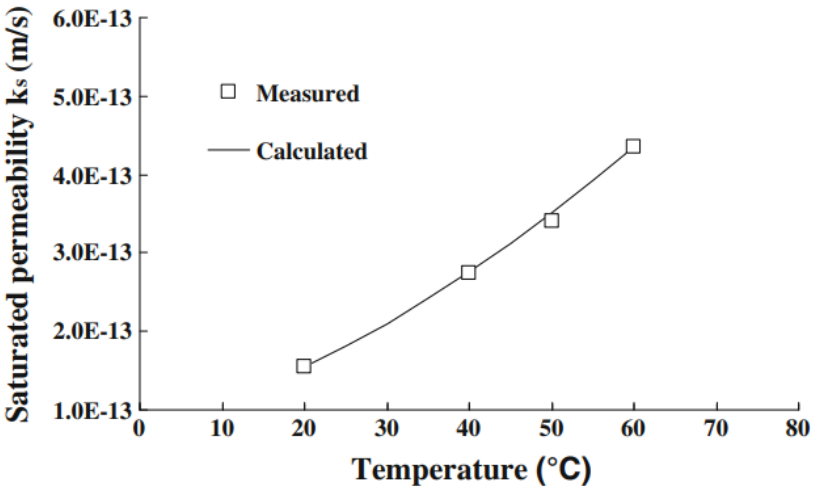

Figure 2.21 Comparison between calculated and measured saturated conductivity of compacted GMZ01 bentonite at various temperatures (Ye et al., 2013)

2.5 Glass Fiber

Fibers are extremely thin, thread-like forms defined by high length to width ratios. These materials play a key role in many industries, applications and composites due to their outstanding strength, flexibility and versatility. These materials are classified into two main categories: natural fibers derived from plants (e.g. bamboo, cotton, cane, flax) or animals (e.g. wool, silk) and man-made synthetic fibers made from different materials (e.g. basalt, carbon, polypropylene, glass). Each type of fiber has unique features that make them suitable for different applications. Natural fibers generally offer breathability and biodegradability, while synthetic fibers are superior in strength, stiffness and durability.

Today, the production of glass fiber starts with the necessary raw materials (sand for silica, clay for alumina, colemanite for boron oxide and limestone or calcite for calcium oxide) being mixed and fed into a furnace at 1600 °C. At this temperature, the raw materials melting in the furnace become glass and form the glass melt. At this stage, the glass melt is directed into channels for flowing. The glass melt, which flows freely through the barrel holes, is mechanically wound on a mandrel rotating at high speed to produce glass fibers of constant diameter.

Many researchers have used glass fiber to reinforce the engineering properties of soils (Maher & Ho, 1994; Consoli et al., 2004; Bouricha et al., 2017; Mukherjee & Mishra, 2021; Valipour et al., 2021) because of glass fiber's high tensile strength, high elastic modulus, environmentally friendly features, etc. Studies have shown that glass fiber addition increased the unconfined compressive strength (Maher & Ho, 1994), shear strength (Bouaricha et al., 2017), hydraulic conductivity (Mukherjee & Mishra, 2021), while decreasing the compression index (Jadda et al., 2021), volumetric strain (Ruan et al., 2020) and desiccation shrinkage (Mukherjee & Mishra 2019) of soils.

CHAPTER THREE
MATERIAL CHARACTERIZATION AND EXPERIMENTAL METHODS

3.1 Material Characterization

In this study, bentonite clay and glass fiber were used as materials. It is a commercial bentonite and was obtained from Unye Madencilik. The bentonite used in the study is given in Figure 3.1. As can be seen from the figure, bentonite is grey in color and in powder form. The specific gravity of bentonite is 2.60, the natural water content is between 6-8% and the bentonite sample passes through No.200 sieve. Various experiments were conducted in the laboratory for the characterization of bentonite. These include hydrometer, consistency limits, pH measurement, X-ray diffraction (XRD), methylene blue index (MBI) and cation exchange capacity (CEC) tests. The physico-chemical properties of bentonite were summarized in Table 3.1.

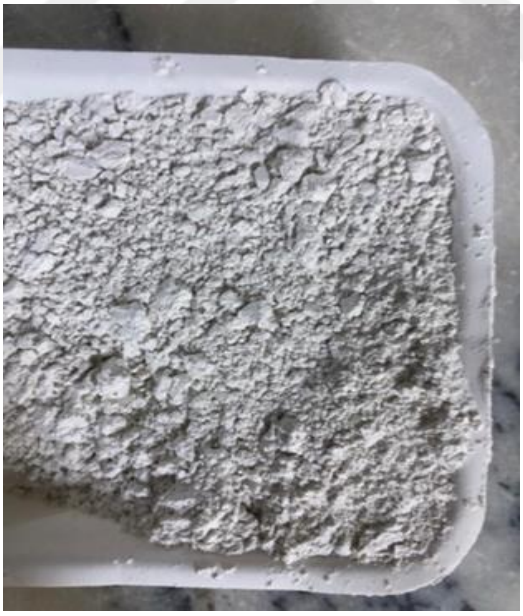

Figure 3.1 Bentonite used in the study (Personal archive, 2022)

The grain size distribution of the bentonite was obtained by hydrometer analysis according to ASTM D422-63 (2007). The grain size distribution curve of bentonite is given in Figure 3.2. According to the results, the clay content of bentonite was found to be 82%.

Table 3.1. The physico-chemical properties of the bentonite

Property	Bentonite
Specific gravity (G_s)	2.6
Passing sieve	- No 200
Natural water content (%)	7
pH	9.13
Liquid limit (%)	270
Plastic limit (%)	63
Clay fraction, <2 μm (%)	82
Cation exchange capacity (meq/100g)	-
Specific surface area (m^2/g)	611

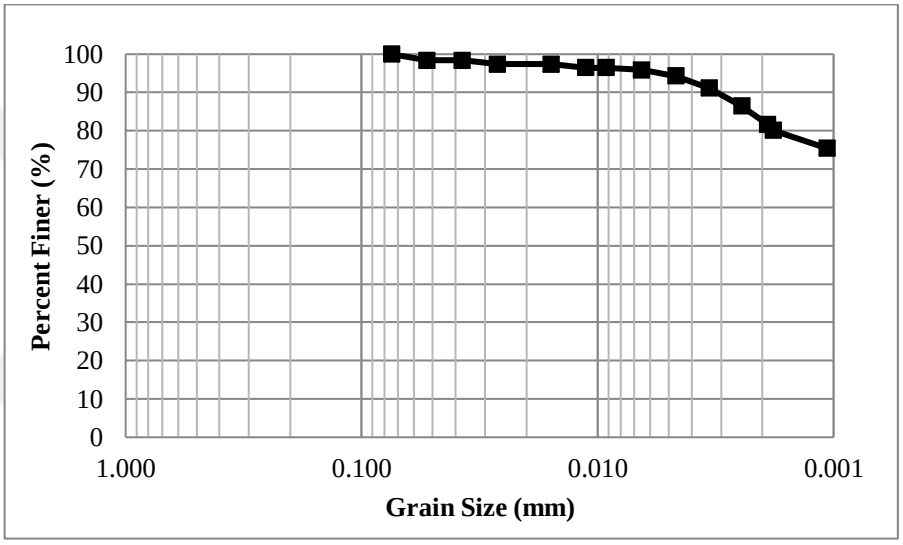

Figure 3.2 Grain size distribution curve of bentonite

Liquid and plastic limit tests were conducted according to ASTM D4318-17e1 (2017). Casagrande and Fall Cone tests were conducted to determine the liquid limit of bentonite and bentonite-glass fiber mixtures. The results are presented in Table 3.2.

Table 3.2 Liquid and plastic limit test results, LL: Liquid limit (%), PL: Plastic limit (%), GF: Glass fiber

Sample	LL (Casagrande Method)	LL (Fall cone method)	PL
Bentonite	270	265	63
0.5% GF	267.7	263.9	59.1
1% GF	263.6	262.3	56.2

The pH measurement of bentonite and glass fiber samples were performed according to ASTM D4972-19 (2019). A 1:1 deionized water-material mixture was prepared for glass fiber and a 1:5 deionized water-material mixture was prepared for bentonite. After approximately one hour of mixing, pH measurements of the materials were taken. According to the results, the pH value of bentonite was found to be 9.13 and the pH value of glass fiber was found to be 7.18. The pH meter test device and the shaker are given in Figure 3.3.

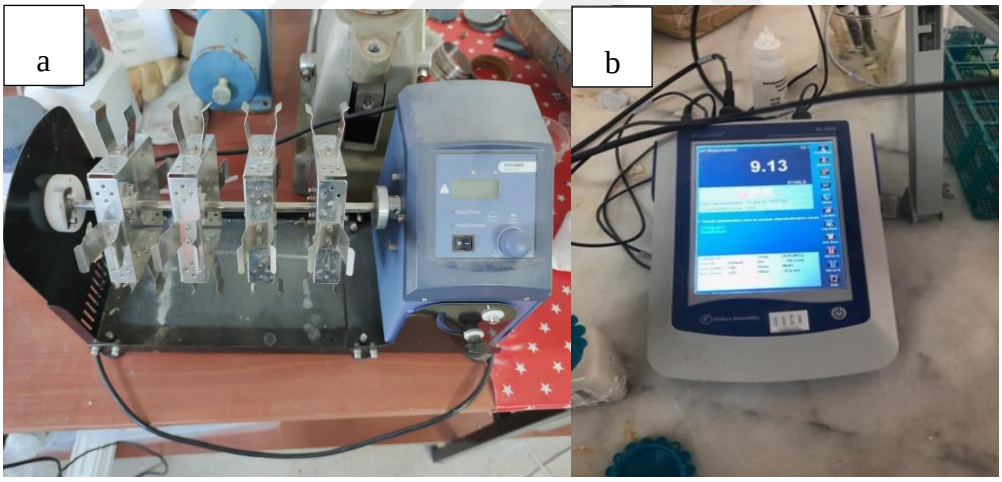

Figure 3.3 The pH measurements a) The shaker b) pH meter (Personal archive, 2023)

X-ray Diffraction (XRD) analyses of bentonite were performed using Thermo Scientific ARL X'TRA device. XRD analyzes were performed with focusing geometry between 0° and 89°, scanning speed at 0.1° 2θ/s and radiation at 60 kV, on Thermo Scientific ARL X'TRA X-Ray diffraction equipment (Figure 3.4). In addition, XRD analyzes of bentonite were conducted both at room temperature and on samples exposed to 80 °C to determine the effect of high temperature on its mineralogy. For

the analysis carried out at room temperature, bentonite was prepared in its original form (as powder), while for the analysis of the material exposed to 80 °C, the sample was placed in the ring in powder form, kept in the thermal pool at 80 °C with the help of a clamped mold for 48 hours, then dried in the oven and broken with the help of a pestle. Then the sample was sieved through a No.200 sieve.

Figure 3.4 Thermo Scientific ARL X'TRA device (Personal archive, 2023)

When the XRD analyses were examined, montmorillonite, quartz, calcite and albite minerals were found in bentonite at room temperature (Figure 3.5a). When the temperature was increased to 80 °C, changes occurred in the structure of bentonite. While the montmorillonite ratio in bentonite decreased, calcite mineral was not observed at high temperatures. (Figure 3.5b).

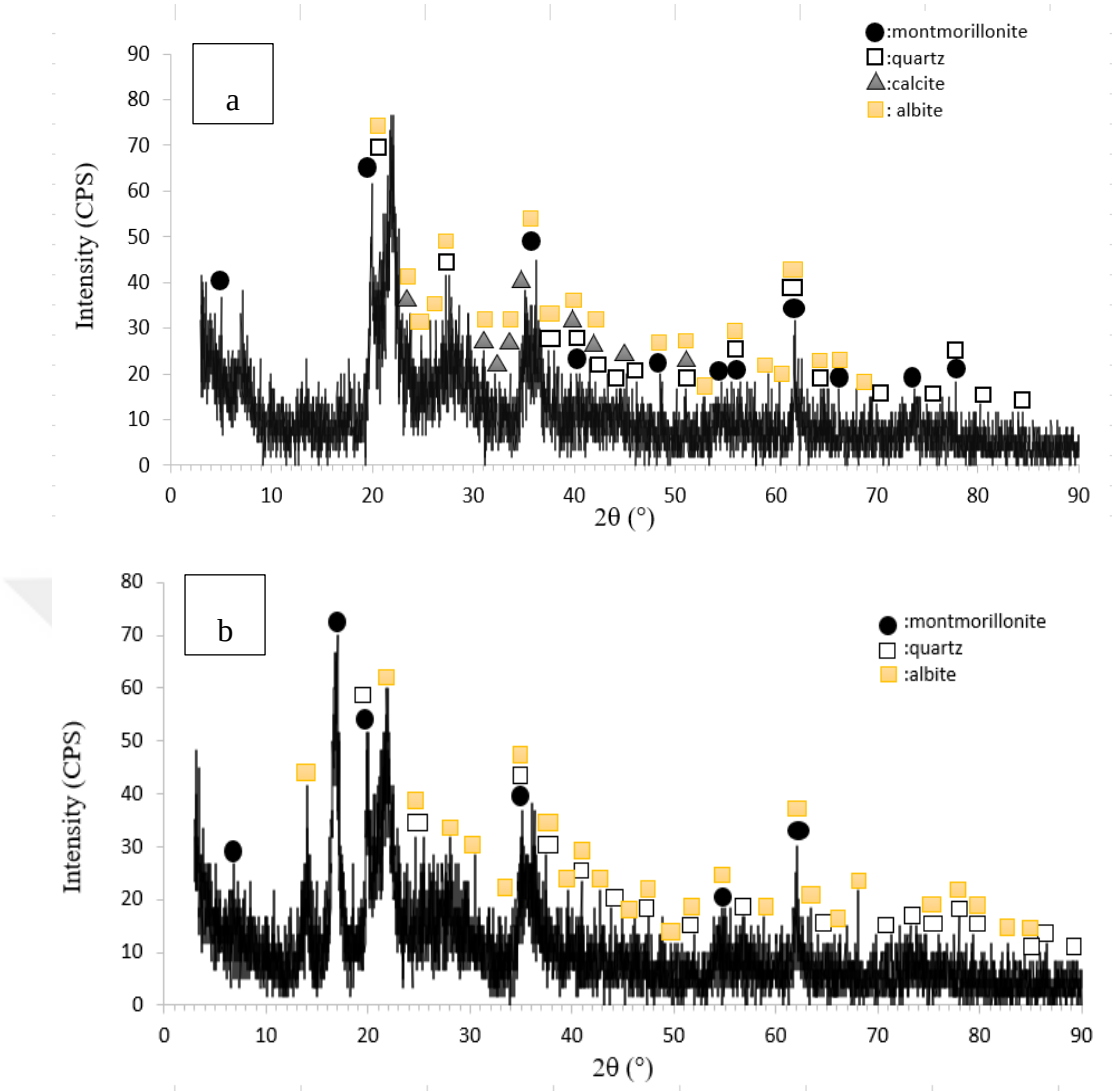

Figure 3.5 XRD analysis results of bentonite a) at room temperature b) at 80 °C

The specific surface area of bentonite was determined by the methylene blue index (MBI) test. Methylene blue solution was prepared 1:200 portion by mixing dry powdered methylene blue-Deionized water. 5 g oven dried bentonite was mixed with 30 ml deionized water and initial 200 ml methylene blue solution. After mixing, a drop taken with the help of a glass rod is placed on a Fisher P5 filter paper and its image is observed. After the first mixing, 10 ml each of methylene blue solution is mixed for 20 minutes and after each mixing, a drop is placed on the filter paper and the image is observed. This procedure ends if the unabsorbed methylene blue creates a permanent blue halo around the soil aggregate dot on the filter paper. It means that the methylene blue has replaced the cations in the double layer and filled the entire

surface (Santamarina et al., 2002). The specific surface area is calculated from the amount of methylene blue needed to achieve the endpoint from the following formula:

$$SSA = \frac{1}{319.87}\frac{1}{200}(0.5N)A_v A_{MB}\frac{1}{5} \quad (3.1)$$

Where N is the number of methylene blue increments being added to the soil suspension solution, A_v is the Avagadro number ($6.02x10^{23}$/mol) and A_{MB} is the area enclosed by a methylene blue molecule (typically assumed to be 130 $Å^2$) (Santamarina et al., 2002). The specific surface area of bentonite in this study was found to be 611 m^2/g. The process of mixing bentonite with methylene blue solution and the light blue halo observed on the filter paper is shown in Figure 3.6.

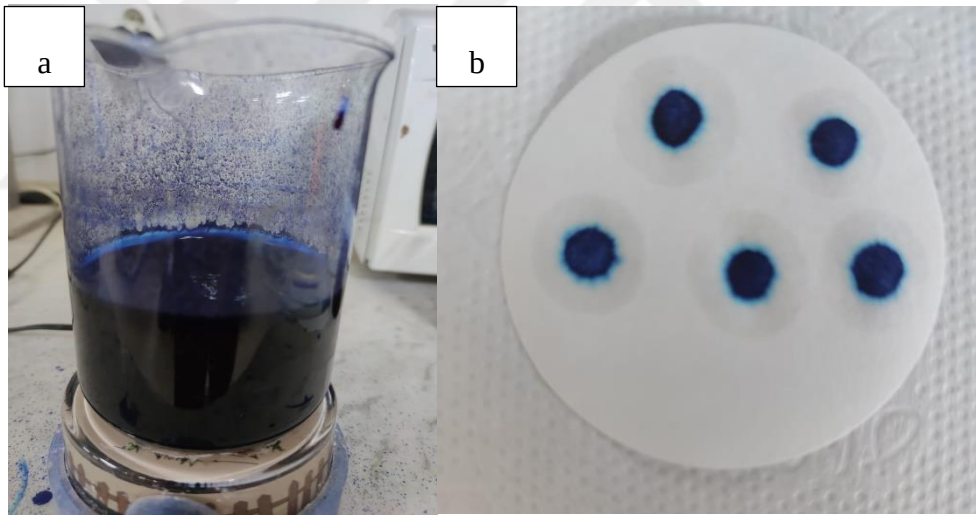

Figure 3.6 a) The mixing process of bentonite with methylene blue solution b) The light blue halo observed after the experiment (Personal archive, 2023)

Fine-grained clayey soils have a negatively charged surface on the mineral surface and this surface is in equilibrium with bound cations. These bound cations can exchange with other cations and are called soluble cations. Cation exchange capacity (CEC) is the measure of the negative charge on the mineral surface. In bentonite, CEC is usually characterized by sodium (Na), calcium (Ca) and magnesium (Mg). Higher CEC implies higher surface activity and therefore higher water adsorption potential.

Clays with greater specific surface area are characterized by higher water adsorption. Table 3.3 shows the different CEC values for different types of clay minerals.

Table 3.3 Cation exchange capacity by clay minerals (Lambe & Whitman, 1969)

Clay Mineral	CEC (meq/100g)
Kaolinite	3.0-15.0
Illite	10.0-40.0
Montmorillonite	80.0-150.0

Cation exchange capacity measurement of bentonite was performed according to ASTM D7503-18 (2018). 10 g of air-dried bentonite and 40 mL of ammonium acetate (NH_4OAc) at a concentration of 1 M were mixed in a plastic bottle. The suspension was stirred in an end over shaker at 30 rpm for 5 minutes. The suspension was then allowed to stand for 24 hours and again stirred at 30 rpm for another 15 minutes. Sample was poured onto Whatman No.42 (2.5 µm) filter paper on a Buchner funnel. Bentonite was first rinsed four times with 30 ml NH_4OAc and three times with 40 ml isopropanol and a vacuum pressure of <10 kPa was introduced during filtration. As the last wash, it was washed four times with KCl at 1 M concentration and 50 ml each, then the collected KCl sediment was analyzed for cation exchange capacity by inductively coupled plasma optical emission spectrophotometer. (Figure 3.7).

The results of the experiments used for the characterization of bentonite described above are sum up in Table 3.5. This table also compares the characteristics of the bentonite used in the study with other bentonites used in nuclear HLW repositories.

Figure 3.7 Inductively coupled plasma optical emission spectrophotometer device (Personal archive, 2023)

Table 3.4 Comparison of physico-chemical properties of bentonite used in the study and other bentonites used in nuclear HLW repositories ([a] Tripathy & Schanz, (2007), [b] Marcial et al., (2002), [c] Tang & Cui, (2005), [d]Villar, (2001), [e] Ye et al., (2014))

Property	Kunigel(a)	FoCa(b)	MX80(c)	FEBEX(d)	GMZ(e)	Bentonite used in the study
Particle <2mm	64.5	-	60	68	60	82
CEC (meq/100 g)	73.2	54	82.3	102	77.3	-
Base cations exchange	Na	Ca	Na-Ca	Ca-Mg	Na-Ca	Na-Ca
Specific Gravity G_s	2.79	2.67	2.76	2.7	2.66	2.6
Liquid limit (%)	474	112	519	102	313	270
Plastic limit (%)	27	50	35	53	38	63
Montmorillonite content (%)	48	80	80	92.3	75.4	-
Activity	6.93	-	8.01	0.81	4.6	2.6
Specific surface area S_s (m^2/g)	687	300	522	725	570	611

The glass fiber used in the thesis was purchased from Dost Kimya company. The technical properties of glass fiber and the sample photo is given in Table 3.6 and Figure 3.8.

Figure 3.8 The photograph of the glass fiber used in the study (Personal archive, 2023)

Table 3.5 Technical properties of glass fiber (Dost Kimya, 2023)

Property	Glass Fiber
Specific Gravity	2.6
Tensile Strength (MPa)	3400
Modulus of Elasticity (GPa)	77
Application Temperature Limits (°C)	-710
Melting Temperature (°C)	1120
pH	7.18
Diameter (µ)	13
Length (mm)	3
Water Absorption Capacity	-

3.2 Experimental Methods

3.2.1 Consolidation Tests

Consolidation tests were performed according to ASTM D2435-11 (2011). Test samples were prepared with a water content of 1.5 times the liquid limit value obtained from the Casagrande experiment. Tap water was used to prepare the mixtures. Mixing of the samples was performed with the help of a mixer (Figure 3.9). The prepared mixtures were kept 24 h in a closed plastic bag for uniform moisture distribution and then placed in a specially manufactured sample preparation apparatus (Figure 3.10).

The purpose of the sample preparation apparatus was to load the seating pressure on the sample and to prepare identical samples.

Figure 3.9 The process of mixing the sample with a mixer (Personal archive, 2023)

The sample preparation apparatus consists of 3 parts. These are the bottom plate, the upper load plate and the part where the sample will be placed. The bottom plate is fixed to the table with screws and consists of 4 steel legs. These legs are connected to the upper load plate and ensure that the load is transferred to the specimen without any inclination and friction. The upper load plate consists of a steel plate, bearing cavities for the steel legs to pass through and a head to transfer the load on top of the specimen.

The other part where the sample will be located consists of a steel drainage container. A water outlet pipe was manufactured at the bottom part of the drainage container to drain the water. Perforated drainage plate, porous stone and filter paper were placed in the steel drainage container, respectively (Figure 3.11). There was a stainless-steel consolidation ring was used in the consolidation tests and there were filter papers on the top and bottom of the sample. The diameters of the steel drainage container, consolidation ring and acryclic glass cell were 7.0 cm. Height of steel

drainage container, consolidation ring and acrylic glass cell was 5 cm, 1.9 cm and 6 cm respectively.

Figure 3.10 Top view of the sample preparation apparatus fixed on the table (Personal archive, 2023)

Samples were placed above the ring height plus up to a height of 2 cm. Tap water was administered from above in a controlled manner to ensure that the water content of the samples did not change throughout the process. The samples were left to be consolidate under seating pressure for 14 days. The seating pressure was 12.25 kPa. The samples removed from the apparatus after 14 days were used by trimming the part outside the consolidation ring.

Figure 3.11 a) Steel drainage container b) Perforated drainage plate c) Porous stone d) Filter paper e) Consolidation ring f) Acryclic cell (Personal archive, 2023)

Consolidation experiments were carried out at room temperature and 80 ℃. Modifications were made to the oedometer cell to carry out the experiments at 80 ℃. The heat ring and thermostat probe placed inside the oedometer cell to maintain constant 80 ℃ temperature inside the cell (Figure 3.12). The temperature was increased by 5 ℃ per hour with the help of thermostat to prevent excess pore water formation. In order to prevent the water inside the consolidation cell from decreasing due to evaporation, a membrane was placed on top of the cell and continuous tap water supplement was given from the top through pipes.

Figure 3.12 Consolidation cell and modifications for high temperatures a) Consolidation cells at room temperature b) Consolidation cells at high temperatures (80 °C) c) Thermostat d) Heat ring (Personal archive, 2023)

To understand the long-term behavior of bentonite, experiments were also carried out on samples which were left to cure in a hot water pool for 6 months and 1 year. For curing, two identical hot water pools were manufactured (Figure 3.14a and b). There were four heat rods on the lower edges of these pools (Figure 3.15). Heat rods were connected to Arduino system thermostats and serve to measure and change the temperature. To prevent the formation of excessive pore water pressure within the samples, the samples, closed with a clamped mold, were kept in a pool, where it will increase by 1 °C per hour, before being released into the other pool at a constant

temperature of 80 °C. The samples prepared in the apparatus in the consolidation ring were placed in the manufactured stainless steel clamped mold with porous stones on top and bottom (Figure 3.13). The samples were taken out of the pool after the curing periods were also subjected to consolidation tests. Thanks to the clamped mold, the swelling of bentonite under water was prevented.

Figure 3.13 The stainless-steel clamped mold (Personal archive, 2023)

Figure 3.14 Hot water pools a) external view b) internal view (Personal archive, 2023)

Figure 3.15 Mounted heat rods to the hot water pools (Personal archive, 2023)

In the consolidation test, the samples were loaded at 24.5, 49, 98, 196, 392 and 784 kPa load levels, respectively. At each load stage, dial gauges with an accuracy of 0.002 mm were used to measure the deformations and when the primary consolidation settlement at one load stage was completed, the next load stage was started. After loading stages were completed, the unloading stages was started by unloading from 784 kPa to 196 kPa and then 49 kPa, respectively. In the consolidation tests, it took approximately 3 months to complete all load stages.

3.2.2 Free Swell Index (FSI) Tests

Free Swell Index (FSI) tests were conducted according to ASTM D5890-19 (2019). The tests were carried out to examine the swelling behavior of bentonite under room temperature and high temperature (80 °C). Since this test is not compatible for bentonite mixtures or glass fiber itself, only bentonite was tested. The experimental procedure consisted of adding 2 g of oven-dried bentonite to 90 mL of distilled water in a 100 mL graduated cylinder at 0.1 g intervals and swelling freely. The specimen was left to hydrate and settle for at least ten minutes for all 0.1 g increments. After the final increment had settled, the water volume was increased to 100 mL by rinsing the adhering particles from the sides of the cylinder. After 24 hours of hydration time, the volume at the top of the settled sample was recorded in milliliters. Experiments performed at room temperature are shown in Figure 3.16. A hot water pool was used to conduct the experiments in the presence of 80 °C (Figure 3.17). 100 mL graduated glass cylinders containing the sample were placed in the thermal pool at a constant

temperature of 80 °C. The water level in the cylinders and pool were kept constant throughout the experiment. The top of the cylinder is covered with aluminum foil to prevent water loss due to evaporation inside the cylinder.

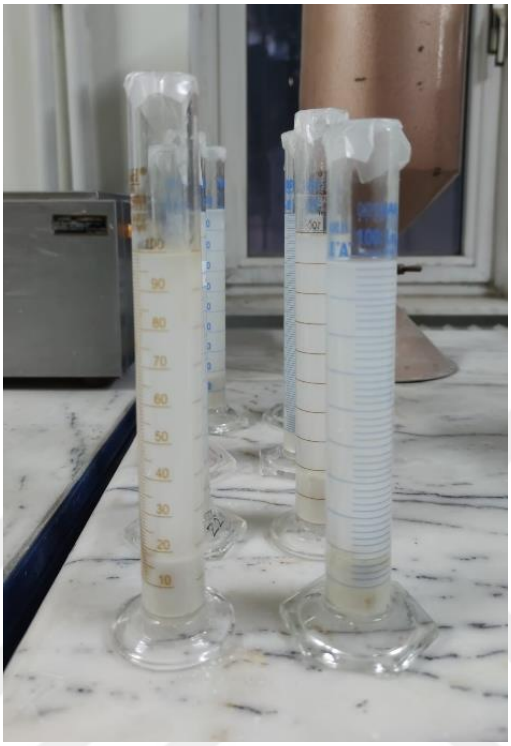

Figure 3.16 FSI tests at room temperature (Personal archive, 2023)

Figure 3.17 FSI tests at 80 °C (Personal archive, 2023)

3.2.3 Suction Tests by Vapor Equilibrium Technique (VET)

Water retention curves (WRCs) and suction values of the compacted and unconfined bentonite samples were carried out according to the Vapor Equilibrium Technique (VET). Compactions of the samples were performed on an unconfined compression test machine (Figure 3.18). A compaction rate of 1.14 mm/min was selected for the compaction process and a load dial with a limit of 5000 kg was used for load control. The samples were mixed and used in their natural state. A 3 mm diameter head, steel collar and rings were fabricated for compaction process (Figure 3.19). The height of the ring was 1.0 cm and the collar was 4.0 cm. Samples were placed inside the ring and the collar above it and the compaction process was started. The compaction pressure required for the specimens was found to be approximately 55 MPa. The dry densities of the samples were 1.4 ±0.01 g/cm^3. The bentonite compacted in the ring was then carefully removed from the ring with a specially manufactured equipment and used as an unconfined sample (Figure 3.20).

Figure 3.18 Unconfined compression test machine (Personal archive, 2023)

Figure 3.19 Sample preparation equipment a) Compression head b) Collar c) Ring (Personal archive, 2023)

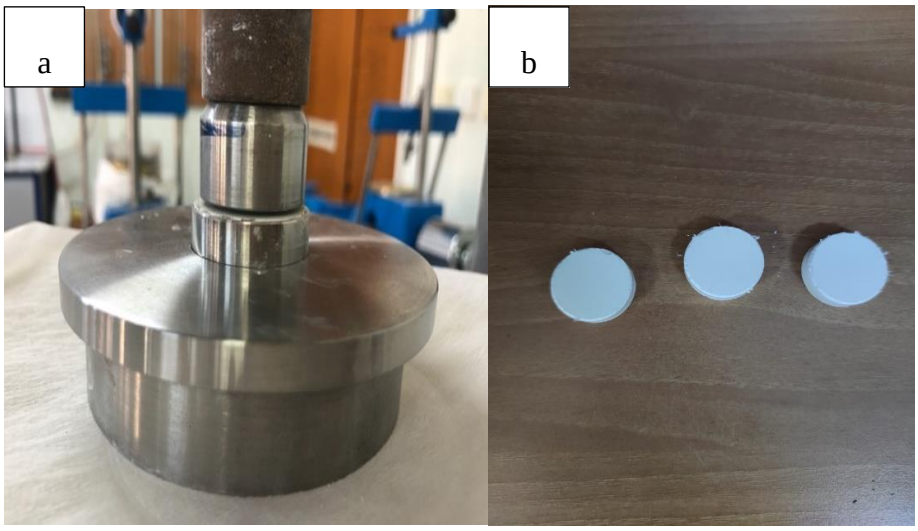

Figure 3.20 Sample preparation process a) Manufactured equipment for removing the sample from the rings b) Unconfined specimens of 3 cm diameter and 1 cm height each (Personal archive, 2023)

In this study, suction experiments were carried out at room temperature and 80 °C using the vapor equilibrium technique (VET). Saturated salt solutions were used to provide the required relative humidity. Salt solutions used in the study were K_2CO_3, $CaNO_3$, $NaNO_2$, NaCl, KCl, $ZnSO_4$ and K_2SO_4, respectively. The chemical components of these salts are given in Table 3.6. As can be seen from the table, the assay value for all salts is >97%. The assay value is an indication of the purity of the salts.

Table 3.6 Chemical components of the salts (Tekkim, 2023)

Percentage (%)	K_2CO_3	$CaNO_3$	$NaNO_2$	NaCl	KCl	$ZnSO_4$	K_2SO_4
Assay	>99.5	>98.0	>99.0	>99.5	>99	>97.0	>97.0
Calcium (Ca)	-	>16.5	-	<0.002	<0.0008	-	-
Magnesium (Mg)	-	-	-	<0.0003	<0.01	-	-
Iron (Fe)	<0.001	-	<0.002	<0.0005	-	<0.2	-
Sulphate (SO_4)	<0.1	-	-	<0.01	<0.01	-	-
Sodium (Na)	<0.5	-	-	-	<0.2	-	-
Chloride (Cl)	<0.02	-	-	-	-	-	<1.0
Aluminum (Al)	<0.1	-	-	-	-	-	-
Chromium (Cr)	<0.0005	-	-	-	-	-	-
Calcium oxide (CaO)	-	>23.0	-	-	-	-	-
Sodium Chloride (NaCl)	-	-	<0.005		-	-	-
Sodium Sulphate (Na_2SO_4)	-	-	<0.05	-	-	-	-
Sodium Nitrate ($NaNO_3$)	-	-	<1.5	-	-	-	-
Arsenic (As)	-	-	-	-	-	<0.0005	-
Zinc (Zn)	-	-	-	-	-	>20.0	-
Lead (Pb)	-	-	-	-	-	<0.0001	-
Potassium Oxide (K_2O)	-	-	-	-	-	-	>51.0

The VET method generally uses desiccators as a closed system with a constant mass. However, due to the large volume of the desiccator, it takes a long time to achieve equilibrium between the salt solution and the sample. To shorten this time, small glass jars with a height of 7.8 cm and a diameter of 5.2 cm were used in this study as a closed system with a constant mass. When saturated salt solutions were prepared in jars, salts were placed to a height of 2.0 cm and saturated with deionized water. At the top of the jar the samples were placed in plastic bottle caps and plastic feet were placed under the plastic caps (Figure 3.21a and b). The experimental system was kept in an incubator with constant temperature (25 °C) and constant relative humidity (70%) so that it would not be affected by the relative humidity and temperature changes outside during the experiment (Figure 3.22).

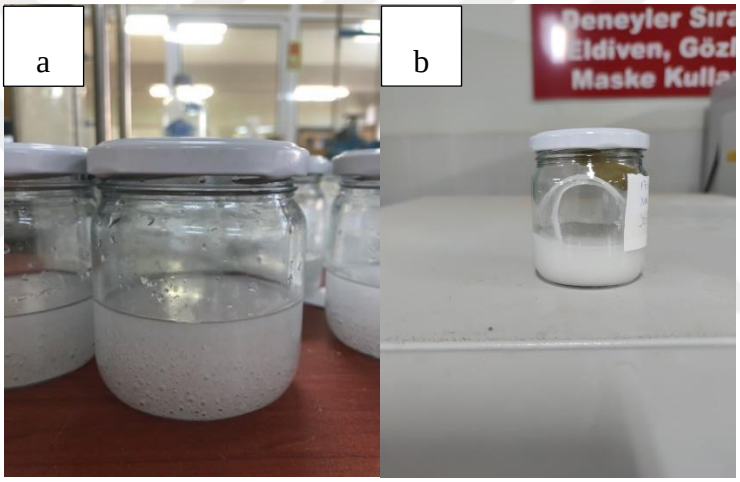

Figure 3.21 a) Preparation of saturated salt solution in jars b) Placing the sample into jars (Personal archive, 2023)

For the 80 °C suction experiments, the samples were prepared in the same way as for the room temperature experiments mentioned above. To maintain a constant 80 °C temperature, an oven in the laboratory was used (Figure 3.23). The jars used in the room temperature experiments could not be used at high temperature because the lid of the jar expanded at different rates compared to the other parts of the jar due to the effect of temperature, so that a closed system could not be obtained in the jar and the salt solutions could escape to the upper part of the jar, where the sample was located, damaging the samples. Therefore, a jar with a glass lid was preferred for the high temperature suction experiment (Figure 3.24).

Figure 3.22 Incubator used in the study a) External view b) Internal view (Personal archive, 2023)

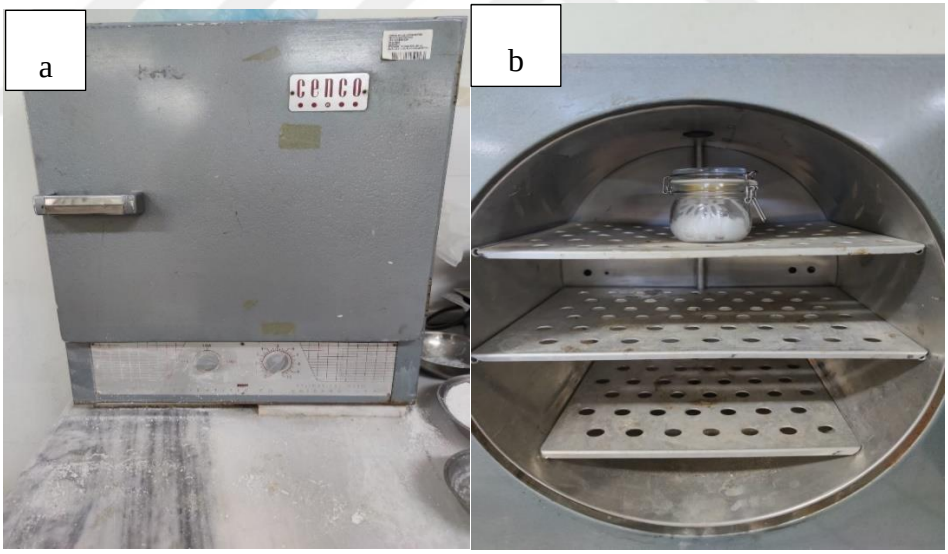

Figure 3.23 The oven used for suction tests a) external view b) internal view (Personal archive, 2023)

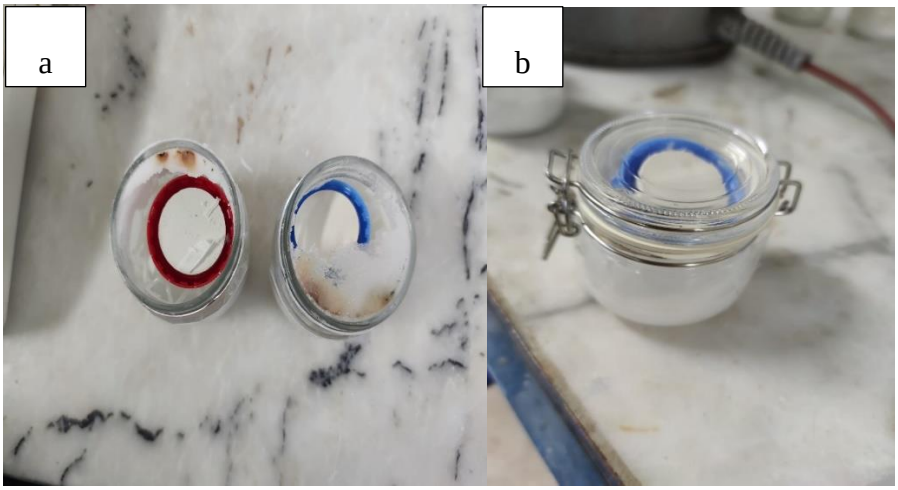

Figure 3.24 Jar system used for high temperature a) Damage caused to the sample by the jar used at room temperature under high temperature b) Jar used at high temperatures (Personal archive, 2023)

Hygrometers measuring relative humidity and temperature were used to control the experiments. The temperature and relative humidity of the experiments, which continued both at room temperature and at 80 °C, were regularly controlled by hygrometers. The samples in jars with plastic lids were weighed on precision scales with regular checks. If a change of less than 0.01 g in the weight of the sample as a result of hydration was observed, the sample was placed in the next jar with a lower suction value and a higher relative humidity saturated salt solution. This process continued with the six saturated salt solutions mentioned above and when the wetting paths of the samples were completed, the same saturated salt solutions were used for the drying path from the lower to the higher suction value. It took approximately 2-3 weeks for a sample to reach equilibrium in any saturated salt solution.

3.2.4 Hydraulic Conductivity Tests

Hydraulic conductivity tests were performed according to ASTM D5084-16a (2016). A flexible wall permeameter was used and the falling head method was applied for the experiments. The experiments were conducted at room temperature and 80 °C. In addition, hydraulic conductivity experiments were also performed on the cured samples where curing process was in the permeameters at 80 °C for 3 months. For hydraulic conductivity tests, flexible wall permeameter cells made of aluminum were manufactured (Figure 3.25). The main reason for producing aluminum cells instead of

acryclic cell is to ensure high temperature resistance. However, acryclic cells were used for experiments at room temperature. The reason for their use was to check whether there was a systemic failure during long-term experiments.

Figure 3.25 Specially designed manufactured flexible wall permeameter test device (Personal archive, 2023)

In addition, the upper and lower heads of the permeameters are also made of aluminum. At the top, there is a space for a heat rod, thermostat probe and thermocouple (Figure 3.26a). There are four pipe inlets in the lower head of the permeameter. These were the cell pressure pipe, the inlet pipe of the sample, the outlet pipe and the pipe used to evacuate the air gap between the sample and the heads inside (Figure 3.26b).While performing the experiments in the presence of high temperature, the thermostat was programmed with Ardunio to increase the temperature by 1 °C per hour to prevent excess pore water pressure in the system due to the rapid temperature increase. The samples were compacted in their natural state under a pressure of approximately 120 MPa in the uniaxial compaction test apparatus shown in Figure 3.27a. The compaction was performed in 5.0 cm diameter by 1.0 cm high steel rings inside a 10 cm diameter 1.0 cm high delrin material (Figure 3.27b). On top of the ring there was a 5.0 cm diameter 5.2 cm high chrome collar. The dry density value of the samples was the same as the value used in the suction tests, which was 1.4 g/cm^3.

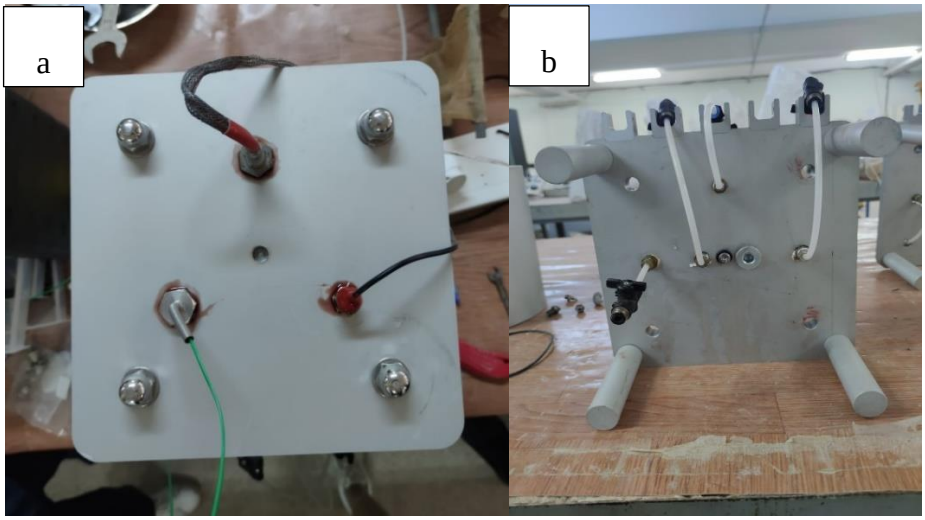

Figure 3.26 The heads of the permeameter a) Upper head b) Lower head (Personal archive, 2023)

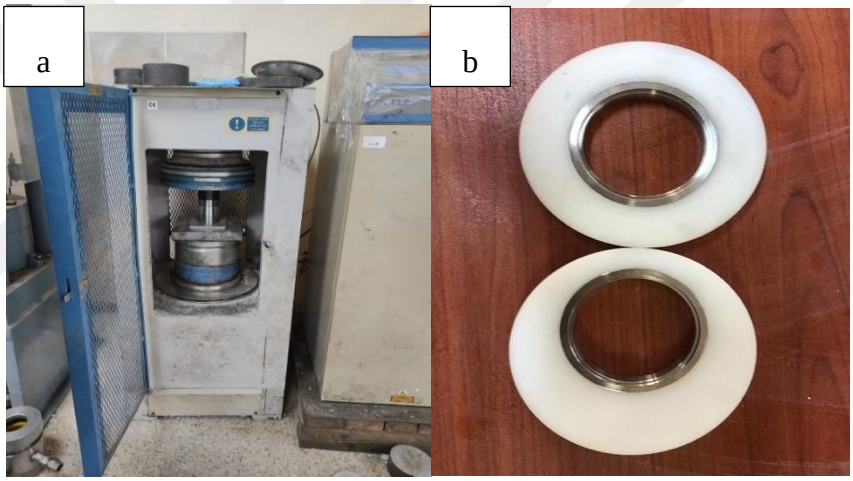

Figure 3.27 The hydraulic conductivity sample preparation devices a) uniaxial compression test apparatus, b) Mold made of delrin outside and steel ring inside (Personal archive, 2023)

The compacted specimens at natural water content were placed in permeameters inside the delrin molds. De-ionized water was used for the inlet water. Since the swelling pressure values of the compacted bentonite are very high, it was not possible to reach cell pressures that will prevent the compacted bentonite from swelling in the flexible-walled permeameter system. Therefore, the flexible-walled permeameter system was modified to behave like a rigid-walled permeameter. Therefore, a clamping system was fabricated on top of the sample to prevent vertical deformations due to swelling of the bentonite sample in the ring. The placement stages are as shown in Figure 3.28. Filter papers were placed under and on top of the samples and non-

woven geotextile was placed on top of the filter papers. The heads were placed above and below the samples placed in the permeameter with the delrin mold. These heads were connected to the inlet and outlet water pipe of the samples and to the pipes used to remove the air generated inside the system. The pipes were made of polyethylene material and had an inner diameter of 4.0 mm.

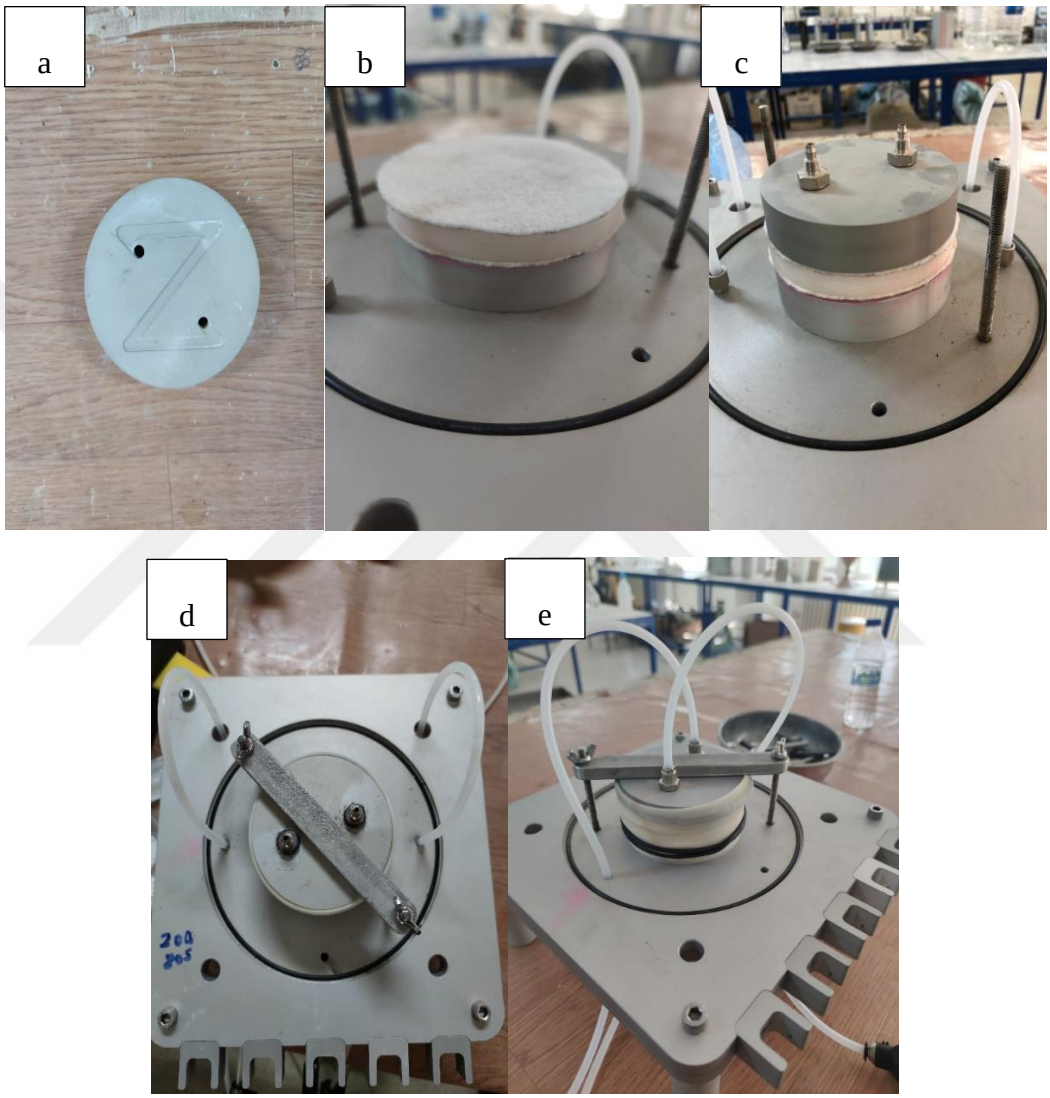

Figure 3.28 Placement of samples in permeameters a) Top and bottom caps with a z-shaped hollow inside b) Delrin mold and non-woven geotextile on top and bottom c) Placing the top cap on top of the specimen d) clamped system used to prevent swelling e) Ready system with membrane o-ring and pipes (Personal archive, 2023)

To provide the cell pressure inside the experimental system, pressurized tanks were used (Figure 3.29a). The principle of pressurization is to increase the air pressure from the lower part of the tank with the help of a pump and to allow the water at the top to

come out in a pressurized way. In the middle of the tank there is a membrane separating the air and water. The more air is pumped into the tank, the higher the water pressure. In this study, a value of 1.5 MPa was preferred for the cell pressure. To control the cell pressure value, a manometer was installed in the pipe where the water outlet of the tanks is located (Figure 3.29b).

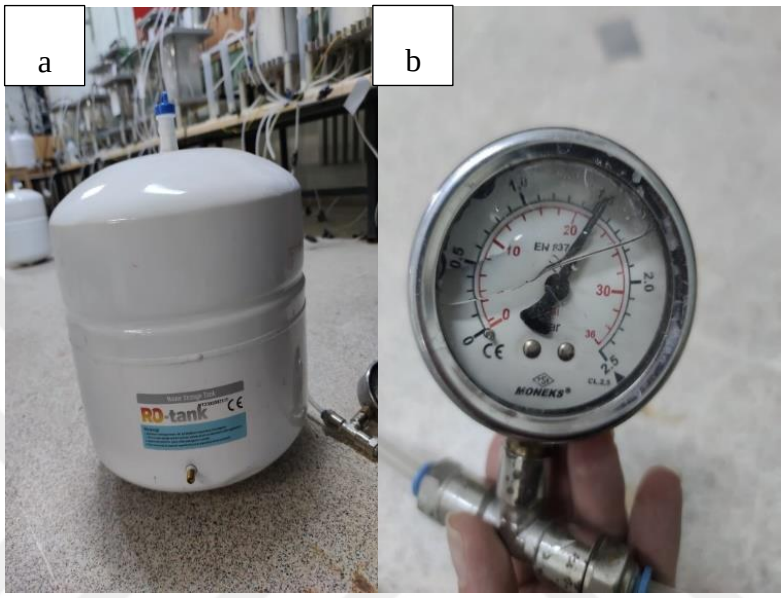

Figure 3.29. a) Water tanks providing the necessary cell pressure for the experimental systems b) Manometer (Personal archive, 2023)

CHAPTER FOUR
RESULTS AND DISCUSSIONS

The results of the experimental studies conducted within the scope of the thesis are given in this chapter. Glass fiber additive was mixed with bentonite 0.5% and 1% contents by dry weight of bentonite. The bentonite samples without glass fiber additives were named as ‘‘Bentonite’’ and the bentonite samples with glass fiber additives were named as 0.5% GF and 1% GF depending on the mixture content. The results of the experiments carried out at room temperature were abbreviated as RT, and the abbreviation of the experiments carried out at 80 °C high temperature was named as 80 °C. The first part of this section presents the results of the consolidation experiments. In this section, the changes in the deformation behavior of bentonite and glass fiber additives at room temperature, in the presence of high temperature and in the presence of high temperature for short and long term were investigated. In the second part, the swelling behavior of bentonite obtained by the free swell index tests at room temperature and at 80 °C were analyzed. In the third part, the suction values and water retention curves (WRCs) of bentonite and glass fiber additive bentonite mixtures were investigated at room temperature and 80 °C. In the last part of this chapter, hydraulic conductivity results of bentonite mixtures are given.

4.1 Consolidation Test Results

Consolidation tests were performed according to ASTM D2435-11 (2011). Within the scope of this thesis, twelve consolidation tests were performed. The experimental setup is shown in Table 4.1.

To determine the consolidation behavior of the specimens, vertical stress-strain plots and normalized e-log p plots were obtained at the end of the experiment. Total compression and swelling moduli values were determined from the vertical stress-strain graphs. Compression moduli values represent the deformation in the range of 24.5-784 kPa, while swelling moduli values represent the deformation in the range of 784-49 kPa from the rebound curve. Since the initial void ratio values of all experiments varied in a wide range between 6.0 and 8.4, normalized e-log p graphs

were presented by starting the initial void ratios of all samples from 1.0 in order to visually explain the void ratio change. Compression index (C_c) and swelling index (C_s) were obtained from the original void ratio values. For C_c values, void ratios in the range 196-784 kPa were considered, while for C_s, void ratios in the range 784-49 kPa were considered.

To investigate the effect of two different contents of glass fiber additives on the consolidation behavior of bentonite under different thermal conditions consolidation tests were performed. These thermal conditions were room temperature, 80 °C temperature, short term (6 months) and long term (1 year) curing periods. The results were discussed and interpreted by comparing the compression index (C_c), swelling index (C_s), compression and swelling moduli, coefficient of consolidation (c_v), coefficient of volume compressibility (m_v) and hydraulic conductivity (k) values obtained indirectly.

Table 4.1 The experimental set-up for consolidation tests

	Room Temperature (R.T.)	At High Temperature (80 °C)	Short Term Curing at 80 °C (6 Months)	Long Term Curing at 80°C (1 Year)
Bentonite	✓	✓	✓	✓
0.5% GF	✓	✓	✓	✓
1% GF	✓	✓	✓	✓

4.1.1 Settlement and Rebound Behavior Under Room Temperature

Consolidation tests of bentonite and glass fiber added bentonite samples were carried out at room temperature. The stress-strain relationships obtained as a result of the experiments are given in Figure 4.1. As can be seen from the graph, the compression moduli of bentonite were 53.3%. The compression moduli values of 0.5% and 1% GF added bentonites were 52.5% and 58.0%, respectively. With 0.5% GF additive, the compression moduli change was -1.4%, while with 1% GF additive, this change was 8.9%. The swelling moduli of bentonite was found to be 7.2% at room

temperature. 0.5% and 1% GF additives improved the swelling moduli of bentonite at room temperature. At 0.5% GF additive, the swelling moduli was 12.0%, while at 1% GF additive it was 17.0% (Table 4.2).

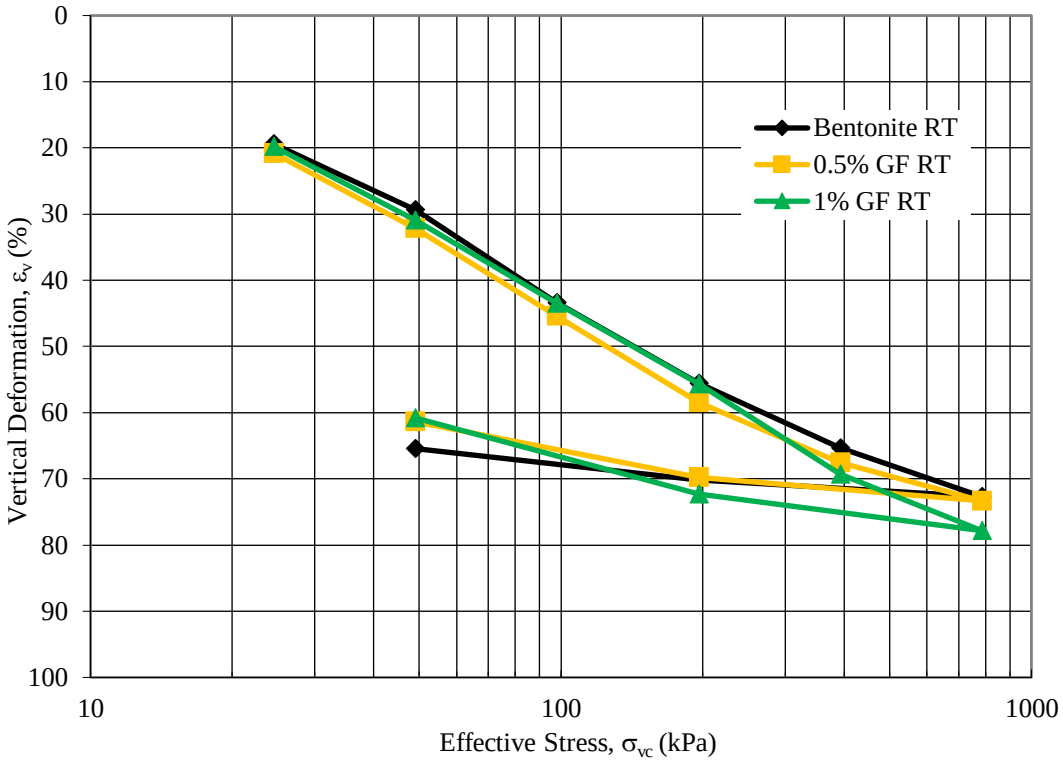

Figure 4.1 Vertical stress-strain curves of glass fiber added bentonite mixtures at room temperature

Table 4.2 The compression and swelling moduli results of the experiments at room temperature

	Temperature	Compression Moduli (%)	Swelling Moduli (%)
Bentonite	RT	53.28	7.24
Bentonite - 0.5% GF		52.53 *(-1.41%)*	11.97 *(+65.3%)*
Bentonite - 1% GF		58.03 *(+8.92%)*	17.03 *(+135.22%)*

Normalized e-log p plots of experiments at room temperature are given in Figure 4.2. Glass fiber additive increased the compression and swelling index values of bentonite at room temperature. The C_c and C_s values and the rates of change of the results with the additives are shown in Table 4.3.

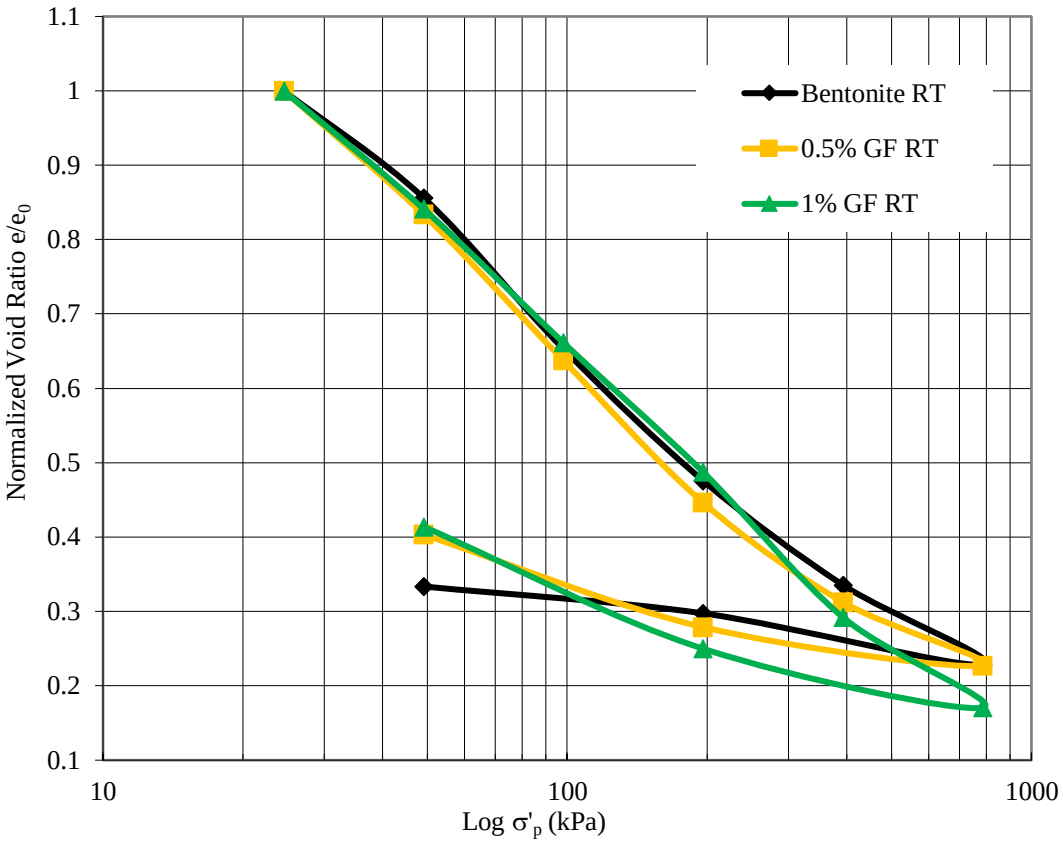

Figure 4.2 Normalized e-logp curves of glass fiber added bentonite mixtures at room temperature

The C_c of bentonite at room temperature was found to be 2.46. With 0.5% GF additive, the C_c changed by -10.4% to 2.21. With 1% GF additive, it changed by 46.2% to 3.6. The C_s of bentonite and mixtures with 0.5% and 1% GF additives were 0.52, 0.88 and 1.38, respectively. The GF additive contents increased the C_s value of bentonite.

Table 4.3 The compression and swelling index results of the experiments at room temperature

	Temperature	Compression Index (C_c)	Swelling Index (C_s)
Bentonite	RT	2.46	0.52
Bentonite – 0.5% GF		2.21 *(-10.44%)*	0.88 *(+69.44%)*
Bentonite – 1% GF		3.60 *(+46.22%)*	1.38 *(+164.84%)*

4.1.2 Settlement and Rebound Behavior Under High Temperature (80 °C)

The results of consolidation tests carried out at 80 °C in the modified oedometer test apparatus for high temperature are as follows. The stress-strain graph of the mixtures is given in Figure 4.3. Compression and swelling moduli values are also given in Table 4.4.

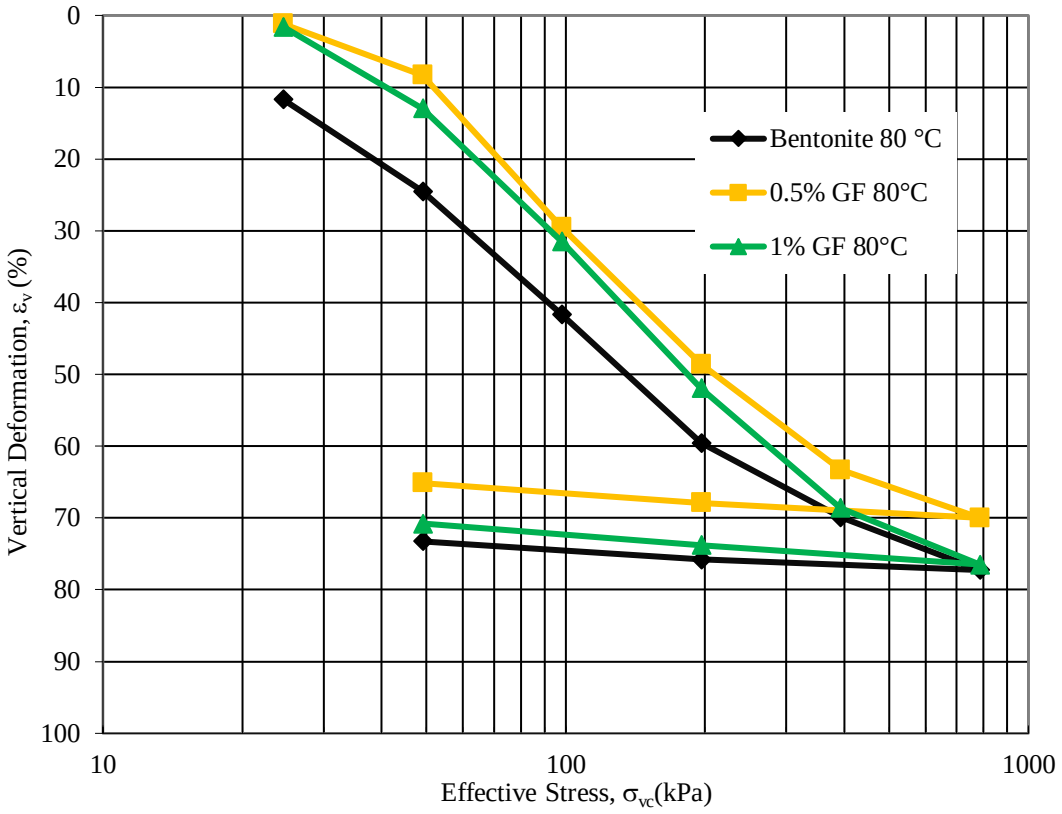

Figure 4.3 Compression and swelling curves of glass fiber added bentonite mixtures at high temperature (80 °C)

Table 4.4 The compression and swelling moduli results of the experiments at high temperature (80 °C)

	Temperature	Compression Moduli (%)	Swelling Moduli (%)
Bentonite	80 °C	65.5	4.0
Bentonite - 0.5% GF		68.8 *(+4.96%)*	4.8 *(+21.37%)*
Bentonite - 1% GF		74.9 *(+14.29%)*	5.7 *(+42.88%)*

According to the results, the compression moduli of bentonite at 80 °C was 65.5%. The compression moduli of bentonite with 0.5% and 1% GF additives were 68.8% and 74.9%, respectively. Glass fiber additive increased the compression moduli of bentonite under high temperature (80 °C).

In terms of swelling moduli, glass fiber additive increased the swelling moduli of bentonite for both contents at 80 °C. While the swelling moduli of bentonite under high temperature was found to be 4.0%, the swelling moduli values increased with 0.5% and 1% GF additives and were found to be 4.8% and 5.7%. The swelling moduli changes with glass fiber additives were 21.4% and 42.9%, respectively.

When the experiments performed at room temperature are compared with the experiments performed in the presence of 80 °C, the compression moduli of all three mixtures increased while the swelling moduli decreased. It was observed that the glass fiber additive increased the compression moduli and swelling moduli of bentonite both at room temperature and at 80 °C, while its effect on the swelling moduli decreased at 80 °C.

The normalized e-log p plots of the experiments at 80 °C temperature is as shown in Figure 4.4. The C_c and C_s of bentonite are 3.31 and 0.37, respectively. Glass fiber additive increased the C_c and C_s of bentonite at 80 °C. With 0.5% GF addition, C_c increased by 1.6% to 3.37, while with 1% GF addition, C_c increased by 10.9% to 3.67. The C_s values also increased with GF additive and increased from 0.37 to 0.38 and 0.43 with 0.5% and 1% GF additives, respectively (Table 4.5).

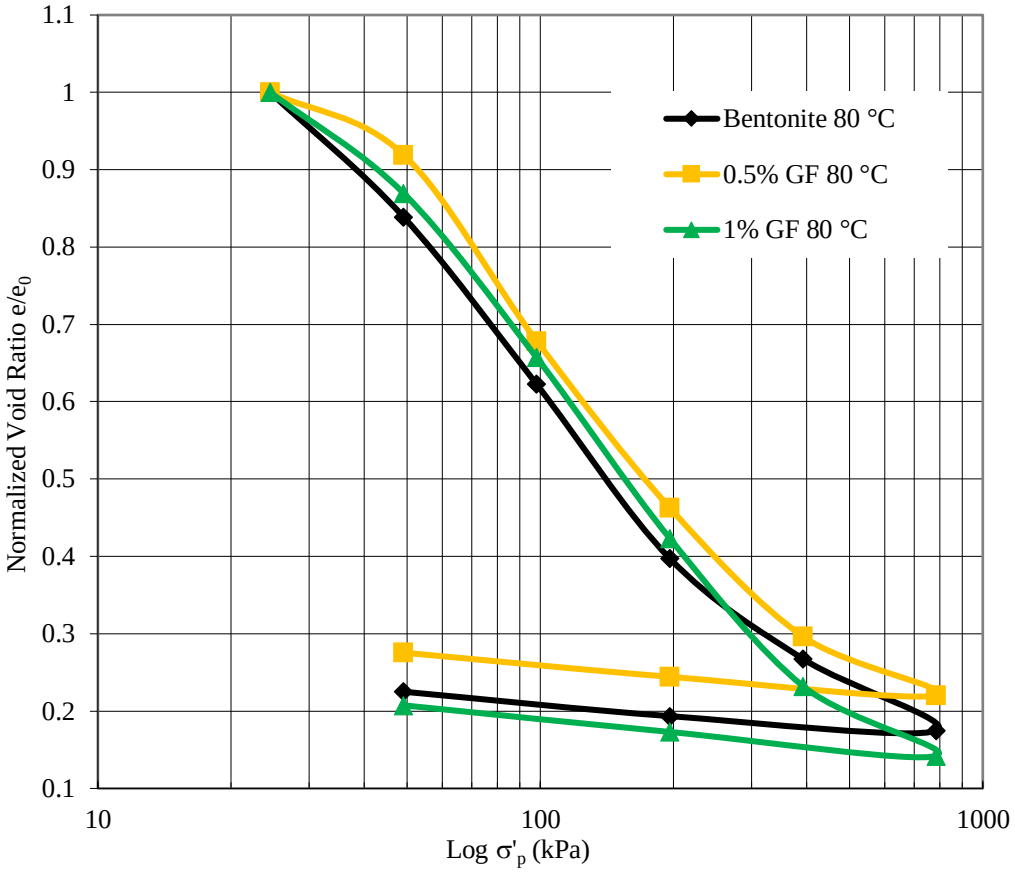

Figure 4.4 Normalized e-logp curves of glass fiber added bentonite mixtures at high temperature (80 °C)

Table 4.5 The compression and swelling index values at high temperature (80 °C)

	Temperature	Compression Index (C_c)	Swelling Index (C_s)
Bentonite 80 °C	80 °C	3.31	0.37
Bentonite - 0.5% GF		3.37 *(+1.63%)*	0.38 *(+2.06%)*
Bentonite - 1% GF		3.67 *(+10.89%)*	0.43 *(+14.10%)*

4.1.3 Settlement and Rebound Behavior Under Six Months Curing Period

The results of consolidation tests performed with specimens left to cure at 80 °C for six months are shown in this section. Stress strain graphs of the specimens are given in Figure 4.5 and compression and swelling moduli values are given in Table 4.6.

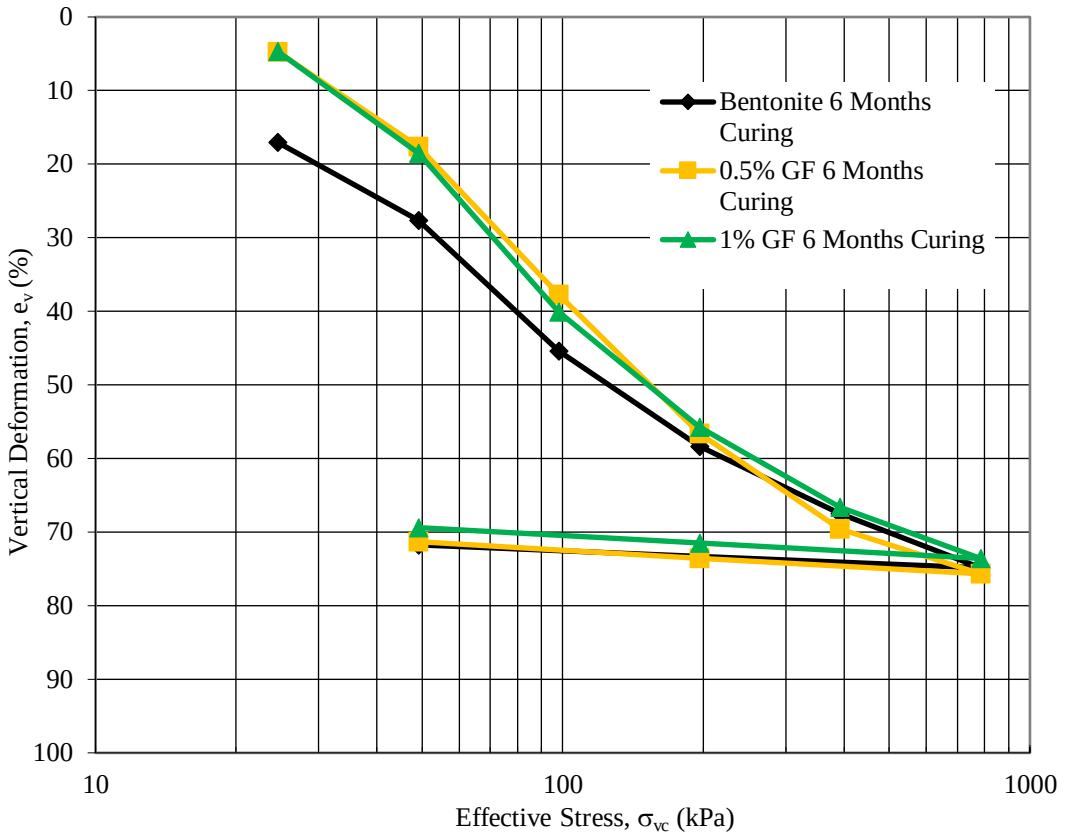

Figure 4.5 Compression and swelling curves of glass fiber added bentonite mixtures at high temperature (6 months curing)

According to the results, the compression moduli values of bentonite, 0.5% and 1% GF added bentonite mixtures under 6 months high temperature curing were 57.8%, 71.0% and 68.9% respectively. In the 6 months curing period, a decreasing effect was observed in the compression moduli with the curing effect in all mixtures except the mixture with 0.5% GF additive. At 6 months curing effect, glass fiber additive caused an increase in the compression moduli of bentonite as in the experiments performed at room temperature and 80 °C. This increase was found to be 22.7% and 19.2% for 0.5 and 1% GF additives, respectively.

The swelling moduli values of bentonite, 0.5 and 1% GF added bentonite mixtures were found to be 3.1%, 4.4% and 4.2%, respectively. 0.5% and 1% GF additives increased the swelling moduli by 42.2% and 35.7%, respectively. Also, a decrease in the swelling moduli of the mixtures was observed with the 6 months curing effect compared to 80 °C mixtures.

Table 4.6 The compression and swelling moduli values at high temperature (6 months curing-80 °C)

	Curing period	Compression Moduli (%)	Swelling Moduli (%)
Bentonite	6 Months	57.8	3.1
Bentonite - 0.5% GF		71.0 *(+22.70%)*	4.4 *(+42.22%)*
Bentonite - 1% GF		68.9 *(+19.17%)*	4.2 *(+35.73%)*

The normalized e-log p graph of the mixtures after 6 months of curing are given in Figure 4.6. C_c values were 2.60, 3.11 and 2.59 for bentonite, 0.5 and 1% GF mixtures respectively. C_s values were 0.24, 0.36 and 0.30 for bentonite, 0.5 and 1% GF additives. The change in C_s value of bentonite with 0.5% and 1% GF additives was 47.1% and 24.6%, respectively (Table 4.7).

Table 4.7 The compression and swelling index results of the experiments at high temperature (6 Months curing)

	Curing period	Compression Index (C_c)	Swelling Index (C_s)
Bentonite	6 Months	2.60	0.24
Bentonite - 0.5% GF		3.11 *(+19.88%)*	0.36 *(+47.09%)*
Bentonite - 1% GF		2.59 *(-0.23%)*	0.30 *(+24.59%)*

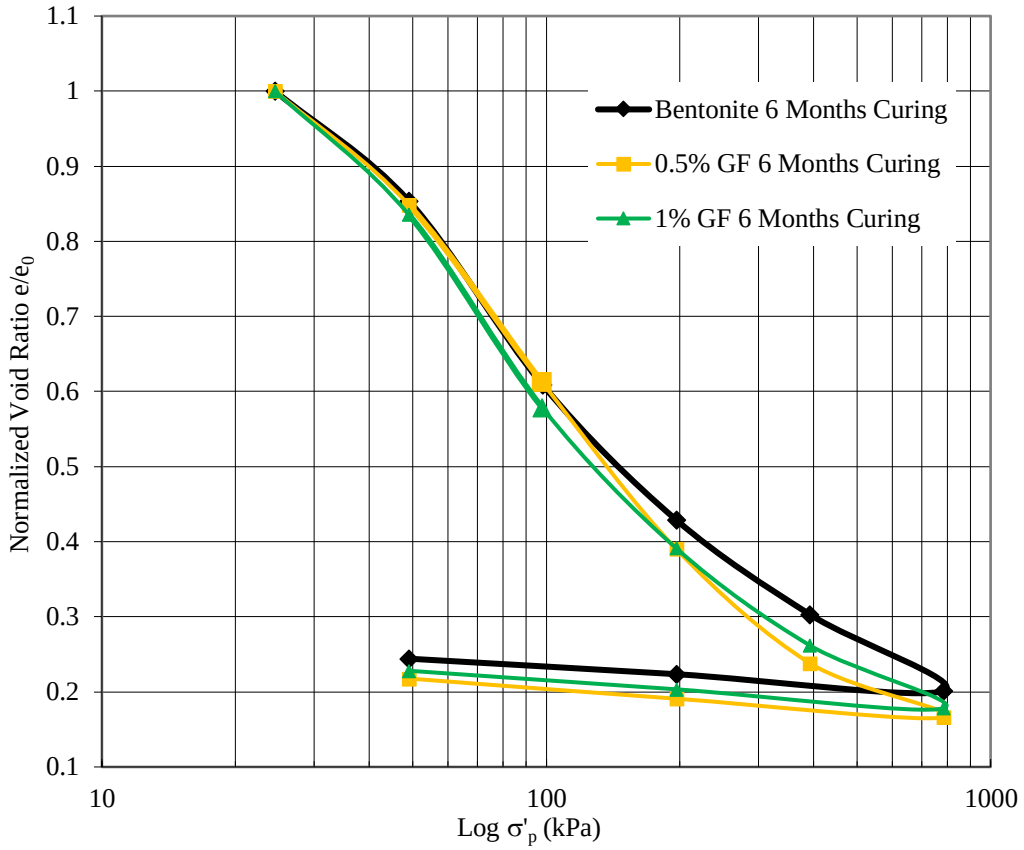

Figure 4.6 Normalized e-logp curves of glass fiber added bentonite mixtures at high temperature (6 months curing)

4.1.4 Settlement and Rebound Behavior Under 1 Year Curing Period

The results of consolidation tests performed on specimens left to cure in the presence of high temperature for 1 year are given below. Stress-strain graphs are given in Figure 4.7 and compression and swelling moduli values are given in Table 4.8.

Table 4.8 The compression and swelling moduli results of the experiments at high temperature (1 year curing)

	Curing period	Compression Moduli (%)	Swelling Moduli (%)
Bentonite	1 Year	62.6	3.6
Bentonite - 0.5% GF		69.6 *(+11.10%)*	3.8 *(+5.60%)*
Bentonite - 1% GF		62.4 *(-0.36%)*	3.5 *(-1.18%)*

There was an insignificant change in the compression moduli than the change with the effect of glass fiber at other temperature conditions. Unlike other temperature conditions, 1% GF additive caused a small decrease in compression moduli. With 0.5% and 1% GF additive, the change in compression moduli was found to be 11.1% and -0.36%, respectively.

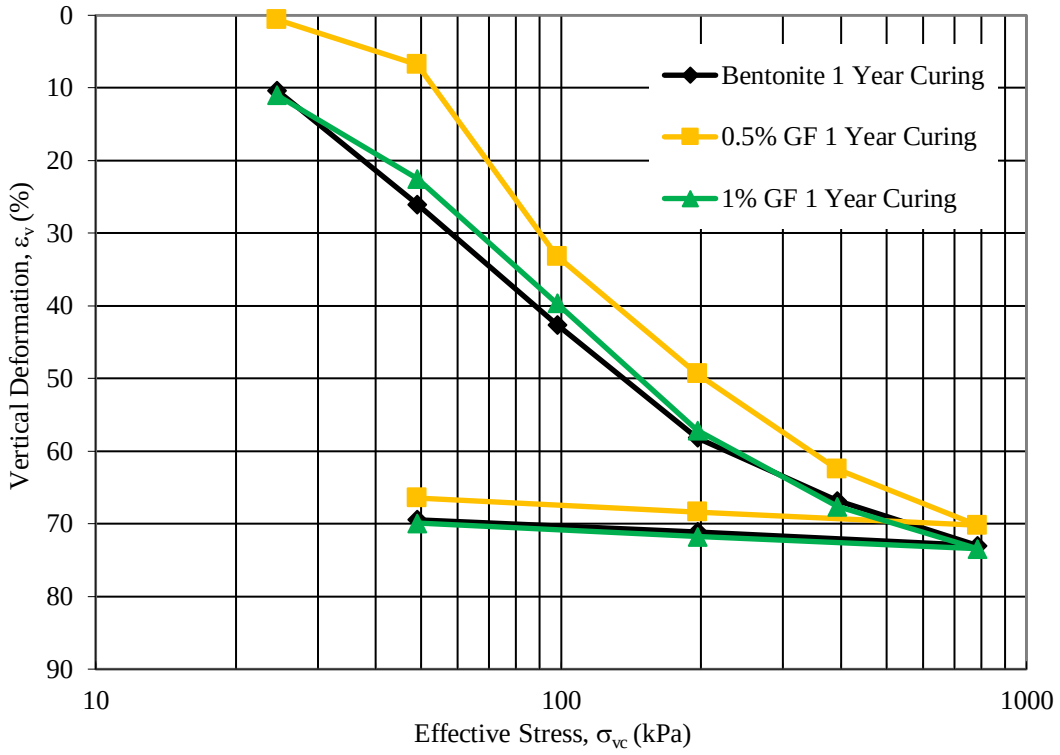

Figure 4.7 Compression and swelling curves of glass fiber added bentonite mixtures at high temperature (1 year curing)

An increase in swelling moduli of bentonite was observed with 1 year curing when compared with 6 months cured samples. However, a decrease was observed in the glass fiber added specimens. It was also observed that the positive effect of glass fiber additive on swelling moduli decreased at 1 year curing effect compared to other thermal conditions. With 0.5% and 1% GF additives, the changes in swelling moduli were 5.6% and -1.2%, respectively.

The normalized e-log p graph of the samples kept at 80 °C for 1 year under curing effect is shown in Figure 4.8. C_c values for bentonite, 0.5 and 1% GF additives were

2.30, 2.99 and 2.78 respectively. C_s values were 0.28, 0.27 and 0.30 for bentonite, 0.5 and 1% GF added samples, respectively (Table 4.9).

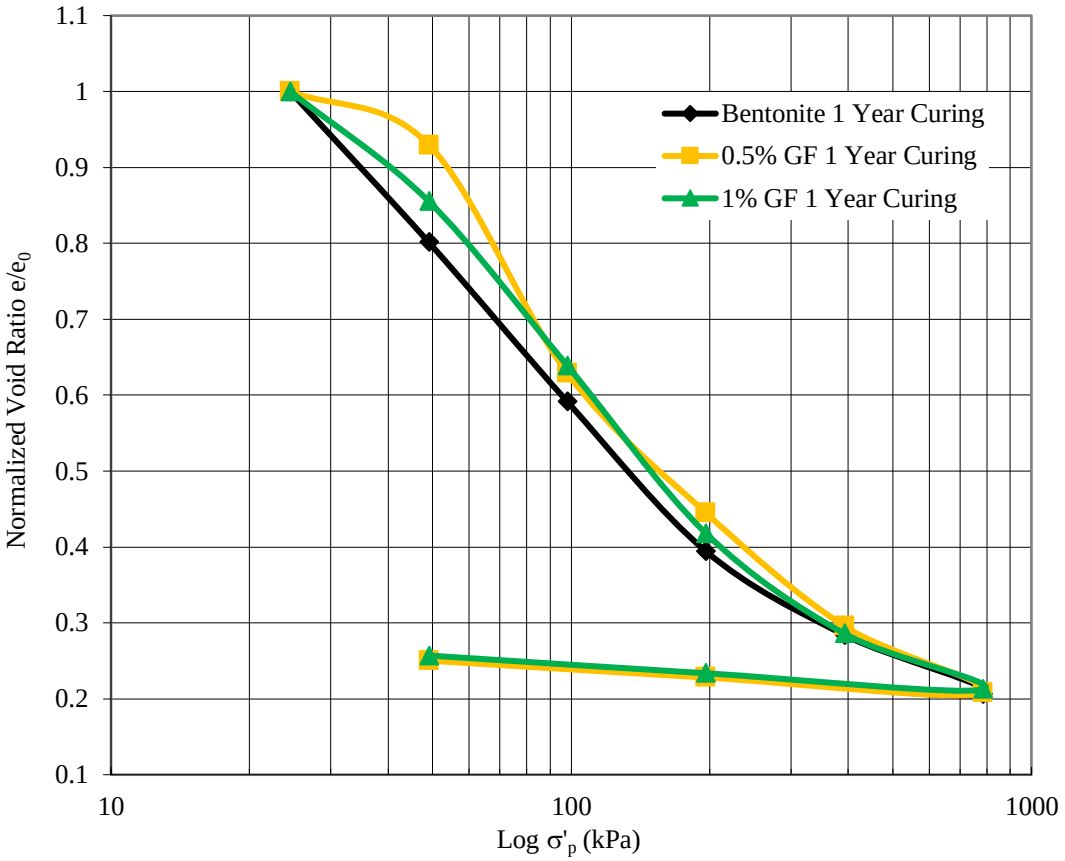

Figure 4.8 Normalized e-logp curves of glass fiber added bentonite mixtures at high temperature (1 year curing)

Table 4.9 The compression and swelling index values under high temperature (1 year curing-80 °C)

	Curing period	Compression Index (C_c)	Swelling Index (C_s)
Bentonite	1 Year	2.30	0.28
Bentonite - 0.5% GF		2.99 *(+30.11%)*	0.27 *(-2.15%)*
Bentonite - 1% GF		2.78 *(+21.13%)*	0.30 *(+9.18%)*

4.1.5 Effects of Curing, High Temperature and Glass Fiber Content on the Volume Deformation

In this thesis, the experiments were carried out at room temperature and at 80 °C to understand the effect of high temperature on consolidation behavior. In order to examine the long term effects of high temperatures, some samples were kept in water pools at 80 °C for 6 months and 1 year and then consolidation experiments were performed. The effect of glass fiber additive on the consolidation behavior of bentonite at these thermal conditions was also investigated. Glass fiber additives were used at 0.5% and 1% by dry weight of bentonite.

The compression moduli, swelling moduli, compression index (C_c) and swelling index (C_s) obtained from the results of the above experiments are summarized in this section. Figure 4.9 shows the bar graph distribution of the compression moduli values found from the experiments. Table 4.10 shows the compression moduli values.

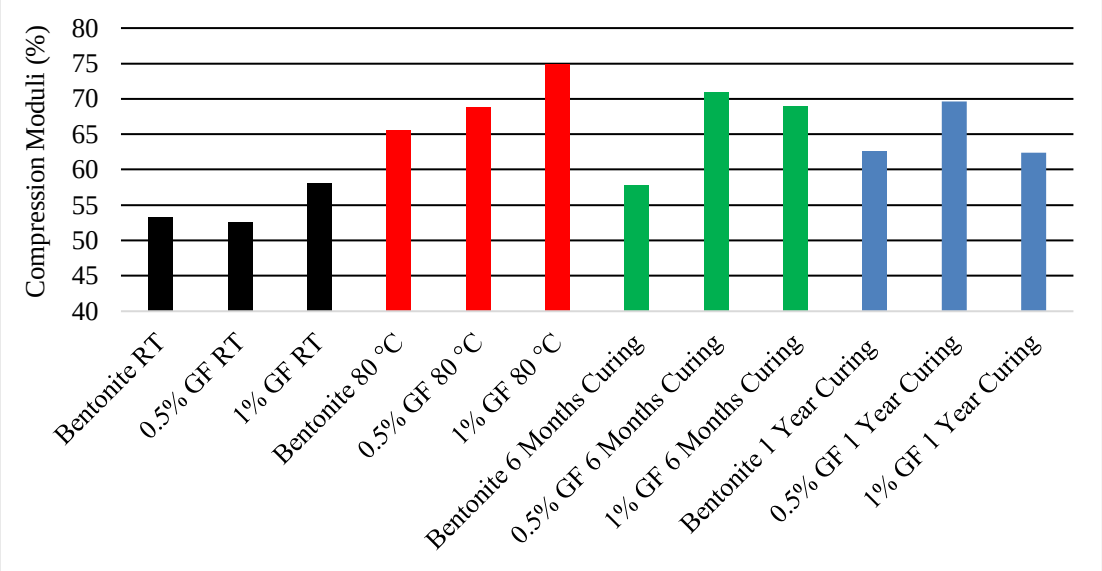

Figure 4.9 Bar graph distribution of the compression moduli values

As can be seen from the Figure 4.9, there is no specific trend in the compression moduli values. However, it can be concluded from the results that the compression moduli of all mixtures increased in the presence of 80 °C temperature. In terms of curing effect, while the compression moduli values of bentonite decreased slightly, no change was observed in 0.5% GF mixtures and the curing effect had a positive effect

as a decrease in 1% GF mixtures. In addition, both contens of glass fiber additives caused an increase in the compression moduli of bentonite at all thermal conditions.

Table 4.10 Compression moduli values of all mixtures

Sample	Temperature	Curing period	Compression Moduli (%)
Bentonite	RT	-	53.3
Bentonite - 0.5% GF			52.5
Bentonite - 1% GF			58.0
Bentonite	80 °C	-	65.5
Bentonite - 0.5% GF			68.8
Bentonite - 1% GF			74.9
Bentonite	80 °C	6 months	57.8
Bentonite - 0.5% GF			71.0
Bentonite - 1% GF			68.9
Bentonite	80 °C	1 year	62.6
Bentonite - 0.5% GF			69.6
Bentonite - 1% GF			62.4

The change in compression index (C_c) according to the mixtures is shown in Figure 4.10 and Table 4.11. As in the compression moduli, C_c also showed an increasing trend in the presence of 80 °C. The insignificant change on the C_c was observed with the effect of high temperature for the 1% GF mixture. There is a decrease in C_c as seen in compression moduli in all mixtures at both curing periods. It can be concluded that the glass fiber additive caused a slight increase in the C_c value of bentonite at all thermal conditions.

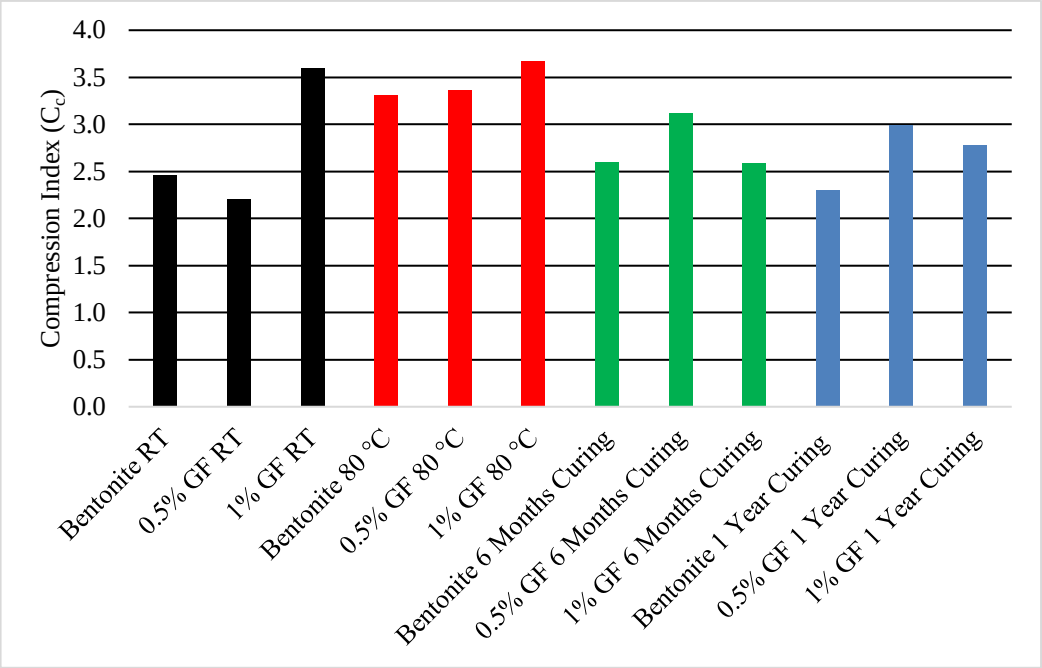

Figure 4.10 The distribution of the compression index values

Table 4.11 Compression index values of all mixtures

Samples	Temperature	Curing period	Compression Index (C_c)
Bentonite	RT	-	2.46
Bentonite - 0.5% GF			2.21
Bentonite - 1% GF			3.60
Bentonite	80 °C	-	3.31
Bentonite - 0.5% GF			3.37
Bentonite - 1% GF			3.67
Bentonite	80 °C	6 months	2.60
Bentonite - 0.5% GF			3.11
Bentonite - 1% GF			2.59
Bentonite	80 °C	1 year	2.30
Bentonite - 0.5% GF			2.99
Bentonite - 1% GF			2.78

It is expected that when soils are exposed to high temperatures, the quantity of energy they possess will increase; therefore, the energy of soil particles will increase. Molecules with elevated energy will become more mobile and thus weaken the existing bonds even more. As a result, the amount of compression in the soil will increase (Gupta et al., 1964; Jarad, 2016). Bag & Rabbani, (2017) reported that the compression index value increased from 0.76 to 0.96 as the temperature increased from 25 °C to 90 °C in their study with Bikaner bentonite.

Considering the effect of glass fiber on the compressibility of bentonite in the study, it can be said that it increases the compressibility as a general trend. However, studies on clayey soils in the literature have given contradictory results. Mukherjee & Mishra, (2019), Jadda et al. (2021) in their studies on sand-bentonite mixtures and clayey soils stated that the compression index decreased slightly with the addition of glass fiber, while Güneri, (2022) and Çirkin, (2023) in their studies with sand-bentonite and zeolite-bentonite mixtures showed that the addition of glass fiber led to a slight increase in the compression index. The compressibility values found in this thesis study gave high values in terms of compression moduli and compression index values due to the fact that the sample used was only bentonite and the initial water content was high. Due to the high water content of the sample in this thesis, glass fiber may not have been able to improve the compressibility by providing adhesion between the clay grains.

In addition, as a general trend, the compressibility behavior of mixtures decreased with curing effect. This may be due to the mineralogical change of bentonite under high temperature curing effect. The montmorillonite mineral may have been transformed into illite mineral with less swelling and compaction properties with prolonged heat.

The variation of swelling moduli and swelling index (C_s) according to the mixtures are given below. Swelling moduli change is given in Figure 4.11. A large positive effect of glass fiber additive on the swelling behavior was observed at room temperature. In the presence of 80 °C, this effect decreased but still had a positive influence. The effect on swelling behavior decreased even more under curing effect. This change is also seen in the C_s values (Figure 4.12). Comparing the mixtures at 80

°C and the mixtures under curing effect, a slight decrease in the swelling behavior of bentonite and glass fiber added mixtures was observed under curing effect. Tables 4.12 and 13 also show the swelling moduli and C_s values of the mixtures.

Some previous studies have indicated that temperature significantly affects the swelling behavior of bentonite. Xiang et al. (2020) stated that the swelling deformation decreased under high temperature with the effect of vertical stress. The Gouy-Chapman equation represents the volume change of clays. The equation is also known as the diffuse double layer (DDL) model and previous studies have reported that the thickness of DDLs increases with increasing temperature. Thus, increasing temperature induces swelling of clays (Ye et al., 2013; Cui et al., 2018).

Table 4.12 Swelling moduli values of all mixtures

Samples	Temperature	Curing period	Swelling Moduli (%)
Bentonite	RT	-	7.2
Bentonite - 0.5% GF			12.0
Bentonite - 1% GF			17.0
Bentonite	80 °C	-	4.0
Bentonite - 0.5% GF			4.8
Bentonite - 1% GF			5.7
Bentonite	80 °C	6 months	3.1
Bentonite - 0.5% GF			4.4
Bentonite - 1% GF			4.2
Bentonite	80 °C	1 year	3.6
Bentonite - 0.5% GF			3.8
Bentonite - 1% GF			3.5

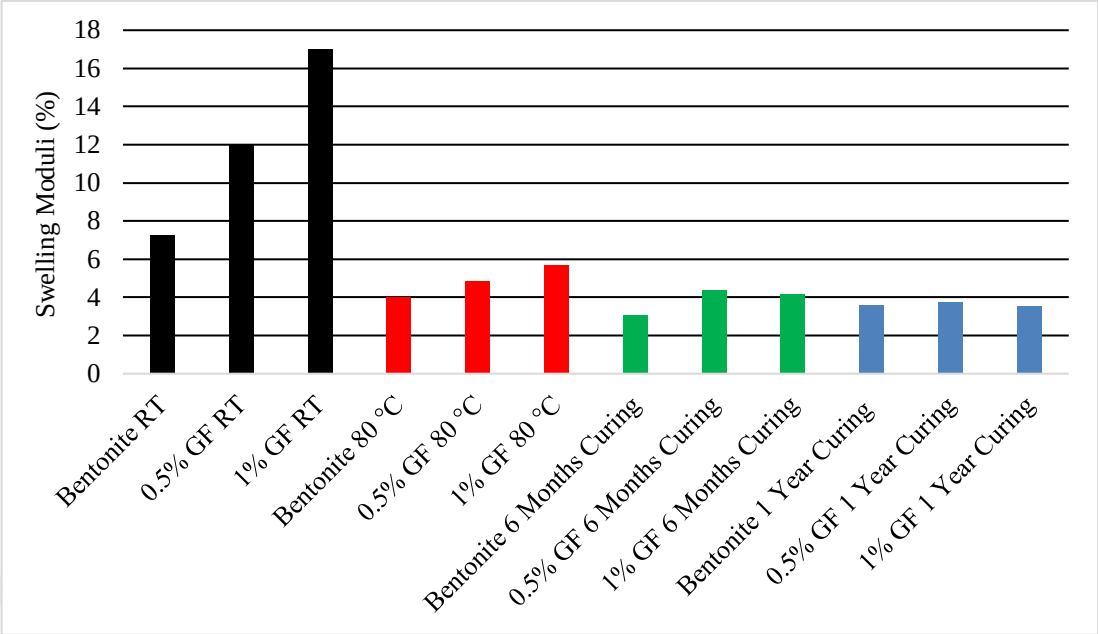

Figure 4.11 The distribution of the swelling moduli values

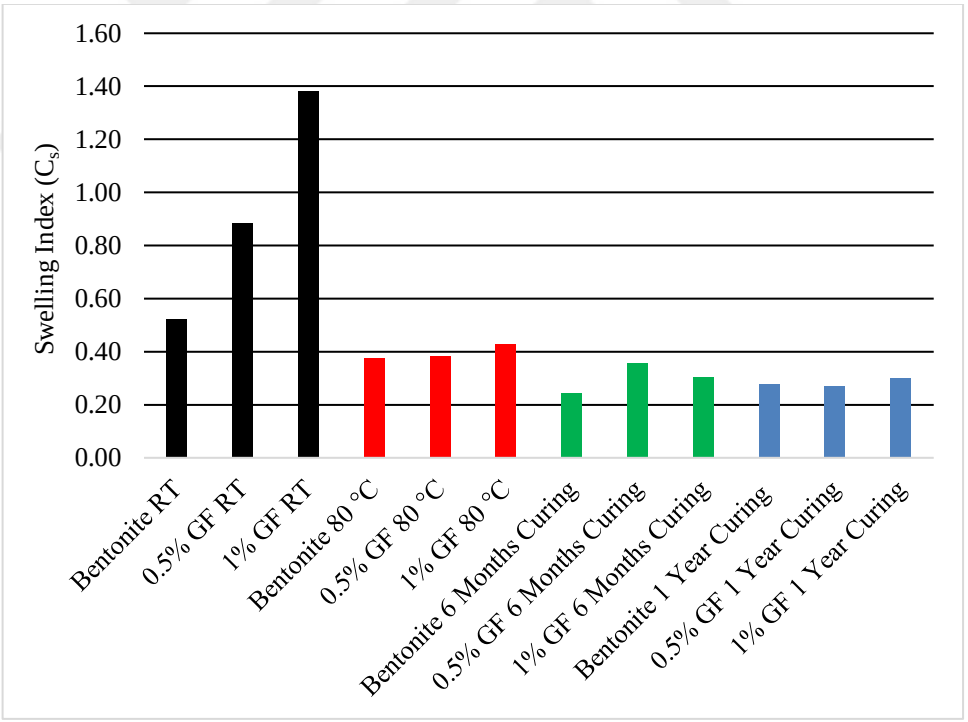

Figure 4.12 The distribution of the swelling index values

Table 4.13 Swelling index values of all mixtures

Samples	Temperature	Curing period	Swelling Index (C_s)
Bentonite	RT		0.52
Bentonite - 0.5% GF			0.88
Bentonite - 1% GF			1.38
Bentonite	80 °C		0.37
Bentonite - 0.5% GF			0.38
Bentonite - 1% GF			0.43
Bentonite	80 °C	6 months	0.24
Bentonite - 0.5% GF			0.36
Bentonite - 1% GF			0.30
Bentonite	80 °C	1 year	0.28
Bentonite - 0.5% GF			0.27
Bentonite - 1% GF			0.30

The values of coefficient of consolidation (c_v), coefficient of volume compressibility (m_v) and hydraulic conductivity (k) obtained from the consolidation test are given below. The values of c_v were taken from 196 kPa load level. The c_v of a consolidated soil represents the rate of consolidation due to the applied vertical pressure. For c_v, log fitting (Casagrande & Fadum, 1940) and square fitting (Taylor, 1948) methods were applied. Casagrande's log fitting method is calculated for a consolidation degree of 50% (U=50%) and is given by the following formula.

$$c_v = \frac{0.197 \mathrm{x} {H_{dr}}^2}{\mathrm{T_{50}}} \tag{4.1}$$

Where H_{dr} is the drainage path of the sample and T_{50} is time for 50% degree of consolidation. The coefficient of consolidation values with square fitting method is also found by the following formula.

$$c_v = \frac{0.848 x {H_{dr}}^2}{T_{90}} \quad (4.2)$$

Where T_{90} is the time for 90% degree of consolidation. In the log fitting method, T_{50} is obtained from the log time-settlement plot, while in the square fitting method, T_{90} is obtained from the square root of time-settlement plot. The c_v values of the mixtures according to log fitting and square fitting methods are given in Figures 4.13, 4.14 and Table 4.14 below. As can be seen from the figures and table, c_v values increased with temperature in both methods. In addition, this increase continued with the curing effect and the c_v values of the samples at 1 year curing time were higher than the c_v values of the samples at 6 months curing time. In addition, glass fiber additive increased the c_v value of bentonite. This increase became more noticeable in the presence of 80 °C.

The coefficient of volume compressibility (m_v) is defined as the ratio between the volume change in relation to the increase in vertical stress per unit volume of the soil sample and is calculated as follows.

$$m_v = \frac{\Delta e}{\Delta \sigma (1 + e_0)} \quad (4.3)$$

Where $\Delta\sigma$ is the change in the vertical stress, Δe is the change in void ratio. The coefficient of volume compressibility (m_v) values was found as in the stress range 98-196 kPa. As in c_v values, it was observed that higher temperature increased the m_v value. Although the curing effect was not clearly seen in the change in m_v, m_v values varied between 2.71×10^{-5} and 3.62×10^{-5} m^2/kg in all experiments performed at 80 °C

temperature. The bar graph and table of values for m_v are given in Figure 4.15 and Table 4.15.

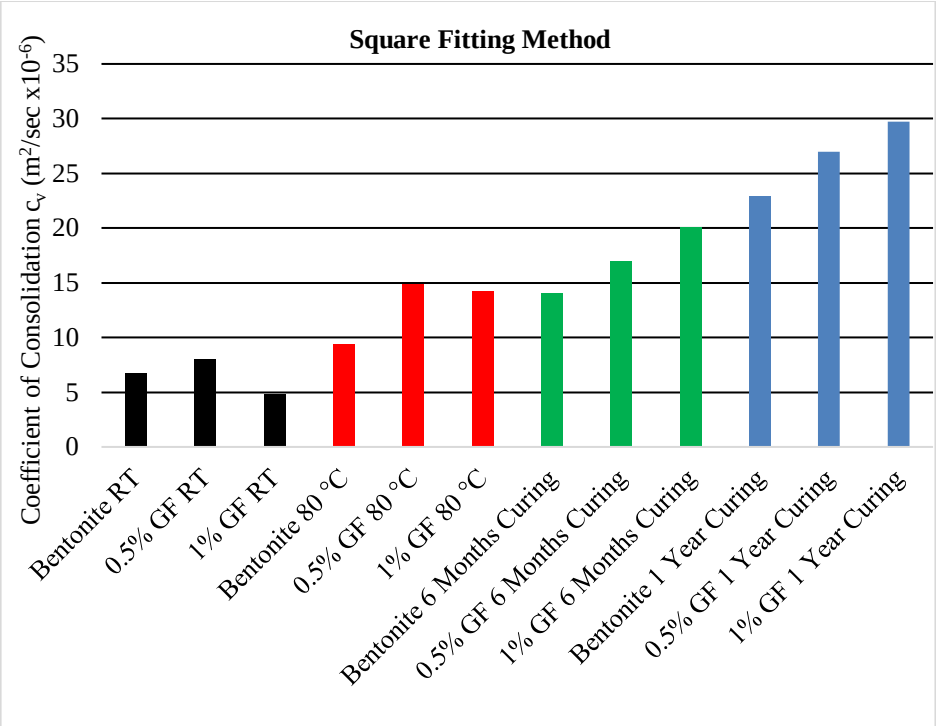

Figure 4.13 The c_v values of the mixtures according to square fitting method

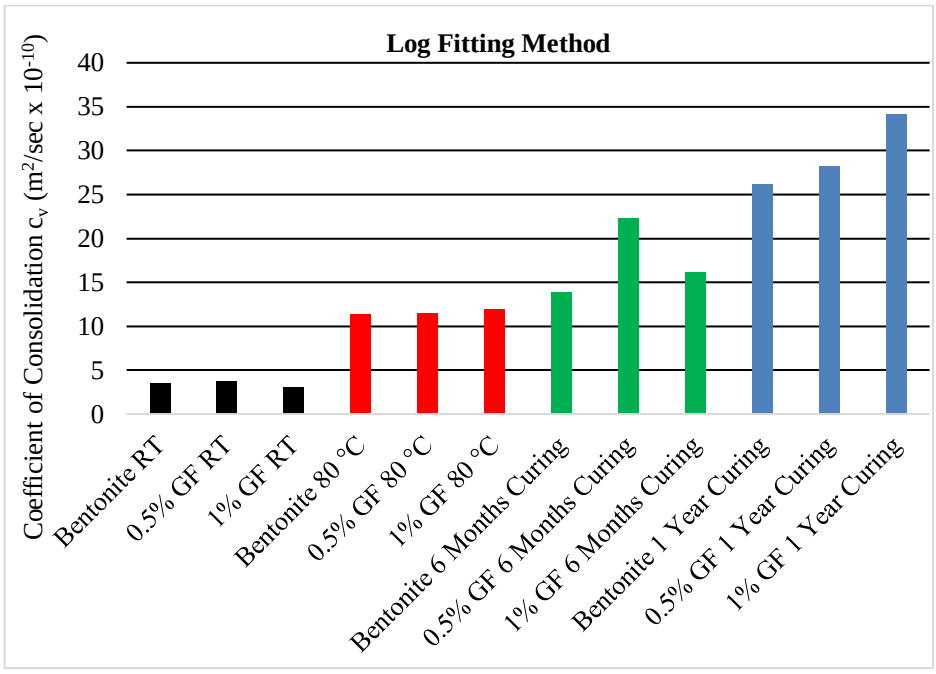

Figure 4.14 The c_v values of the mixtures according to log fitting method

Table 4.14 The c_v values of the mixtures according to log fitting and square fitting method

Samples	Temperature	Curing period	Log Fitting (m^2/sec 10^{-10})	Square Fitting (m^2/sec x 10^{-6})
Bentonite	RT	-	3.50	6.75
Bentonite - 0.5% GF			3.66	8.00
Bentonite - 1% GF			3.03	4.81
Bentonite	80 °C	-	11.35	9.33
Bentonite - 0.5% GF			11.43	14.85
Bentonite - 1% GF			11.94	14.20
Bentonite	80 °C	6 months	13.80	14.01
Bentonite - 0.5% GF			22.30	16.91
Bentonite - 1% GF			16.16	20.10
Bentonite	80 °C	1 year	26.19	22.93
Bentonite - 0.5% GF			28.23	26.96
Bentonite - 1% GF			34.08	29.75

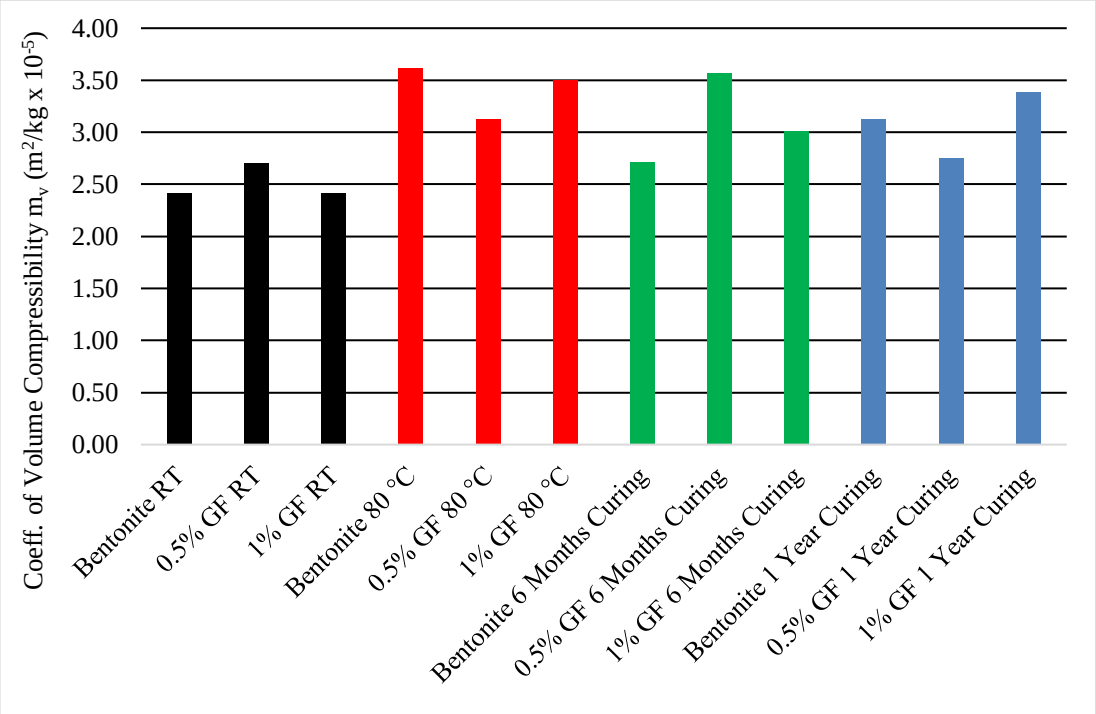

Figure 4.15 The distribution of m_v values

Table 4.15 The m_v values of the mixtures

Samples	Temperature	Curing period	m_v (m^2/kg x 10^{-5})
Bentonite	RT		2.42
Bentonite - 0.5% GF			2.70
Bentonite - 1% GF			2.42
Bentonite	80 °C		3.62
Bentonite - 0.5% GF			3.13
Bentonite - 1% GF			3.50
Bentonite	80 °C	6 months	2.71
Bentonite - 0.5% GF			3.57
Bentonite - 1% GF			3.01
Bentonite	80 °C	1 year	3.13
Bentonite - 0.5% GF			2.75
Bentonite - 1% GF			3.39

Indirect hydraulic conductivity measurement from the consolidation experiment is based on Terzaghi's one-dimensional consolidation theory (Terzaghi, 1943) and hydraulic conductivity (k) is found by the following formula.

$$k = c_v m_v \gamma_w \tag{4.4}$$

Where γ_w is the unit weight of water. In order to determine the hydraulic conductivity, c_v values found from the square fitting method were used. At 80 °C, the unit volume weight of water is different from room temperature. Therefore, while finding the hydraulic conductivity value of the experiments carried out at 80 °C, the unit volume weight of water at 80 °C was used. The results of indirect hydraulic conductivity measurements in the experiments are given in the bar graph in Figure 4.16. Numerical values are also given in Table 4.16. As can be seen from the results,

an increase in the hydraulic conductivity values found by consolidation test was observed at 80 °C temperature. It was also found that the curing effect increased the hydraulic conductivity. And finally, it was observed that glass fiber additive increased the hydraulic conductivity of bentonite at all thermal conditions.

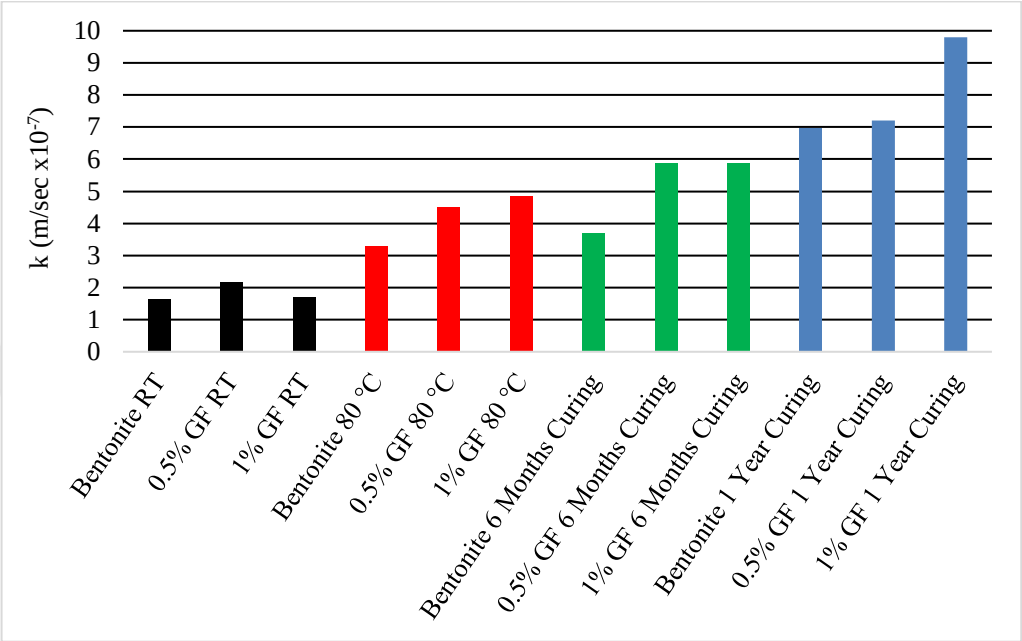

Figure 4.16 The indirect hydraulic conductivity values

Table 4.16 The indirect hydraulic conductivity values of the experiments

Samples	Temperature	Curing period	k (m/sec x 10^{-7})
Bentonite	RT		1.63
Bentonite - 0.5% GF			2.15
Bentonite - 1% GF			1.69
Bentonite	80 °C		3.28
Bentonite - 0.5% GF			4.52
Bentonite - 1% GF			4.83
Bentonite	80 °C	6 months	3.69
Bentonite - 0.5% GF			5.87
Bentonite - 1% GF			5.88
Bentonite	80 °C	1 year	6.98
Bentonite - 0.5% GF			7.20
Bentonite - 1% GF			9.80

4.2 Free Swell Index (FSI) Test Results

The free swell index (FSI) tests were performed for bentonite without glass fiber additives at room temperature and 80 °C (Figure 4.17). While the average swell index value of the experiments performed at room temperature was 20 mL/2g, the average swell index value of the experiments performed at 80 °C was found to be 19 mL/2g.

A slight decrease in the swell index was observed in the presence of high temperature. The reason for this may be explained by the weakening of the bonds between the clay minerals at high temperatures and the decrease in their water retention capacity. It was revealed by literature studies that there is a relationship between free swell and hydraulic conductivity. In the study conducted with 15 different Na-bentonites, it was stated that the hydraulic conductivity decreased approximately ten times as the swell index increased from 6 to 20 mL/2g, and the hydraulic conductivity value remained almost constant in the free swell after 20 mL/2g (Mishra et al., 2011). Studies also show that a bentonite with a swell index higher than

20 mL/2g can be an excellent hydraulic barrier for landfill liners with a hydraulic conductivity value of $k<10^{-9}$ m/sec (Katsumi et al., 2008; Shan & Lai, 2002).

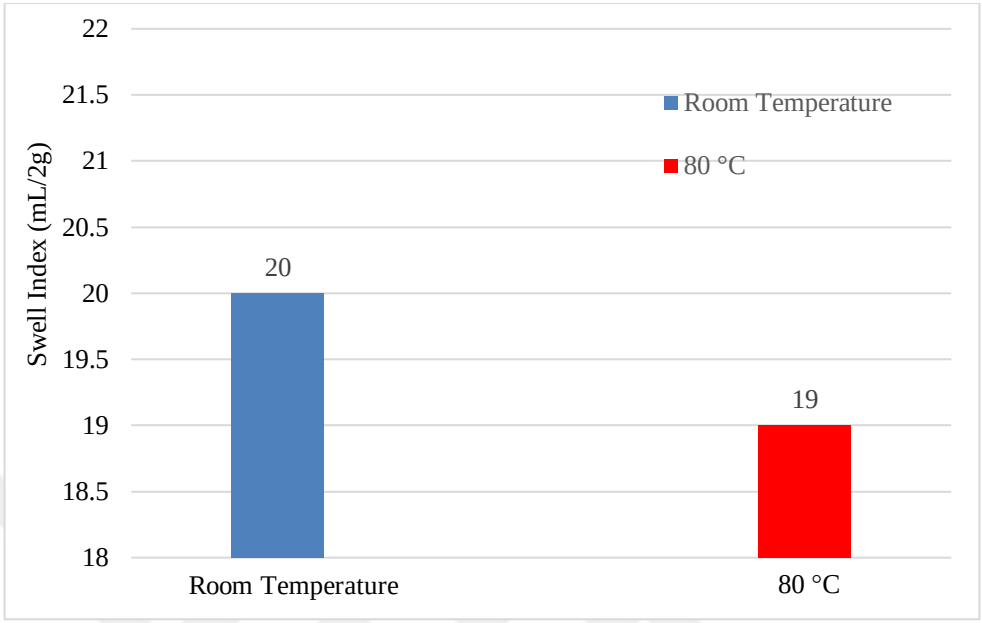

Figure 4.17 Free swell index test results

4.3 Suction Test Results

The suction and water retention curves (WRCs) of bentonite and glass fiber added bentonite mixtures were investigated according to the vapor equilibrium technique (VET). The experiments were carried out both at room temperature and at 80 °C with different samples. The mixtures were compacted as unconfined compacted specimens at a dry density of 1.4 g/cm^3 in the air-dry state in unconfined compression testing machine. When applying the vapor equilibrium technique, saturated salt solutions with different relative humidity and suction values were used.

The saturated salt solutions and unconfined compacted samples were kept in jars until the water transfer change in the vapor phase reached equilibrium and then the WRCs of the samples were observed by continuing this process in saturated salt solutions with higher relative humidity and lower suction value. With this process, the wetting paths of the samples were determined. In addition, drying paths were also obtained for the hysteretic behavior of the curve by drying the samples in the same salt solutions after the wetting path.

The reason for choosing jars as a closed and constant mass system is to shorten the equilibrium times by reducing the volume of the system. Thus, the equilibrium periods of 3-4 months in relatively larger systems such as desiccators were reduced to 3-4 weeks with jars. Constant temperature and relative humidity conditions were created to prevent the experimental system from being affected by changes in ambient temperature and relative humidity. An incubator was used for experiments at room temperature, while an oven was used for experiments at 80 °C.

The salts used in the suction tests are given in Table 4.17 below. The relative humidity of the saturated salt solutions was determined using hygrometers before placing the samples in the jars. The suction values of the solutions were also determined by the formula given in equation 2.5.

Table 4.17 Relative humidity (RH) and suction values of salts at room temperature and high temperature

Salts	Room Temperature		High Temperature (80 °C)	
	Relative Humidity (%)	Suction (MPa)	Relative Humidity (%)	Suction (MPa)
K_2CO_3	44	112	-	-
$CaNO_3$	51	92	-	-
$NaNO_2$	66	57	65	65
NaCl	75	39	75	45
KCl	84	24	79	37
$ZnSO_4$	91	13	89	18
K_2SO_4	97	4	96	6

In the experiments conducted at room temperature, bentonite and glass fiber added bentonite mixtures were first kept in the K_2CO_3 saturated salt solution. However, as a result, it was observed that the bentonite mixtures dried slightly, i.e. the water content decreased. This shows that the total suction value of bentonite and glass fiber added

bentonite mixtures is lower than the suction value of K_2CO_3 salt solution which is 112 MPa. The samples were then placed in the $CaNO_3$ salt solutions with lower suction value (92 MPa) and higher relative humidity. $CaNO_3$ saturated salt solution was found to be the salt solution with the highest suction value increasing the water content of bentonite mixtures at room temperature. This means that the total suction values of bentonite mixtures at room temperature were in the range of 92-112 MPa. The initial water content of bentonite was 7.5%, whereas 0.5% and 1% GF mixtures were 7.5% and 7.4% respectively. The water content corresponding to the suction value in each salt solution was calculated and a suction-water content graph was created. The suction-water content graphs and tables obtained in the experiments conducted at room temperature are given in Figure 4.18 and Table 4.18 below.

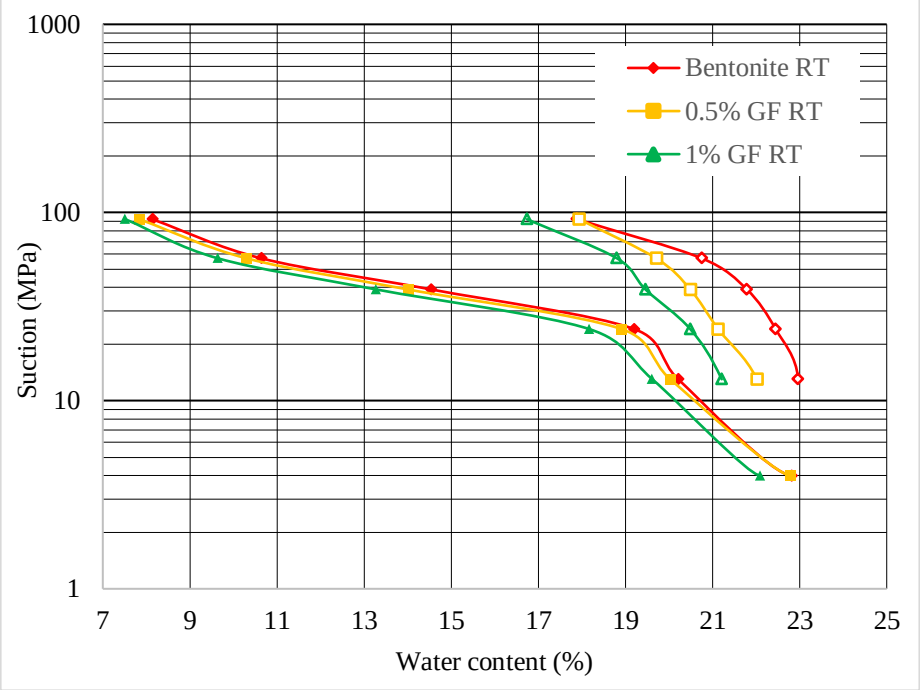

Figure 4.18 Suction-water content graph of the bentonite mixtures at the room temperature (filled symbols: wetting, hollow symbols: drying)

Table 4.18 The water contents at which the attained equilibrium in the suction tests performed at room temperature

Path	Salt	Suction (MPa)	Water Content (%)		
			Bentonite RT	0.5% GF RT	1% GF RT
Wetting	$CaNO_3$	92	8.1	7.8	7.4
	$NaNO_2$	57	10.7	10.3	9.7
	NaCl	39	14.5	14.0	13.3
	KCl	24	19.2	18.9	18.2
	$ZnSO_4$	13	20.2	20.4	19.6
	$K2SO_4$	4	22.8	22.8	22.1
Drying	$ZnSO_4$	13	23.0	22.0	21.2
	KCl	24	22.5	21.1	20.5
	NaCl	39	21.8	20.5	19.5
	$NaNO_2$	57	20.8	19.7	18.8
	$CaNO_3$	92	17.9	17.9	16.7

As can be seen from the Fig. 4.18 and Table 4.18, glass fiber additive decreased the water retention capacity of bentonite. Figure 4.18 shows that at the same water content, the suction value of bentonite was higher than the glass fiber added mixtures. Likewise, the water retention capacity decreased when the glass fiber ratio increased from 0.5 to 1%. This decrease can also be explained by the downward shift of the wetting path. However, at high suctions, the decrease in water retention capacity caused by glass fiber additive is negligible. For example, if the suction values of the samples are compared at 15% water content, it is seen that the suction of bentonite is again the highest, but the change is limited to a few MPa. At low suctions (<24 MPa) a bend in the water retention curve occurred in all three mixtures. It was also observed that the water retention curve of the 1% GF mixture at low suction values, i.e. at high water content, diverged away from the bentonite and 0.5% GF mixture.

After the wetting paths were completed, the drying paths formed in the samples dried by the same method gave consistent results between each other. A hysteretic behavior was not observed in the water retention behavior of the samples with drying

paths. That is, there is a difference between the water content at which it reaches equilibrium at any suction value in the wetting path and the water content at which it reaches equilibrium at the same suction value in the drying path. At low suction values in the drying path, the samples reached equilibrium at higher water contents without reaching the water content at which they reached equilibrium in the wetting path. At low suction values, the difference in water content at the same suction value in the wetting and drying path was between 2-3%, while at high suction values (>24 MPa) this difference increased even more. For example, bentonite reached equilibrium with a water content of 20.2% at 13 MPa suction value in the wetting path, while the water content at equilibrium in the drying path was 23.0%. The equilibrium water content of bentonite at 57 MPa suction value was found to be 10.7% in the wetting path and 20.8% in the drying path.

For the experiments carried out at 80 °C, the initial salt solution was NaCl with a suction value of 45 MPa. $CaNO_3$ and $NaNO_2$ salt solutions with higher suction values decreased the water content of the samples, i.e. dried them. The suction value of $NaNO_2$ and NaCl salt solutions at 80 °C is 65 and 45 MPa, respectively. This means that the total suction values of the samples at 80 °C were in the range of 45-65 MPa. Suction-water content relationship graphs and water content values where it reaches equilibrium at certain suction value are presented in Figure 4.19 and Table 4.19. In the experiments carried out at 80 °C, the glass fiber additive shifted the water retention curve slightly downwards as observed in the experiments carried out at room temperature. As getting to lower suction values (<37 MPa), the difference between the water retention curves of the mixtures became more pronounced. In addition, at low suction, the negative effect of glass fiber additive on the water retention capacity became more pronounced.

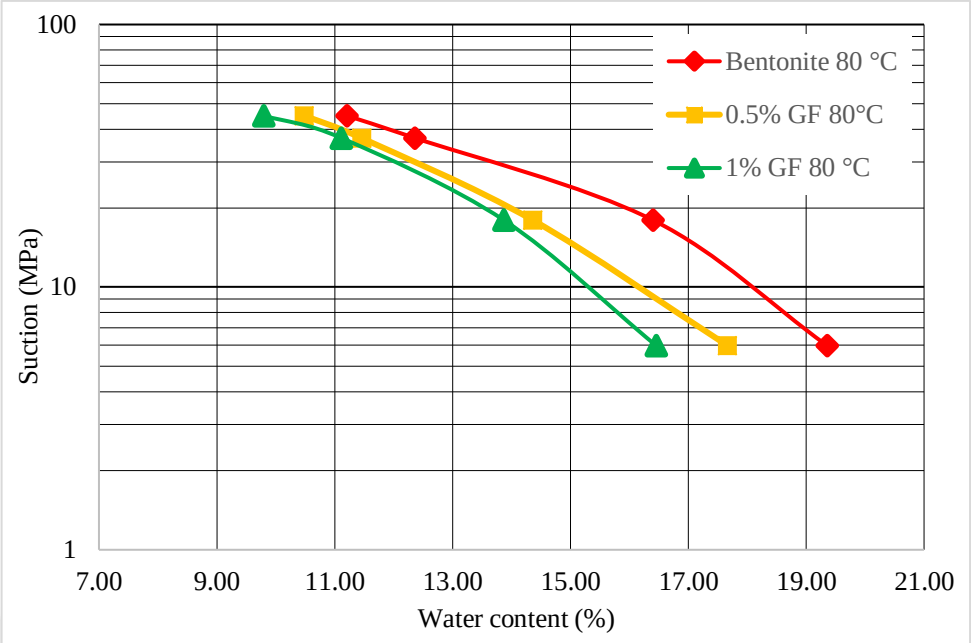

Figure 4.19 Suction-water content graph of the bentonite mixtures at 80 °C

Table 4.19 The water contents at equilibrium in the suction tests performed at 80 °C

Path	Suction (MPa)	Water Content (%)		
		Bentonite 80 °C	0.5% GF 80 °C	1% GF 80 °C
Wetting	45	11.20	10.48	9.79
	37	12.36	11.45	11.11
	18	16.40	14.36	13.87
	6	19.35	17.66	16.45

The change of pore water characteristics with temperature clearly affects the water retention behavior of soils. The water characteristic that can have the most impact on the retention capacity of a soil is surface tension due to its reflection in capillary phenomena (Villar & Lloret, 2004). Romero et al. (2001) also found that the effect of temperature on the retention capacity of compacted kaolinitic-illitic clay (Boom clay) cannot be solely caused by the thermal variation of surface tension and that the clay texture and the fluid chemistry within the aggregate may change with temperature. Ye et al. (2009) concluded that the evolution of the clay texture and the water in the aggregate plays an important role in the water retention capacity. With increasing

temperature, a lot of intra-aggregate water moves towards the macropores. Excess water flows out of the macropore because the degree of saturation is invariant in the macropores at a given suction. Therefore, the water retention capacity of bentonite decreases. At low suction values, the change in the water retention behavior of glass fiber with high temperature became more pronounced. According to Jadda et al. (2021), this may be due to the reduction of macropores in the clay with the addition of fibers.

4.4 Hydraulic Conductivity Test Results

Hydraulic conductivity tests were conducted according to ASTM D5084-16a (2016). Falling head and constant tailwater method was applied for the tests. Bentonite mixtures were compacted in air dry condition at a dry density of 1.4 g/cm^3. Hydraulic conductivity values of these unsaturated highly compacted bentonite mixtures were determined in an unconfined state in a 5.0 cm diameter 1.0 cm high ring. In all experiments, 1.5 MPa was used as cell pressure. The hydraulic gradient values of the experiments vary in the 175-225 range.

The experiments were carried out in a specially manufactured flexible-walled permeameter test apparatus. The experiments were performed with bentonite and glass fiber reinforced bentonite mixtures at room temperature, at 80 °C and cured at 80 °C for 3 months. The samples that completed the experiment at room temperature were then exposed to 80 °C and the experiment was continued at 80 °C. The samples cured for 3 months were kept at 80 °C and then the experiments were started. Since the duration of the experiments was very long, the samples, which were tested at room temperature, took a long time to transition to 80 °C temperature. Therefore, no more data could be obtained at 80 °C, but the experiments at 80 °C and cured for 3 months are still ongoing.

The hydraulic conductivity changes of the mixtures were determined according to Q_{out}/Q_{in} ratio and pore volume of flow (a pore volume is defined as the volume of voids in the sample). It took more than 200 days to get results from the experiments, yet only maximum five readings were taken and the average of the readings was taken as the hydraulic conductivity value. The hydraulic conductivity test results of bentonite and

glass fiber added bentonite mixtures at room temperature are shown in Figures 4.20-22 and at cured for 3 months are shown in Figures 4.23-25.

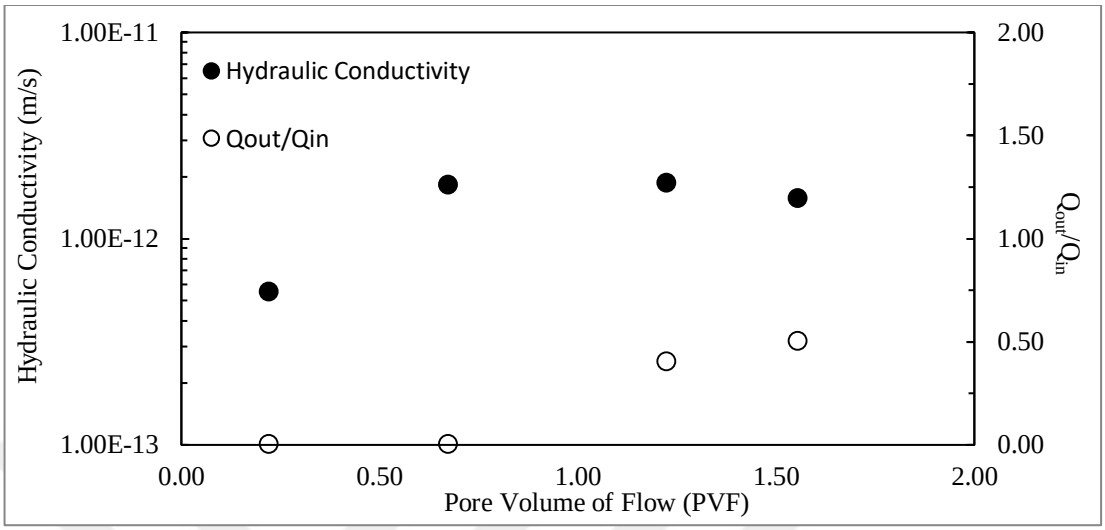

Figure 4.20 Hydraulic conductivity test results of bentonite at room temperature

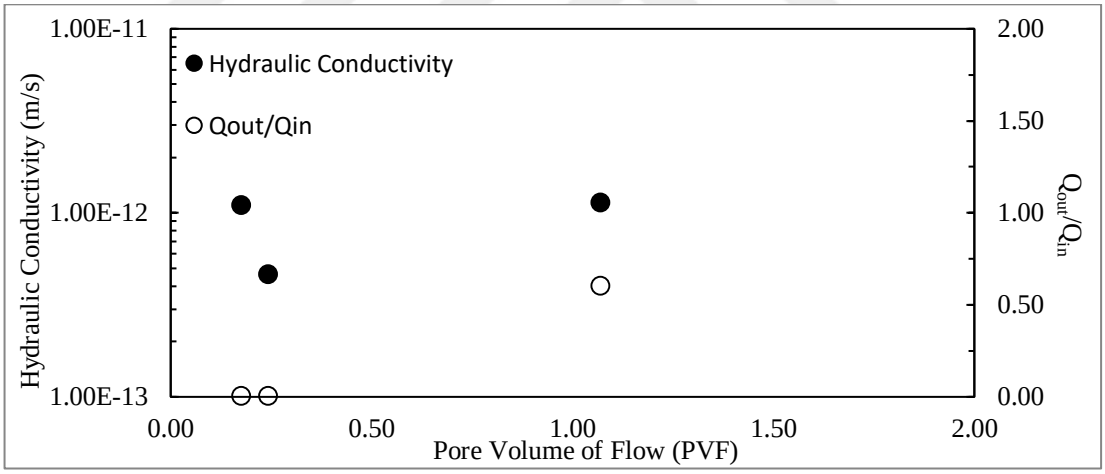

Figure 4.21 Hydraulic conductivity test results of 0.5%GF mixture at room temperature

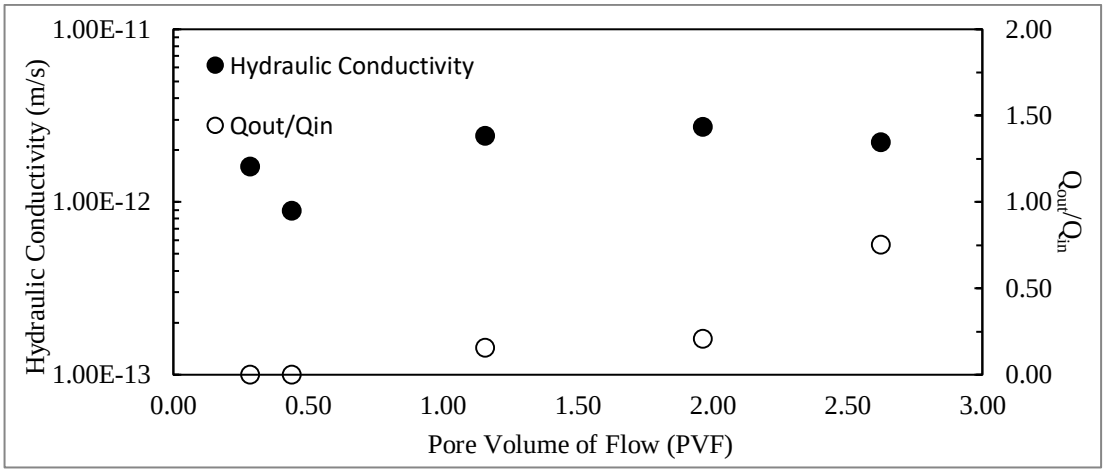

Figure 4.22 Hydraulic conductivity test results of 1%GF mixture at room temperature

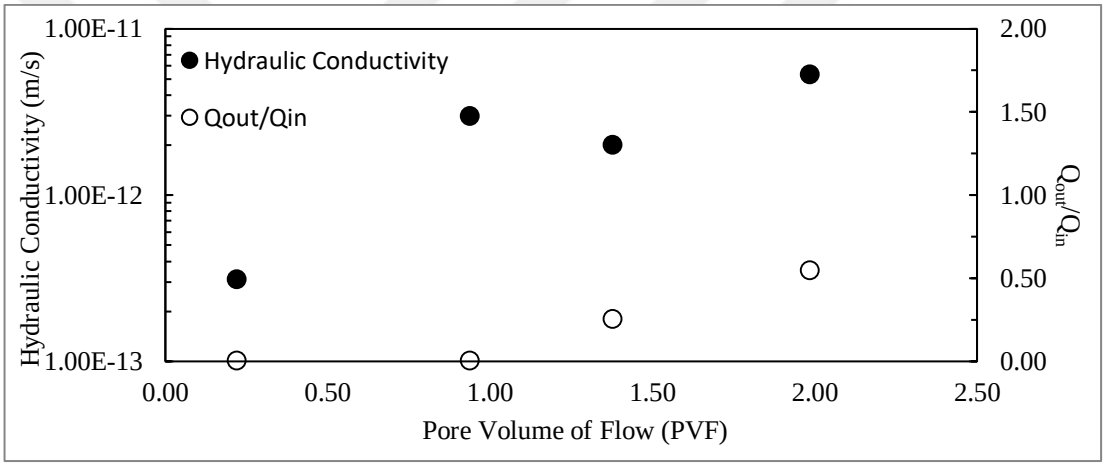

Figure 4.23 Hydraulic conductivity test results of bentonite for cured 3 months at 80 °C

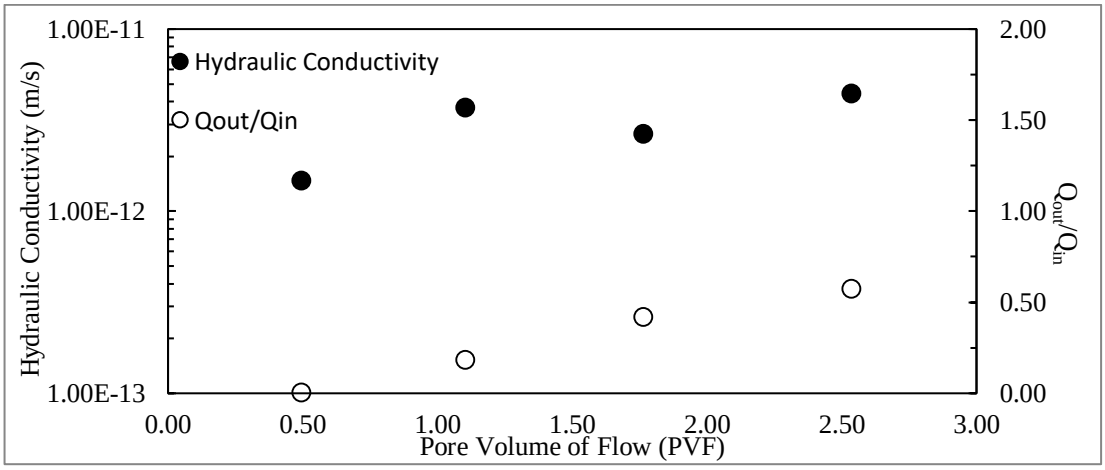

Figure 4.24 Hydraulic conductivity test results of 0.5% GF mixture for cured 3 months at 80 °C

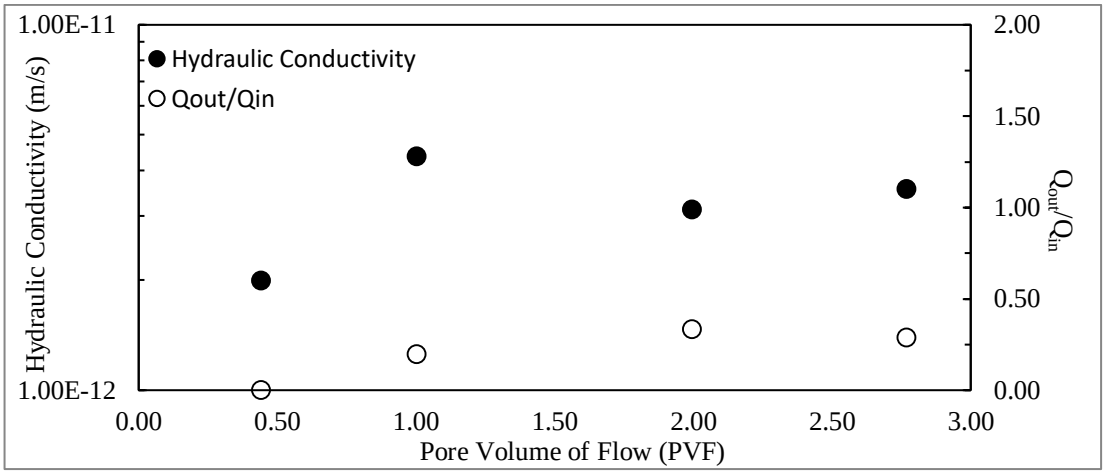

Figure 4.25 Hydraulic conductivity test results of 1% GF mixture for cured 3 months at 80 °C

The average hydraulic conductivity values obtained from the experiments are presented in Table 4.20. According to the results, an increase in hydraulic conductivity values was observed in the mixtures cured at 80 °C for 3 months with the effect of temperature and curing.

Table 4.20 Average hydraulic conductivity values obtained from the experiments

Samples	Temperature	Curing Period	k_{av} (m/s)
Bentonite	RT	-	1.44×10^{-12}
0.5% GF			8.92×10^{-13}
1% GF			1.96×10^{-12}
Bentonite	80 °C	3 Months	2.63×10^{-12}
0.5% GF			3.04×10^{-12}
1% GF			3.26×10^{-12}

Except for the 0.5% GF mixture at room temperature, the other glass fiber added samples caused an increase in the hydraulic conductivity value of bentonite (Figure 4.26). Also, when the mixtures cured at 80 °C for 3 months were examined, 0.5% and 1% GF mixtures increased the hydraulic conductivity value of bentonite by 1.15 and 1.24 times, respectively. In the equation below, the change in hydraulic conductivity due to the change in density and viscosity of water with the change in temperature can be found.

$$\frac{k(T)}{k(To)} = \frac{\mu(T)\gamma w(T)}{\mu(T0)\gamma w(T0)} \quad (4.5)$$

Where μ(T) and μ(T_0) are the viscosity of water at 80 °C and room temperature, γ_w(T) and γ_w(T_0) are the density of water at 80 °C and room temperature, respectively. According to the equation, the hydraulic conductivity at room temperature at 25 °C is expected to increase 2.5 times in the presence of 80 °C temperature. The hydraulic conductivity of bentonite increased 1.83 times from 1.44 x 10^{-12} to 2.63 x 10^{-12} m/s after 3 months of 80 °C curing. This change with 80 °C curing was determined as 3.40 and 1.66 times for 0.5% and 1% GF mixtures, respectively.

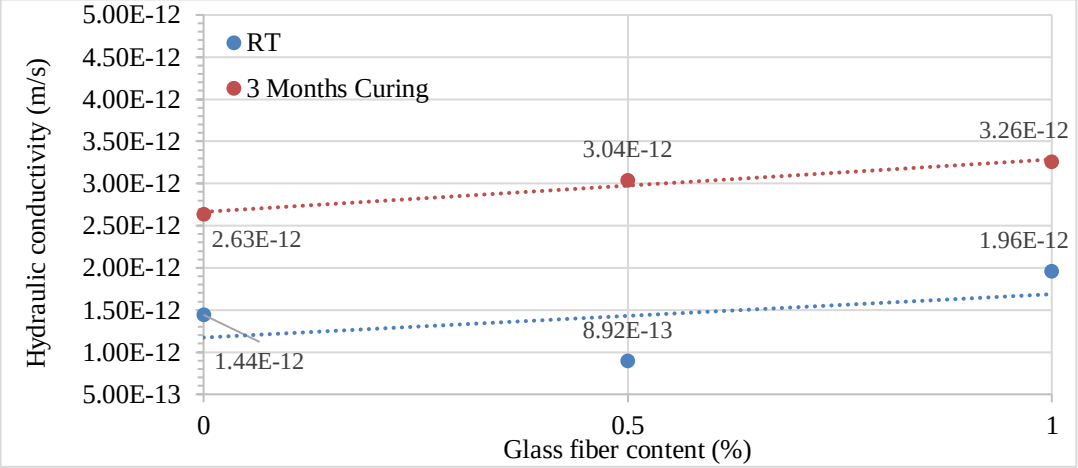

Figure 4.26 Change in hydraulic conductivity according to glass fiber ratio

The increase in hydraulic conductivity at high temperature is mostly attributed to the increase in viscosity of the fluid used with increasing temperature. According to Habibagahi (1977), at a certain temperature, the adsorbed water molecules do not mobilize and free flow of water through the confined channels takes place, thus decreasing the water layer thickness and increasing the hydraulic conductivity.

The hydraulic conductivity increased both at room temperature and at high temperature with the addition of glass fiber. The reason for this increase, according to Mukherjee & Mishra (2021), is that the fibers inside the sample can create a drainage

path that allows water to pass through. The reason for the decrease in hydraulic conductivity at room temperature in the 0.5% GF mixture may be due to the dispersion of the fibers in such a way that they do not form a drainage path.

CHAPTER FIVE

CONCLUSIONS AND RECOMMENDATIONS

5.1 Conclusions

Engineering properties of bentonite used as a buffer material in high-level nuclear waste storage sites were investigated in this thesis. In addition, glass fiber additives were added to bentonite at the rate of 0.5% and 1% by dry weight to improve its engineering properties. Within the scope of the thesis study, consistency limits, hydrometer, X-Ray diffraction (XRD), Methylene blue index (MBI), Cation exchange capacity (CEC) and pH measurement tests were carried out for the characterization of the materials and mixtures. A number of experiments were carried out to determine the volumetric deformation, hydraulic conductivity and water retention behavior of glass fiber added bentonite mixtures at room temperature and 80 °C. These tests were consolidation, hydraulic conductivity, free swell index (FSI) and vapor equilibrium technique (VET) tests. The results obtained from the experiments are summarized below:

An insignificant decrease was observed in the liquid and plastic limit values of bentonite with glass fiber additive.

In consolidation experiments conducted at room temperature, glass fiber additive caused an increase in rebound behavior. This increase increased as the glass fiber content increased and while the swelling index value of the bentonite without additive was 0.52, it increased to 0.88 and 1.38 with 0.5% and 1% GF additive, respectively. Rebound behavior of the mixtures decreased significantly in the presence of 80 °C temperature.

At 80 °C temperature, glass fiber addition increased the compressibility. However, the change remained negligible. Compression index values are 3.31, 3.37 and 3.67 for bentonite, 0.5% and 1% GF mixtures, respectively.

In the specimens kept under 80 °C temperature for a curing period of 6 months, a decrease in compressibility was observed in the specimens due to the curing effect. There was also a decrease in swelling behavior.

The change in compressibility and swelling behavior with the increase in curing time from 6 months to 1 year is negligible.

When the indirect hydraulic conductivity values obtained from consolidation test results were compared, it was observed that the glass fiber additive increased the hydraulic conductivity value of bentonite at all temperatures and curing conditions. This increase increased at 80 °C temperature conditions. The increase was also observed with the curing effect. The lowest calculated value was $1.6x10^{-7}$ m/s in the bentonite mixture at room temperature, while the highest value was 9.8×10^{-7} m/s in the 1% GF sample cured for 1 year.

The FSI test results of bentonite at room temperature and 80 °C were 20mL/2g and 19mL/2g, respectively. It is interpreted that the effect of temperature will reduce the swelling behavior of bentonite and increase the hydraulic conductivity behavior accordingly.

Total suction value was found in the range of 92-112 MPa in suction experiments performed with bentonite mixtures at room temperature. In the experiments performed at 80 °C, the total suction range was found in the range of 45-65 MPa. A decrease in water retention behavior was observed with the effect of temperature.

A slight downward shift in the water retention curve was observed as a negative effect due to the glass fiber effect both at room temperature and at 80 °C. Nevertheless, this change was limited to only a few MPa, i.e. negligible.

At low suction values (<24 MPa for room temperature, <37 MPa for 80 °C) the negative effect of glass fiber became more pronounced.

In terms of hydraulic conductivity values, when the samples at room temperature and at 80 °C for 3 months cured were compared, an increase in the hydraulic conductivity values of bentonite mixtures was observed in the presence of 80 °C temperature.

While the hydraulic conductivity of bentonite at room temperature was found to be 1.44 x 10^{-12} m/s, this value increased 1.83 times to 2.63 x 10^{-12} m/s at 80 °C.

Glass fiber additive increased the hydraulic conductivity of bentonite both at room temperature and at 80 °C. However, this increase was found to be less than two times.

The bentonite and glass fiber added bentonite mixtures used in the thesis exceeded the desired limit of 10^{-12} m/s hydraulic conductivity values in nuclear waste repositories.

5.2 Recommendations for Future Studies

The engineering behavior of bentonite, a buffer material used in high-level nuclear waste (HLW) repositories, under temperature is critical for the continuity performance of HLW's. Therefore, it is necessary to investigate the hydraulic conductivity and water retention behavior of bentonite at various dry densities at different temperature values and also over temperature cycles. In addition to this, swelling pressure experiments of bentonite and its change and improvement under increasing temperature conditions are necessary for further studies. Working with different OCR values while examining the compressibility behavior is also one of the topics that can be examined. In addition, instead of glass fiber, different materials such as carbon fiber or basalt fiber that show good thermal properties can be considered for the improvement of bentonite.

REFERENCES

Abuel-Naga, H. M., Bergado, D. T., Ramana, G. V., Grino, L., Rujivipat, P., & Thet, Y. (2006). Experimental evaluation of engineering behavior of soft Bangkok clay under elevated temperature. *Journal of geotechnical and geoenvironmental engineering*, 132(7), 902-910.

Abuel-Naga, H. M., Bergado, D. T., Bouazza, A., & Ramana, G. V. (2007). Volume change behaviour of saturated clays under drained heating conditions: experimental results and constitutive modeling. *Canadian Geotechnical Journal*, 44(8), 942-956.

ANDRA (2005) Synthesis: evaluation of the feasibility of a geological repository in an argillaceous formation, Meuse/Haute Marne site. *Tech rep*, Paris, France.

ASTM: D2435-11 (2011). Standard test methods for one-dimensional consolidation properties of soils using incremental loading. *ASTM International, West Conshocken, PA, USA*, 1-8.

ASTM: D422-63. (2007). Standard test method for particle-size analysis of soils (Withdrawn 2016), *ASTM International, West Conshohocken, PA, USA*, 1-8.

ASTM: D4318-17e1. (2017). Standard test methods for liquid limit, plastic limit, and plasticity index of soils. *ASTM International, West Conshohocken, PA, USA*, 1- 20.

ASTM: D4972-19. (2019). Standard test methods for ph of soils. *ASTM International, West Conshohocken, PA, USA*, 1-6.

ASTM: D5084-16a. (2016). Standard test methods for measurement of hydraulic conductivity of saturated porous materials using a flexible wall permeameter. *ASTM International, West Conshohocken, PA, USA*, 1–24.

ASTM: D5890-19. (2019). Standard Test Method for Swell Index of Clay Mineral Component of Geosynthetic Clay Liners. *ASTM International, West Conshocken, PA, USA*, 1-9.

ASTM: D7503-10. (2018). Standard Test Method for Measuring the Exchange Complex and Cation Exchange Capacity of Inorganic Fine-Grained Soils. *ASTM International, West Conshohocken, PA, USA*, 1–9.

Bag, R., & Rabbani, A. (2017). Effect of temperature on swelling pressure and compressibility characteristics of soil. *Applied Clay Science*, 136, 1-7.

Baldi, G., Hueckel, T., & Pellegrini, R. (1988). Thermal volume changes of the mineral–water system in low-porosity clay soils. *Canadian geotechnical journal*, 25(4), 807-825.

Blatz, J. A., Cui, Y. J., & Oldecop, L. (2009). Vapour equilibrium and osmotic technique for suction control. *Laboratory and field testing of unsaturated soils*, 49-61.

Bouaricha, L., Henni, A. D., & Lancelot, L. (2017). A laboratory investigation on shear strength behavior of sandy soil: effect of glass fiber and clinker residue content. *Studia Geotechnica et Mechanica*, 39(4), 3-15.

Campanella, R. G., & Mitchell, J. K. (1968). Influence of temperature variations on soil behavior. *Journal of the Soil Mechanics and Foundations Division*, 94(3), 709-734.

Casagrande, A., & Fadum, R. E. (1940). Notes on soil testing for engineering purposes.

Cekerevac, C., & Laloui, L. (2004). Experimental study of thermal effects on the mechanical behaviour of a clay. *International journal for numerical and analytical methods in geomechanics*, 28(3), 209-228.

Cho, W. J., Lee, J. O., & Chun, K. S. (1999). The temperature effects on hydraulic conductivity of compacted bentonite. *Applied clay science*, 14(1-3), 47-58.

Cho, W. J., Lee, J. O., & Kwon, S. K. (2012). An analysis of the factors affecting the hydraulic conductivity and swelling pressure of Kyungju Ca-bentonite for use as a clay-based sealing material for a high-level waste repository. *Nuclear Engineering and Technology*, 44(1), 89-102.

Consoli, N. C., Prietto, P. D., & Ulbrich, L. A. (1998). Influence of fiber and cement addition on behavior of sandy soil. *Journal of geotechnical and geoenvironmental engineering*, 124(12), 1211-1214.

Consoli, N. C., Montardo, J. P., Donato, M., & Prietto, P. D. (2004). Effect of material properties on the behaviour of sand—cement—fibre composites. *Proceedings of the Institution of Civil Engineers-Ground Improvement*, 8(2), 77-90.

Cui, S. L., Du, Y. F., Wang, X. P., Huang, S., & Xie, W. L. (2018). Influence of temperature on swelling deformation characteristic of compacted GMZ bentonite-sand mixtures. *Journal of Central South University*, 25(11), 2819-2830.

Çirkin, İ. (2023). The effect of pumice, perlite and fiber glass additives on the thermal conductivity, compressibility and shear strength behavior of zeolite-bentonite and sand-kaolin mixtures under high temperatures (M.Sc. Thesis, Dokuz Eylül University, The Graduate School of Natural and Applied Sciences).

Delage, P., Sultan, N., & Cui, Y. J. (2000). On the thermal consolidation of Boom clay. *Canadian Geotechnical Journal*, 37(2), 343-354.

Delage, P., Cui, Y. J., & Tang, A. M. (2010). Clays in radioactive waste disposal. *Journal of Rock Mechanics and Geotechnical Engineering*, 2(2), 111-123.

Dixon, D. A., Graham, J., & Gray, M. N. (1999). Hydraulic conductivity of clays in confined tests under low hydraulic gradients. *Canadian Geotechnical Journal*, 36(5), 815-825.

Dixon, D. A. (2000). Porewater salinity and the development of swelling pressure in bentonite-based buffer and backfill materials.

Dost Kimya. (2023, 15 October). https://www.dostkimya.com/tr/urunler/elyaf-katkilar//cam-elyaf-kirpilmis

El Tawati, A. (2010). Impact of the rate of heating on the thermal consolidation of compacted silt (Doctoral dissertation, University of Colorado at Boulder).

Fredlund, D. G., & Rahardjo, H. (1993). Soil mechanics for unsaturated soils. John Wiley & Sons.

Gao, Y. (2017). Soil-water retention behavior of compacted soil with different densities over a wide suction range and its prediction. *Computers and Geotechnics*, 91, 17-26.

Gray, H. (1936, June). Progress report on research on the consolidation of fine-grained soils. In Proceedings, *First International Conference on Soil Mechanics and Foundation Engineering* (Vol. 2, pp. 138-141).

Gupta, B. (1964). Creep of saturated soil at different temperatures (Doctoral dissertation, University of British Columbia).

Güneri, E. (2022). Development of thermally resistant soil material with pumice, perlite and fiber glass additives (P.hD. Thesis, Dokuz Eylül University, The Graduate School of Natural and Applied Sciences).

Habibagahi, K. (1977). Temperature effect and the concept of effective void ratio. *Indian Geotechnical Journal*, 7(1), 14-34.

Hedin, A. (2006). Long-term safety for KBS-3 repositories at Forsmark and Laxemar-a first evaluation. Main Report of the SR-Can project.

Herbert, H. J., & Moog, H. C. (1999). Cation exchange, interlayer spacing, and water content of MX-80 bentonite in high molar saline solutions. *Engineering Geology*, 54(1-2), 55-65.

Hoseinimighani, H., & Szendefy, J. (2022). A Review on Mechanisms of Thermally Induced Volume Changes in Fine Soil. *Minerals*, 12(5), 572.

Imbert, C., & Villar, M. V. (2006). Hydro-mechanical response of a bentonite pellets/powder mixture upon infiltration. *Applied Clay Science*, 32(3-4), 197-209.

Ito, H., & Komine, H. (2008). Dynamic compaction properties of bentonite-based materials. *Engineering Geology*, 98(3-4), 133-143.

Jadda, K., Injamala, S. K., & Bag, R. (2021, May). Hydro-mechanical behavior of glass fiber reinforced clay barriers. *In Proceedings of the Indian Geotechnical Conference 2019: IGC-2019 Volume II* (pp. 145-156). Singapore: Springer Singapore.

Jarad, N. (2016). Temperature impact on the consolidation and creep behaviour of compacted clayey soils (Doctoral dissertation, Université de Lorraine).

Katsumi, T., Ishimori, H., Onikata, M., & Fukagawa, R. (2008). Long-term barrier performance of modified bentonite materials against sodium and calcium permeant solutions. Geotextiles and Geomembranes, 26(1), 14-30. Kim, J. S., Kwon, S. K., Sanchez, M., & Cho, G. C. (2011). Geological storage of high level nuclear waste. *KSCE Journal of Civil Engineering*, 15, 721-737.

Kim, J. S., Kwon, S. K., Sanchez, M., & Cho, G. C. (2011). Geological storage of high level nuclear waste. *KSCE Journal of Civil Engineering*, 15, 721-737.

Komine, H., & Ogata, N. (1996). Prediction for swelling characteristics of compacted bentonite. *Canadian geotechnical journal*, 33(1), 11-22.

Kompozit.net (2023, November 13) https://www.kompozit.net/cam-elyaf-fiberglas

Lambe, T. W., & Whitman, R. V. (1969). Soil mechanics. John Willey & Sons. Inc., New York, 553.

Lee, J. M., & Shackelford, C. D. (2005). Impact of bentonite quality on hydraulic conductivity of geosynthetic clay liners. *Journal of Geotechnical and Geoenvironmental Engineering*, 131(1), 64-77.

Lee, J. O., Cho, W. J., & Kwon, S. (2011). Suction and water uptake in unsaturated compacted bentonite. *Annals of Nuclear Energy*, 38(2-3), 520-526.

Liu, Y., Xu, G., Liu, S., & Chen, Z. (2001). Study on the basic property of Gaomiaozi bentonite, Inner Mongolia (No. CNIC--01552). China Nuclear Information Centre.

Maak, P. (2006). Used fuel container requirements. Ontario Power Generation Preliminary Design Requirements. Ontario, Canada.

Maher, M. H., & Ho, Y. C. (1994). Mechanical properties of kaolinite/fiber soil composite. *Journal of Geotechnical Engineering*, 120(8), 1381-1393.

Marcial, D., Delage, P., & Cui, Y. J. (2002). On the high stress compression of bentonites. *Canadian Geotechnical Journal*, 39(4), 812-820.

Mishra, A. K., Ohtsubo, M., Li, L., & Higashi, T. (2011). Controlling factors of the swelling of various bentonites and their correlations with the hydraulic conductivity of soil-bentonite mixtures. *Applied Clay Science*, 52(1-2), 78-84.

Mukherjee, K., & Mishra, A. K. (2019). Hydro-mechanical properties of sand-bentonite-glass fiber composite for landfill application. *KSCE Journal of Civil Engineering*, 23, 4631-4640.

Mukherjee, K., & Mishra, A. K. (2021). Impact of glass fibre on hydromechanical behaviour of compacted sand–bentonite mixture for landfill application. *European Journal of Environmental and Civil Engineering*, 25(7), 1179-1200.

Nakashima, Y. (2006). H2O self-diffusion coefficient of water-rich MX-80 bentonite gels. *Clay minerals*, 41(2), 659-668.

Pan, H., Qing, Y., & Pei-yong, L. (2010). Direct and indirect measurement of soil suction in the laboratory. *Electronic Journal of Geotechnical Engineering*, 15(3), 1-14.

Posiva, O. (2003). Nuclear Waste Management of the Olkiluoto and Loviisa Power Plants: Programme for Research, Development and Technical Design for 2004-2006 (No. POSIVA-TKS--2003). Posiva Oy.

Pusch, R. (1983). Use of clays as buffers in radioactive repositories (No. SKBF-KBS-TR--83-46). Svensk Kaernbraenslefoersoerjning AB.

Pusch, R., Karnland, O., & Hökmark, H. (1990). GMM-a general microstructural model for qualitative and quantitative studies of smectite clays (No. SKB-TR--90-43). Swedish Nuclear Fuel and Waste Management Co.

Richards BG (1974) Behaviour of unsaturated soils. In: Lee IK (ed), Soil mechanics—new horizons. *American Elsevier, New York*, pp 112–157.

Romero, E., Gens, A., & Lloret, A. (2001). Temperature effects on the hydraulic behaviour of an unsaturated clay. *Unsaturated soil concepts and their application in geotechnical practice*, 311-332.

Ruan, B., Zheng, S., Teng, J., Ding, H., & Ma, C. (2020). Analysis on the triaxial shear behavior and microstructure of cement-stabilized clay reinforced with glass fibers. *Advances in Civil Engineering*, 2020, 1-12.

Santamarina, J. C., Klein, K. A., Wang, Y. H., & Prencke, E. (2002). Specific surface: determination and relevance. *Canadian Geotechnical Journal*, 39(1), 233-241.

Schneider, A. (1960). Neue Diagramme zur Bestimmung der relativen Luftfeuchtigkeit über gesättigten wässerigen Salzlösungen und wässerigen Schwefelsäurelösungen bei verschiedenen Temperaturen: Institut für Holzforschung und Holztechnik der Universität München. *Holz als Roh-und Werkstoff*, 18(7), 269-272.

Shan, H. Y., & Lai, Y. J. (2002). Effect of hydrating liquid on the hydraulic properties of geosynthetic clay liners. Geotextiles and Geomembranes, 20(1), 19-38.

Shao, J., Zeng, Z., & Sun, D. A. (2022). Effect of heating time on hydro-mechanical behaviour of MX80 bentonite. *Environmental Earth Sciences*, 81(20), 483.

Tang, G. X., Graham, J., & Wan, A. W. L. (1998, August). On yielding behaviour of an unsaturated sand-bentonite mixture. *In Proceedings of the 2nd international conference on unsaturated soils* (Vol. 1, pp. 149-154).

Tang, A. M., & Cui, Y. J. (2005). Controlling suction by the vapour equilibrium technique at different temperatures and its application in determining the water retention properties of MX80 clay. *Canadian Geotechnical Journal*, 42(1), 287-296.

Tang, A. M., Cui, Y. J., & Barnel, N. (2007). A new isotropic cell for studying the thermo-mechanical behavior of unsaturated expansive clays. *arXiv preprint arXiv:0710.1400*.

Tang, A. M., Cui, Y. J., & Le, T. T. (2008). A study on the thermal conductivity of compacted bentonites. *Applied Clay Science*, 41(3-4), 181-189.

Taylor, D. W. (1948). Fundamentals of soil mechanics (Vol. 66, No. 2, p. 161). LWW.

Tekkim. (2023, December 25). https://www.tekkim.com.tr/index.php

Terzaghi, K. (1943). Theoretical soil mechanics.

Towhata, I., Kuntiwattanaku, P., Seko, I., & Ohishi, K. (1993). Volume change of clays induced by heating as observed in consolidation tests. *Soils and Foundations*, 33(4), 170-183.

Tripathy, S., & Schanz, T. (2007). Compressibility behaviour of clays at large pressures. *Canadian Geotechnical Journal*, 44(3), 355-362.

Valipour, M., Shourijeh, P. T., & Mohammadinia, A. (2021). Application of recycled tire polymer fibers and glass fibers for clay reinforcement. *Transportation geotechnics*, 27, 100474.

Villar, M. V. (1999). Investigation of the behaviour of bentonite by means of suction-controlled oedometer tests. *Engineering Geology*, 54(1-2), 67-73.

Villar, M. (2001). Caracterización termo-hidro-mecánica de una bentonita de Cabo de Gata (Doctoral dissertation).

Villar, M. V., & Lloret, A. J. A. C. S. (2004). Influence of temperature on the hydro-mechanical behaviour of a compacted bentonite. *Applied clay science*, 26(1-4), 337-350.

Villar, M. V. (2006). Infiltration tests on a granite/bentonite mixture: Influence of water salinity. *Applied Clay Science*, 31(1-2), 96-109.

Virdi, S. P. S., & Keedwell, M. J. (1988). Some observed effects of temperature variation on soil behaviour. *In International conference on rheology and soil mechanics* (pp. 336-354).

Wang, J. (2008). Geological disposal of high level radioactive waste: progress and challenges. *Engineering Sciences*, 10(3), 58-65.

Xiang, G., Lv, L., & Ge, L. (2020). Simple method for evaluating swelling of GMZ01 Na-bentonite affected by temperature at osmotic swelling. *Soils and Foundations*, 60(5), 1312-1321.

Xu, L., Ye, W. M., Chen, B., Chen, Y. G., & Cui, Y. J. (2016). Experimental investigations on thermo-hydro-mechanical properties of compacted GMZ01 bentonite-sand mixture using as buffer materials. *Engineering Geology*, 213, 46-54.

Ye, W. M., Wan, M., Chen, B., Chen, Y. G., Cui, Y. J., & Wang, J. (2009). Effect of temperature on soil-water characteristics and hysteresis of compacted Gaomiaozi bentonite. *Journal of Central South University of Technology*, 16(5), 821-826.

Ye, W. M., Zhang, Y. W., Chen, B., Zheng, Z. J., Chen, Y. G., & Cui, Y. J. (2012). Investigation on compression behaviour of highly compacted GMZ01 bentonite with suction and temperature control. *Nuclear Engineering and Design*, 252, 11-18.

Ye, W. M., Wan, M., Chen, B., Chen, Y. G., Cui, Y. J., & Wang, J. (2013). Temperature effects on the swelling pressure and saturated hydraulic conductivity of the compacted GMZ01 bentonite. *Environmental earth sciences*, 68, 281-288.

Ye, W. M., Borrell, N. C., Zhu, J. Y., Chen, B., & Chen, Y. G. (2014). Advances on the investigation of the hydraulic behavior of compacted GMZ bentonite. *Engineering geology*, 169, 41-49.

Ye, W. M., Wang, Y., Wang, Q., Chen, Y. G., & Chen, B. (2020). Stress-dependent temperature effect on the swelling behavior of compacted GMZ bentonite. *Bulletin of Engineering Geology and the Environment*, 79, 3897-3907.

Zhang, M., Zhang, H., Cui, S., Jia, L., Zhou, L., & Chen, H. (2012). Engineering properties of GMZ bentonite-sand as buffer/backfilling material for high-level waste disposal. *European journal of environmental and civil engineering*, 16(10), 1216-1237.

Zhang, J., Zhang, J., & Zhang, L. (2013). Swelling characteristics of GMZ bentonite and its mixtures with sand. *Applied Clay Science*, 83, 224-230.

Zhenyao, S., Guoding, L., & Shushen, L. (2000). Coupled calculation of dose rate and temperature in the near field of a high-level radioactive waste disposal repository. *Radiation Protection* (Taiyuan), 20.

Zhou, X., Xu, Y., Tan, Y., & Xu, Y. (2021). Three-dimensional thermal–hydraulic coupled analysis in the nuclear waste repository. *Annals of Nuclear Energy*, 151, 107866.